

**MECHANISTIC INSIGHTS INTO RETIGABINE
MODULATION OF NEURONAL KCNQ CHANNELS**

by

Robin Yongkyu Kim

B.Sc., The University of British Columbia, 2013

A THESIS SUBMITTED IN PARTIAL FULFILLMENT OF
THE REQUIREMENTS FOR THE DEGREE OF

DOCTOR OF PHILOSOPHY

in

THE FACULTY OF GRADUATE AND POSTDOCTORAL STUDIES

(Pharmacology)

THE UNIVERSITY OF BRITISH COLUMBIA
(Vancouver)

August 2017

© Robin Yongkyu Kim, 2017

Abstract

Epilepsy is among the most prevalent neurological disorders, affecting approximately 1% of the human population. There are many types of epilepsies, with diverse aetiologies, and many therapies that target ion channels as a means to combat neuronal hyper-excitability. However, most anti-epileptic drugs today target a limited number of ion channel types, mainly voltage-gated sodium and calcium channels. Retigabine is a recently approved anti-epileptic drug that operates through a novel mechanism of activating voltage-gated potassium channels. Previous research has established neuronal KCNQ channels as the therapeutic target of retigabine. However, detailed insights regarding the molecular mechanisms of retigabine action are lacking, such as its mode of binding, the factors underlying its ability to stabilize channel opening, and the stoichiometry of its action. A lack of such knowledge hampers the development of more potent and specific channel openers devoid of side effects associated with this first-generation drug.

The work presented in this thesis utilizes various research techniques to investigate retigabine pharmacology at a molecular level. In the first objective, retigabine binding to KCNQ3 channels is investigated using unnatural amino-acid mutagenesis. The data pinpoint an essential hydrogen-bonding interaction that likely occurs between an S5 tryptophan residue and a carbonyl oxygen moiety present in most KCNQ activating drugs, providing the highest resolution understanding of the retigabine pharmacophore to date. In the second objective, voltage-clamp fluorometry is used to track conformational changes of the voltage-sensing domain of KCNQ3 channels. The data illustrate a network of interactions between the voltage-sensing and ion conducting regions of the channel protein that is dependent on the anionic membrane phospholipid PIP₂; these interactions are not only essential for channel function, but also for retigabine binding to modulate channel voltage sensing downstream of binding in the pore domain. Finally, using

concatenated KCNQ3 constructs to express channels with variable stoichiometry of retigabine binding sites, we demonstrate that a minimum of one retigabine sensitive channel subunit is required for functional pharmacological effects. Overall, this work provides novel insights applicable to the development of retigabine derivatives with greater therapeutic impact, and improves our understanding of lipid and drug regulation of KCNQ channels.

Lay Summary

Currently, despite the availability of over 30 anti-epileptic therapies, seizure prevention is inadequate in approximately 25% of patients. Retigabine is a recently discovered compound proven to be effective in reducing seizures in patients resistant to previously existing drugs, and it uniquely operates through a mechanism of opening voltage gated KCNQ potassium channels in the brain. The research in this thesis explores the detailed mechanisms of retigabine using advanced approaches in electrophysiology and molecular biology. The experiments reveal that retigabine interactions with KCNQ channels relies on the formation of a hydrogen bond between a specific amino acid sidechain in the channel pore region, and an oxygen molecule in the drug. Additionally, the membrane lipid PIP₂ plays an important role in altering channel function in response to retigabine binding. These findings can be used to guide the development of more effective drugs for the treatment of epilepsy.

Preface

A version of chapter 3 has been published. **Kim, R.Y.**, Yau, M.C., Galpin, J.D., Seebohm, G., Ahern, C.A., Pless, S.A., and Kurata, H.T. (2015). Atomic basis for therapeutic activation of neuronal potassium channels. *Nat. Commun.* 6, 8116. I conducted a majority of the experiments and data analysis. Writing of the first draft was performed by H.T. Kurata, and subsequent versions were modified and edited by myself and other authors. S.A. Pless and M.C. Yau conducted experiments and contributed to study design along with myself and H.T. Kurata. J.D. Galpin and C.A. Ahern performed chemical synthesis of crucial reagents, and G. Seebohm performed molecular dynamics simulations.

A version of chapter 4 is currently under review, as a manuscript titled “PIP₂ modulates functional coupling and pharmacology of neuronal KCNQ channels”. I solely performed all the experiments in this chapter, and designed experiments with H.T. Kurata along with guidance and input from S.A. Pless. I wrote the first draft of this manuscript and the submitted work was revised and edited by S.A. Pless and H.T. Kurata.

Chapter 5 is currently in preparation for submission of a manuscript titled “Functional stoichiometry of retigabine binding in KCNQ channels”. I performed approximately 40% of the experiments in this chapter, and contributed to writing of the manuscript and experimental design along with H.T. Kurata, M.C. Yau and S.A. Pless. M.C. Yau. R.Y. Yang helped with synthesis of constructs.

Oocyte preparation for all experiments were carried out using a protocol approved by the University of British Columbia Animal Care Committee, in accordance with the Canadian Council for Animal Care guidelines (certificate B14-0009).

Table of Contents

Abstract.....	ii
Lay Summary	iv
Preface	v
Table of Contents	vi
List of Tables.....	viii
List of Figures	ix
List of Abbreviations.....	x
Acknowledgements.....	xi
Dedication	xii
Chapter 1: Introduction.....	1
OVERVIEW	1
KCNQ CHANNELS.....	3
<i>Discovery of KCNQ, or “M” channels</i>	<i>3</i>
<i>KCNQ channel structural overview and evolutionary origins</i>	<i>6</i>
<i>Knockout studies reveal critical roles of KCNQ2/3 genes</i>	<i>9</i>
<i>Physiological roles of M-channels in different neuron types</i>	<i>11</i>
<i>M-channels in sympathetic neurons.....</i>	<i>11</i>
<i>M-channels in sensory neurons.....</i>	<i>12</i>
<i>M-channel functions in CNS neurons.....</i>	<i>13</i>
<i>Speculated roles of M-channels in neuronal circuits</i>	<i>15</i>
<i>Mechanism of KCNQ channel regulation by PIP₂.....</i>	<i>17</i>
<i>Regulation by CaM/Ca²⁺ and AKAP5/PKC signalling</i>	<i>22</i>
<i>Additional regulatory mechanisms.....</i>	<i>26</i>
<i>Molecular determinants of subunit assembly, heteromerization, and localization</i>	<i>29</i>
<i>Mechanisms of BFNC pathogenesis.....</i>	<i>31</i>
RETIGABINE AND KCNQ CHANNEL PHARMACOLOGY	33
<i>Overview of commonly used AED therapies and their mechanisms</i>	<i>33</i>
<i>The discovery of retigabine and its development as an AED.....</i>	<i>36</i>
<i>Current mechanistic understanding of retigabine action on KCNQ channels.....</i>	<i>37</i>
<i>Scope of thesis investigation</i>	<i>39</i>
Chapter 2: Methods.....	41
MOLECULAR BIOLOGY	41
WESTERN BLOT, ANTIBODIES	42
HARVESTING XENOPUS LAEVIS OOCYTES	44
UNNATURAL AMINO ACID MUTAGENESIS	44
TWO ELECTRODE VOLTAGE CLAMP	45
VOLTAGE CLAMP FLUOROMETRY	45
DATA ANALYSIS	46
CONSTRUCTION OF MOLECULAR MODEL.....	47
Chapter 3: H-bonding with W265 is Essential for Retigabine Effects.....	48
BACKGROUND AND SUMMARY	48
RESULTS.....	49
<i>Retigabine modulation of KCNQ channels through an S5 Trp.....</i>	<i>49</i>
<i>Unnatural amino acid mutagenesis of KCNQ3 channels.....</i>	<i>52</i>
<i>Loss of retigabine effects after removal of W265 H-bonding.....</i>	<i>54</i>
<i>Tuning the strength of the W265-retigabine interaction:</i>	<i>56</i>
<i>Relative contributions of putative drug binding residues:</i>	<i>60</i>
<i>Identification of a likely H-bond acceptor in retigabine:.....</i>	<i>63</i>
DISCUSSION.....	66
Chapter 4: PIP₂ Modulates Functional Coupling and Pharmacology of KCNQ3 Channels.....	71
BACKGROUND AND SUMMARY	71
RESULTS.....	72

<i>Voltage clamp fluorometry of KCNQ3 channels</i>	72
<i>Close coupling of the KCNQ3 voltage sensor and pore</i>	73
<i>PIP₂ influences pore coupling and VSD movement</i>	76
<i>Retigabine protects channels from Ci-VSP mediated rundown</i>	79
<i>Structural basis for PIP₂-mediated VSD:PD coupling</i>	83
<i>The C-terminus is essential for normal pore-VSD coupling</i>	84
<i>Residual PIP₂-independent coupling of retigabine effects</i>	86
DISCUSSION.....	89
Chapter 5: Functional Stoichiometry of Retigabine Binding in KCNQ3 Channels	93
BACKGROUND AND SUMMARY	93
RESULTS.....	93
<i>Biphasic conductance-voltage relationships at intermediate retigabine concentrations</i>	93
<i>Generation of a tetrameric KCNQ3* construct</i>	96
<i>A single sensitive subunit encodes a large retigabine effect:</i>	97
<i>Auxiliary retigabine binding residue mutations produce pronounced biphasic features</i>	100
DISCUSSION.....	101
Chapter 6: General Discussion and Conclusions	104
IMPLICATIONS FOR DRUG DEVELOPMENT	104
Q3*VCF REVEALS IMPORTANT FEATURES OF KCNQ3 CHANNEL BIOPHYSICS	107
MECHANISM OF RETIGABINE INDUCED CHANNEL ACTIVATION.....	111
STOICHIOMETRY OF RETIGABINE EFFECTS	112
LIMITATIONS AND OUTLOOK ON FUTURE EXPERIMENTS	113
SUMMARY.....	117
References	118

List of Tables

Table 2.1: List of Mutagenic Primers.....	43
Table 3.1. Activation gating parameters for unnatural amino acid substitutions of KCNQ3*[W265TAG] channels.....	56
Table 5.1: Values for double-Boltzmann fits of recordings from KCNQ3* in different RTG concentrations	96

List of Figures

Figure 1.1: Defining features of M-channels.....	9
Figure 1.2: Multi-modal regulation of KCNQ2/3 channels.....	25
Figure 3.1: Multiple retigabine molecules modulate KCNQ2 and KCNQ3 channel subunits via an S5 Trp side chain.....	51
Figure 3.2: Nonsense suppression for amino-acid incorporation in KCNQ3* channels	53
Figure 3.3: The position of the Trp 265 indole nitrogen is essential for retigabine sensitivity	55
Figure 3.4: The polarity of the W265 indole nitrogen modulates retigabine sensitivity	59
Figure 3.5: Detailed characterization of secondary retigabine binding residues and alternative binding site orientations	62
Figure 3.6: ML-213 exhibits a stronger electrostatic surface potential and higher potency than retigabine for KCNQ3* activation	63
Figure 3.7: Effects of retigabine analogues correlate with electrostatic surface potential.....	65
Figure 3.8: Diverse structures of KCNQ openers.....	68
Figure 4.1: Cysteine mutagenesis of KCNQ3* S3-S4 linker residues and identification of Q218C as the ideal position for fluorophore labelling	73
Figure 4.2. Characterization of retigabine effects on Q3*VCF fluorescence.....	75
Figure 4.3: PIP ₂ depletion alters Q3*VCF fluorescence	77
Figure 4.4. PIP ₂ depletion produces a voltage independent increase Q3*VCF fluorescence and acceleration of deactivation kinetics	78
Figure 4.5: RTG induced strengthening of channel PIP ₂ interactions relies on C-terminal basic residues ...	81
Figure 4.6: Functional characterization of Q3*VCF charge neutralization mutants	82
Figure 4.7: RTG effects on the VSD are partially mediated by C-terminal residues involved in VSD-PD coupling	84
Figure 4.8. S6-KRRK mutations abolish RTG effects on Q3*VCF fluorescence deactivation, but not activation	86
Figure 4.9. RTG activates the VSD in 'PIP ₂ -less' Q3*VCF [S6-AARK] channels	88
Figure 5.1: A biphasic conductance-voltage relationship emerges at intermediate RTG concentrations.....	95
Figure 5.2: Conductance-voltage relationships for KCNQ3* in different RTG concentrations.....	95
Figure 5.3: Generation of KCNQ3* concatamers with variable stoichiometry of RTG sensitive subunits ..	97
Figure 5.4: A single RTG-sensitive subunit encodes a large RTG effect.....	98
Figure 5.5: Effects of RTG on the activation and deactivation kinetics of KCNQ3* tetramers.....	99
Figure 5.6: Super-shifted RTG-binding site mutants highlight all-or-none shift	100

List of Abbreviations

<u>Amino Acid</u>	<u>3 Letter Code</u>	<u>1 Letter Code</u>
Alanine	Ala	A
Arginine	Arg	R
Asparagine	Asn	N
Aspartate	Asp	D
Cysteine	Cys	C
Glutamate	Glu	E
Glutamine	Gln	Q
Glycine	Gly	G
Histidine	His	H
Isoleucine	Ile	I
Leucine	Leu	L
Lysine	Lys	K
Methionine	Met	M
Phenylalanine	Phe	F
Proline	Pro	P
Serine	Ser	S
Threonine	Thr	T
Tryptophan	Trp	W
Tyrosine	Tyr	Y
Valine	Val	V

AED – anti-epileptic drug
BFNC – benign familial neonatal convulsions
RTG – retigabine
TEA⁺ – tetraethylammonium
PKC – protein kinase C
PKA – protein kinase A
AKAP5 – A-kinase anchoring protein 5
K_v – voltage gated potassium channel
Na_v – voltage gated sodium channel
GABA – gamma-aminobutyric acid
PLC – phospholipase C
Ci-VSP – *ciona intestinalis* voltage sensitive phosphatase
s – seconds
ms – milliseconds
mV – millivolts
μA – microamperes
μM – micromolar
PIP₂ – phosphatidylinositol 4,5-bisphosphate
Ind – indole
VSD – voltage sensing domain
PD – pore domain
DAG – diacylglycerol
s.e.m – standard error of the mean
UAA – unnatural amino acid
VCF – voltage clamp fluorometry
AP – action potential
RMP – resting membrane potential
AIS – axon initial segment
HVA – high voltage activated
VGCC – voltage gated calcium channel

Acknowledgements

I feel extremely fortunate to have met the people that I have worked with throughout my degree. First and foremost, I express my gratitude for the mentorship and friendship of my supervisor, Harley Kurata, whose consideration for the people in his lab and understanding that gaining a genuine interest in something precedes motivation or commitment, went a long way in cultivating the energy that I had for working on my projects. Stephan Pless went out of his way to teach me essential techniques that I applied in my research, and set a really strong example for professionalism in the lab. My committee members, Steven Kehl and David Fedida, pushed me to gain a better understanding of electrophysiology. Our enduring lab tech Runying must be thanked for her unwavering lack of hesitation in helping me with important tasks throughout the years. I have met many wonderful students during this time, who I am proud to call my friends. Victoria, Alice, Caroline and Damayante were great companions both in and outside of the lab, and thanks to Logan and other members of the Fedida lab for joining us for extracurricular activities that made grad school more enjoyable.

Against his wishes, my father never had the opportunity to study science as a young adult due to oppressive regulations which deemed that color blindness made one unsuitable for such pursuits. I have a feeling that being colorblind would not have made my VCF experiments any more difficult. I am aware of my parents' immense efforts in enabling a better life for us, and for that I am eternally grateful. Lastly, I would like to thank Kerry for being extremely patient and understanding through this journey, and being my greatest source of support these past few years.

Dedication

I had the privilege of knowing Karen Li, who was a beloved sister, daughter, and friend to many. In the limited time that I had to get to know her, I realized that she is one of those rare individuals you could describe as having a pure and completely selfless kindness towards others. During the last few years of her life, she fully committed herself towards obtaining her PhD in clinical psychology, and she had a passion for working with children. I am very fortunate to have had the health and support to continue along with my own research endeavors, and will never take that for granted. This is for you, Karen.

Chapter 1: Introduction

OVERVIEW

Epilepsy is a condition of recurring, unprovoked seizures and is one of the most common neurological disorders. Adding complexity to the widespread prevalence of this disease is the fact that there are many types of epilepsy, which vary in their clinical manifestations. Moreover, the causes of these epileptic syndromes are seldom determined, only in rare cases when a single gene is found to underlie a familial disorder. A probable explanation for this observation is that any mechanism that disrupts the proper temporal and spatial regulation of neuronal communication has the potential to cause epileptic activity. When considering the vast complexity of our brains in the context of the number of genetic, epigenetic, and environmental players governing its activity, the possible permutations leading to electrical disorders seem limitless. This notion is supported by a recent study demonstrating a lack of detectable genotypic discrepancy between healthy and epileptic individuals (Klassen *et al.*, 2011), likely underlying some of the challenges involved in devising appropriate therapeutic interventions.

In terms of sheer numbers, the therapeutic toolkit for preventing epileptic seizures is large, with approximately 30 compounds approved for use. However, the diversity in the electrical signaling mechanisms targeted by these drugs is lacking, and this is suggested to be a reason for the continued persistence of drug-resistant epilepsies which account for approximately 30% of epilepsies (Kwan and Brodie, 2000). In a broad sense, the current therapeutic strategy for seizure prevention is to modulate membrane proteins that regulate neuronal excitability. Blockade of voltage-gated sodium and calcium channels and enhancement of GABA signaling are the primary mechanisms utilized by currently prescribed first-line, broad spectrum anti-epileptic drugs (AEDs), such as carbamazepine and sodium valproate.

In 2011, after multiple clinical trials to assess efficacy in patients with drug-resistant partial epilepsy, retigabine became the first voltage-gated potassium (K_v) channel activator approved for human use, and the first AED to operate on K_v channels (Brodie *et al.*, 2010; Porter *et al.*, 2007). In the decade following the discovery that retigabine alters potassium conductance in neurons (Rundfeldt, 1997), studies demonstrated that retigabine specifically activates neuronal KCNQ channels to hyperpolarize neurons and suppress excitability (Main *et al.*, 2000; Rundfeldt and Netzer, 2000; Wickenden *et al.*, 2000). Furthermore, genotyping studies have identified congenital forms of epilepsy and neurological disorders caused by mutations in KCNQ2 and KCNQ3 genes (Lerche *et al.*, 2013), providing a basis for understanding the physiological importance of these channel types. Such knowledge regarding the genetic underpinning of different epilepsies may eventually contribute to the development of more effective strategies for deploying KCNQ channel openers in clinical settings, and necessitates expanding our knowledge of their mechanism(s) of action.

In contrast to the large number of reports investigating effects of retigabine in animal models of disease, relatively few studies have targeted the molecular mechanisms of this drug or its many emerging analogs. Understanding the principles underlying activity and specificity of retigabine towards KCNQ channels may accelerate the development of compounds with enhanced potency, specificity and ultimately, improved therapeutic applications. There is no better indication for the need for such compounds than recent news from GlaxoSmithKline announcing intentions to discontinue retigabine production, due to a lack of commercial success. Unpleasant symptoms caused by off-target effects of retigabine may have contributed to low patient adherence and a decline in its popularity as an adjuvant therapy. Furthermore, its novelty and limited proven

efficacy in a wide range of conditions (compared to other established AEDs), may have prevented it from being adopted into entrenched AED prescription practices.

The general approach taken to investigate retigabine pharmacology in this thesis was to apply a combination of electrophysiology, chemical biology, and fluorometric recording techniques to probe different facets of drug action. This introductory chapter will cover the physiological roles and regulatory mechanisms of KCNQ channels, with a particular emphasis on neuronal KCNQ2/3 channels which are the primary therapeutic target of retigabine. The current knowledge regarding the pharmacology of these channels and the molecular mechanisms of retigabine will be discussed to illuminate the gaps in knowledge that we set out to address in our studies.

KCNQ CHANNELS

Discovery of KCNQ, or “M” channels

As early as 1968, scientists recognized the existence of slow post-synaptic potentials that were elicited in the absence of an increase in membrane conductance (Kobayashi and Libet, 1968). In these early studies, recordings from curarized ganglionic preparations from rabbit and frogs demonstrated the generation of slow EPSPs that were distinct from the well characterized fast EPSPs associated with activation of nicotinic acetylcholine receptors. Weight and Votava showed that the reversal potential of this slow EPSP coincided with that of the after-hyperpolarization and that changing extracellular chloride concentration had no appreciable effect, which lead them to propose that the most plausible mechanistic explanation for slow EPSPs was a decrease in the post-synaptic membrane conductance to potassium (1970).

In 1980, through a set of carefully devised electrophysiological measurements, Brown and Adams showed that in frog sympathetic ganglia, muscarinic stimulation leads to blockade of a K^+

current that is distinct from TEA⁺-sensitive A-type current (Brown and Adams, 1980). In this seminal paper, they revealed some features of this current, which they coined “M-current”, now viewed as hallmarks of neuronal KCNQ channel function: activation at subthreshold potentials, a lack of inactivation, and that muscarinic inhibition leading to diminished current levels (but not altered voltage-dependence). They proposed that M-current is involved in regulating the firing frequency of neurons in a stimulus-dependent and muscarinic receptor regulated fashion, laying the foundations for our current understanding of M-channels.

The gene(s) encoding M-currents were not identified until the late 1990s. In 1996, the K_vLQT1 gene was discovered, named in reference to its role in causing acquired forms of long-QT syndrome (Wang *et al.*, 1996). In today’s nomenclature, K_vLQT1 is referred to as KCNQ1, or K_v7.1, and represents the first identified member of the KCNQ family of voltage-gated potassium channels. KCNQ1 is arguably the most unique member of this ion channel family. Often referred to as the ‘cardiac isoform’, it is the only KCNQ channel expressed in the heart, where it is crucial for cardiomyocyte repolarization. KCNQ1 channels do not form heteromeric ion channel complexes with other KCNQ types, but associate with non-pore forming auxiliary KCNE subunits that regulate channel function (Barhanin *et al.*, 1996; Sanguinetti *et al.*, 1996; Schroeder *et al.*, 2000a). Importantly, KCNQ1 is the only isoform that is insensitive to the action of retigabine (Schenzer *et al.*, 2005), allowing the drug to be devoid of cardiac toxicity. This feature also plays an important role in scientific developments leading to the elucidation of the retigabine binding site, and will be revisited when discussing retigabine pharmacology.

KCNQ2 and KCNQ3 genes were subsequently discovered and classified based on homology to KCNQ1, and accompanied by data revealing that mutations in these genes were present in patients with benign familial neonatal convulsions (BFNC, or BFNS)(Biervert *et al.*,

1998; Charlier *et al.*, 1998; Singh *et al.*, 1998). This condition is characterized by infantile seizures that occur within the first weeks of life, followed by an increased susceptibility to epilepsy during adulthood in otherwise normal individuals. These hallmark symptoms of BFNC highlight the subtle involvement of KCNQ2/3 in the developing brain, and how neuronal plasticity can neutralize the impact of aberrant channel function. There are over 35 mutations in KCNQ2 and KCNQ3 that account for the majority of BFNC cases; interestingly, the majority of these mutations are in KCNQ2, and possible reasons for this will be discussed later.

Similar to the identification of previous KCNQs based on associations to known hereditary disorders, KCNQ4 was later discovered by using KCNQ3 fragments to probe for novel genes implicated in acquired deafness (Kubisch *et al.*, 1999). In this study, KCNQ4 transcripts were found in cochlear and vestibular tissue, consistent with its implication in hearing loss, as well as in the brain at lower levels. Genetic mapping of KCNQ4 resulted in overlap with a DFNA2 locus in chromosome 1, which is linked to a form of autosomal dominant non-syndromic hearing loss (Coucke *et al.*, 2010). Screening of families affected by dominant deafness revealed one particular French family in which all deaf individuals possessed a copy of a missense mutation resulting in a serine residue in place of the first glycine in the K⁺ channel trademark “GYG” consensus sequence. Expression of KCNQ4 channels carrying this mutation in cells imposes a dominant negative phenotype which likely contributes to the gradual loss of hearing in these patients.

Finally, KCNQ5 channels were identified and characterized to complete the family of KCNQ voltage-gated potassium channels that we are familiar with today (Lerche *et al.*, 2000; Schroeder *et al.*, 2000b). Unlike KCNQ1-4, mutations in KCNQ5 have not yet been identified in patients with disorders of excitability, despite several lines of evidence suggesting that it may fulfil similar physiological functions. For example, KCNQ5 transcripts are found in most brain regions

(Schroeder *et al.*, 2000b), and electrophysiology experiments indicate that KCNQ5 channels assemble with KCNQ3 to produce highly expressing channels with functional characteristics similar to classical KCNQ2/3 “M-channels” (Lerche *et al.*, 2000). It is a possibility that the expression of KCNQ5 in the brain is redundant beyond more subtle functions that it may provide that are yet to be understood, and that its more significant functions may lie in vascular and other smooth muscle tissues, where it is also detected in the absence of KCNQ2 or KCNQ3 (Jepps *et al.*, 2009, 2009; Ng *et al.*, 2011).

With respect to the “M-Current” identified and characterized by Brown and Adams (1980), it is now accepted that the principal contributors to this K⁺ current are heteromeric ion channels consisting of KNCQ2 and KCNQ3. Several lines of evidence suggests this to be the case: the pharmacological sensitivity of M-current in SCG neurons to channel blockers matches the sensitivity of KCNQ2/3 heteromers expressed in *Xenopus laevis* oocytes, but not KCNQ2 homomers (Wang *et al.*, 1998). KCNQ3 subunits alone are unable to form functional channels, but its expression in neurons coincides with the expression of KCNQ2, and it has been shown that either of the two subunits can be co-immunoprecipitated along with the complementary subunit (Cooper *et al.*, 2000; Schroeder *et al.*, 1998). Numerous studies, including experiments done in our lab, demonstrate that co-expression of KCNQ2 and KCNQ3 increases currents by an order of magnitude relative to expression of KCNQ2 alone. Based on these findings, heteromeric channels consisting of KCNQ2 and KCNQ3 are expected to give rise to the majority of M-current in the nervous system.

KCNQ channel structural overview and evolutionary origins

It is interesting to note that the KCNQ family was the last major family of voltage-gated ion channels to be discovered (Cooper, 2011). What distinguishes KCNQ channels from other

known voltage-gated K⁺ channels and what similarities do they share? In terms of overall architecture, KCNQ channels possess six transmembrane domains that contain the voltage-sensing (S1-S4) and pore forming (S5-S6) domains (Fig. 1.1), with close homology to the transmembrane segments of other K_v channels. Beyond these similarities, there is considerable divergence in the sequences of the C- and N- termini, which account for some of the unique properties of KCNQ channels. Unlike K_v1 - K_v4 channels, KCNQ channels lack N-terminal T1 tetramerization domains, which enable assembly and heteromerization within K_v1-4 channel subfamilies (Xu *et al.*, 1995). Instead, KCNQ channels possess a C-terminal stretch of ~100 amino acids referred to as the “A-domain” which contains residues that enable the formation of coiled-coil structures within homomeric and heteromeric channels of specific KCNQ composition (Schwake *et al.*, 2003, 2006). Chimeras of KCNQ1 channels possessing the C-termini of KCNQ2 and KCNQ3 channels can form functional channels with WT KCNQ2/KCNQ3 subunits, revealing the importance of this domain in subunit assembly (Schwake *et al.*, 2003). Furthermore, the large C-terminus of KCNQ channels (300-500 residues long) encodes regions that enable channel interactions with AKAP79/150, PKC, calmodulin, PIP₂, and ankyrin-G (in KCNQ2/3) (Haitin and Attali, 2008). These interactions are vital for proper channel function and will be discussed later in detail.

In an effort to understand the possible physiological consequences of the emergence of unique KCNQ-channel features, Pan *et al.* (2006) investigated the evolutionary origins of KCNQ channels by comparing KCNQ sequences obtained from various organisms. Specifically, they were curious with regards to the origin of the ankyrin-G binding domain present in KCNQ2/3 subunits, which is homologous to a motif in the intracellular loop between domains II and III in Na_v channels (Fig. 1.1). While this domain appears to have emerged in Na_v channels before the appearance of chordates (spinal organisms), KCNQ channels acquired this property much later

through convergent evolution. In models of early vertebrates, such as the sea lamprey, KCNQ1, KCNQ4 and KCNQ5 orthologues exist but not KCNQ2/3, and neurons are also unmyelinated; it appears that a KCNQ4 gene duplication event lead to the emergence of a new KCNQ gene which evolved a C-terminal domain that interacts with ankyrin-G, followed by another gene duplication event resulting in KCNQ2 and KCNQ3 in a common ancestor of modern jawed vertebrates (Cooper, 2011). Indeed, KCNQ2/3 is only present in jawed vertebrates and coincides with the emergence of myelinated axons and saltatory conduction. The excitozone hypothesis postulates that the emergence of ankyrin-dependent axonal clustering of Na_v channels was critical for the development of larger, more complex brains in chordates (Cooper, 2011). Similarly, it is presumable based on evolutionary evidence that the ability to target KCNQ channels to critical regions of neurons through ankyrin-G interactions was important for the evolution of novel neuronal mechanisms in extant jawed vertebrates, including humans.

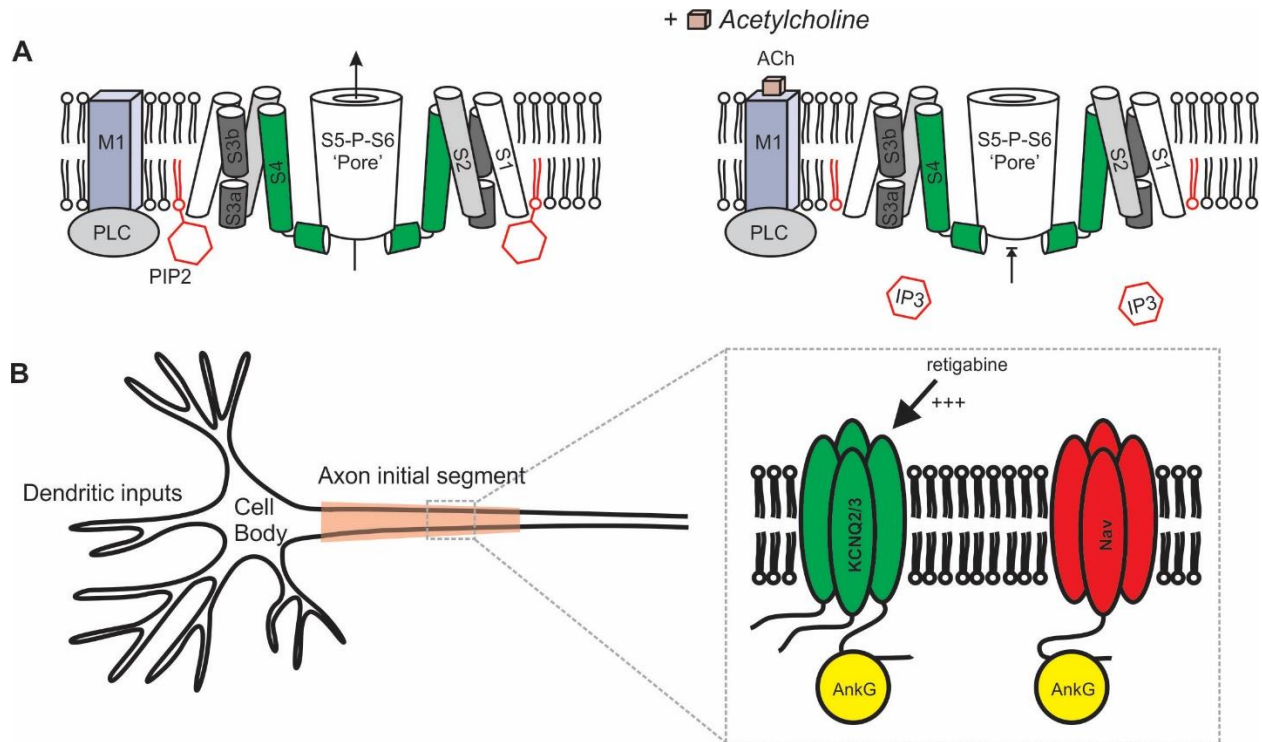


Figure 1.1: Defining features of M-channels. (A) KCNQ2/3 subunits assemble to form a transmembrane structure resembling canonical K_v channels consisting of voltage sensing (S1-S4) and pore forming (S5-S6) domains. Sensitivity to regulation by various endogenous signalling pathways, such as G_q -protein coupled M1 muscarinic receptors, and their positioning at axon initial segments (B) and nodes of Ranviers, enable these channels to play a unique role in the control of neuronal excitability.

Knockout studies reveal critical roles of KCNQ2/3 genes

Several knock-out and knock-in studies have highlighted the broad importance of KCNQ2/3 channels, adding sophistication to the early understanding that their dysfunction can cause neonatal epilepsy (Peters *et al.*, 2005; Soh *et al.*, 2014; Watanabe *et al.*, 2000). From these studies, coupled with our understanding that only a moderate loss of M-current activity can lead to BFNC (Schroeder *et al.*, 1998), it can be inferred that highly disruptive mutations in KCNQ2 genes are likely to be lethal or result in rare, but significant forms of neurological defect. Indeed, the first KCNQ knock-out study by Watanabe *et al.* (2000) showed that homozygous knockout of KCNQ2 genes in mice results in immediate post-natal lethality. Surprisingly, complete knockout of KCNQ3 produces viable mice, but the neurological characteristics of these mice have not been

analyzed in detail (Tzingounis and Nicoll, 2008). In a study employing a more subtle approach to disturb M-current expression in mice using inducible expression of a dominant negative KCNQ2 allele, Peters *et al.* (2005) showed that a substantial loss of M-current causes epilepsy, behavioral hyperactivity, and morphological changes in the hippocampus causing impaired learning. By inhibiting expression of the dominant-negative KCNQ2[G279S] allele during a short post-natal time period, they were able to demonstrate that many of these deficits can be attributed to aberrant hippocampal development that occur in early stages of life, a finding that is consistent with the fact that mild loss of KCNQ function in humans typically manifests as infantile seizures.

More recently, Soh *et al.* (2014) generated mice in which KCNQ2 and KCNQ3 genes were selectively knocked out in pyramidal neurons using the Cre/loxP approach, and showed that KCNQ2 but not KCNQ3 knockdown in these cells caused death in nearly all mice by the third week of life. Electrophysiology recordings from pyramidal CA1 hippocampal neurons demonstrated that KCNQ2 knockdown had a far greater impact on reducing M-current expression, resulting in a dramatic rise in excitability that is not observed after KCNQ3 knockdown. Loss of KCNQ2 expression in these neurons caused a reduction in not only KCNQ3 levels but also KCNQ5, which is surprising given other evidence demonstrating that KCNQ2 is not likely to co-assemble with KCNQ5 (Schroeder *et al.*, 2000b). This suggests that the loss of KCNQ2 and its impact on neuronal excitability may alter the expression of related ion channel genes, but how this may occur is unclear. The results of this study however, suggest that while KCNQ3 genes are important (and it is likely that a more careful examination of KCNQ3 KO mice will reveal more subtle neurological defects), KCNQ2 genes are indispensable for proper control of neuronal excitability, and required for life.

Physiological roles of M-channels in different neuron types

The presence of a unique C-terminal ankyrin-G binding domain in KCNQ2-3 channels hints at the physiological roles these proteins have adapted to serve in jawed vertebrates. This domain positions KCNQ2/3 channels at specific neuronal locations, specifically the axon initial segment (AID) and Nodes of Ranvier (Pan *et al.*, 2006), where they are predicted to play important roles in neuronal excitability. However, unlike KCNQ1 and KCNQ4 subunits which are predominantly expressed in the heart and ear respectively, KCNQ2/3 subunits display a broad pattern of expression throughout the CNS and PNS, with transcripts identified in sympathetic neurons, sensory neurons, and extensively throughout the brain (Brown and Passmore, 2009; Wang *et al.*, 1998). The expression of M-channels in these neurons of diverse function is likely to exert similar, overlapping effects on their electrical properties; however, differences in how these channels contribute to neuronal function are likely to arise depending on the specific cellular milieu of other ion channel types, regulatory receptors, and second messengers. The emergence of retigabine and selective KCNQ blockers such as XE-991 has enabled further dissection of neuronal currents and have aided in elucidating some specific functions of M-channels.

M-channels in sympathetic neurons

In sympathetic neurons, where M-currents were first identified based on their sensitivity to muscarinic agonists (Brown and Adams, 1980), it is well established that the presence of KCNQ2/3 channels regulate the firing properties of neurons in response to depolarizing stimuli, with muscarinic inhibition of these channels causing increased neuronal excitability and a shift from phasic to tonic firing patterns in response to excitatory stimuli (Brown and Passmore, 2009). Analysis of sympathetic neurons isolated from different ganglia show that the baseline firing properties of these neurons in terms of displaying phasic versus tonic firing in response to a

depolarizing stimuli can be accounted for by differential expression levels of M-current (Wang and McKinnon, 1995). Basic KCNQ2/3 channel properties such as their slow activation and deactivation, lack of inactivation, and activation at sub-threshold potentials enable a clear conception of how the recruitment of these channels in response to neuronal excitation would allow for this; indeed, computational modelling studies show that recruitment of outward M-currents upon neuronal depolarization raises the subsequent threshold for the neuronal firing, explaining the phasic adaptations displayed in neurons with sufficient M-current density (Wang and McKinnon, 1995; Zaika *et al.*, 2006).

The modulation of M-channels in sympathetic neurons is not only limited to cholinergic signaling pathways, but to other endogenous receptor/ligand systems that are coupled through G_q signaling pathways. For example, Zaika *et al.* (2006) showed that application of angiotensin II to cultured superior cervical ganglion neurons results in neuronal depolarization, increased AP firing and reduced spike frequency; these effects were antagonized by PLC inhibition and upregulation of PIP₂, demonstrating a mechanism of M-channel inhibition very similar to M1 receptor activation. Additionally, bradykinin (Cruzblanca *et al.*, 1998) as well as ATP (Akasu *et al.*, 1983) have been shown to enhance sympathetic neuron excitability through the inhibition of M-currents. These examples highlight the diversity in the pathways that can regulate M-currents through a convergent mechanism of PIP₂ hydrolysis.

M-channels in sensory neurons

Several studies have implicated M-currents in regulating sensory signal transduction. Recordings from dissociated neurons from a dorsal root ganglion (DRG) preparation revealed the presence of M-currents sensitive to blockade by XE-991 and potentiation by retigabine in various sensory neuron types (Passmore *et al.*, 2003a). In this study, retigabine attenuated the excitatory

response of the dorsal horn in response to the stimulation of A δ and C-type fibers, afferents responsible for the sensation of noxious stimuli. Consistent with the expression of M-channels in DRG sensory neurons is the efficacy of retigabine in attenuating pain responses evoked peripherally through various methods (Du *et al.*, 2014; Hayashi *et al.*, 2014; Passmore *et al.*, 2003b). Du *et al.* (2014) demonstrated that M-currents make a significant contribution to the resting potential of DRG cell bodies by using selective blockers and channel openers, and proposed that the regulation of M-currents at the t-junction of sensory neurons may play a role in regulating the threshold of axon potential propagation from distal axons to the spine. Interestingly, another study demonstrated that injection of retigabine directly into the paw of rats attenuates pain induced by formalin (Hayashi *et al.*, 2014), suggesting an involvement of M-channels throughout the length of the sensory neuraxis. In these studies, retigabine induced M-current upregulation silenced neurons to attenuate pain responses, but they did not demonstrate that M-currents are involved in normal sensory processing. This issue may be addressed by the demonstration that XE-991 application enhances the firing of A δ afferent fibers in response to thermal or mechanical stimuli in skin (Brown and Passmore, 2009), and enhances baroreceptor discharges in response to increasing intra-aortic pressure (Wladyka *et al.*, 2008). Collectively, these studies demonstrate that KCNQ2/3 channels are involved in the physiology of sensation, and suggest that targeting these channels for anti-pain therapy may be viable.

M-channel functions in CNS neurons

Much of what is known regarding the role of KCNQ channels in the brain has been determined based on electrophysiology experiments from rat hippocampus *in vitro*. From these experiments, the contribution of M-current to the firing properties of neurons has been characterized, and these mechanisms are generally assumed to be at play where KCNQ channels

are expressed. In the brain, KCNQ2/3 subunits appear to be the primary constituents of M-currents; however, there is evidence that KCNQ5 channels also contribute as homotetramers (Huang and Trussell, 2011) or in complex with KCNQ3 (Shah *et al.*, 2002). There are three ‘classic’ examples of how M-channels control neuronal firing patterns in hippocampal neurons (Brown and Passmore, 2009); they promote a decrease in firing frequency in response to a depolarizing stimulus (tonic to phasic conversion), they prevent burst firing in response to a single short depolarizing stimulus (by inhibiting the after-depolarization), and their activation in the sub-threshold range contributes to the RMP, and threshold for AP firing. Interestingly, it was shown that disrupting the targeting of KCNQ2/3 channels to the AIS by injecting a peptide that competes with channel binding to ankyrin-G results in enhanced neuronal excitability that cannot be explained by M-current inhibition alone (Shah *et al.*, 2008), demonstrating that the relative AIS-somatic distribution of these channels also governs neuronal excitability.

In CNS and PNS neurons, KCNQ mediated currents contribute to the apamin-insensitive medium afterhyperpolarizations following action potentials (mAHP), and it is the presence or absence of this repolarizing influence that largely influences the firing processes described above. The relative contributions of M-currents to the mAHP of neurons is cell-type specific; for example, in CA1 hippocampal pyramidal neurons there is strong evidence that they are the primary constituent of I(mAHP)(Gu *et al.*, 2005; Yue and Yaari, 2004), whereas SK channels have been demonstrated to predominantly mediate mAHPs in other neuron types, such as in neocortical pyramidal neurons (Abel *et al.*, 2004). Furthermore, the relative contribution of KCNQ2, 3, and even 5 subunits to these currents is cell type dependent(Tzingounis *et al.*, 2010), and their levels are likely to be regulated not only by cell-specific transcription factors, but by reciprocal feedback

mechanisms, as selective knockdown of KCNQ2 or KCNQ3 subunits alone did not appreciably inhibit I(mAHP) in hippocampal pyramidal neurons (Tzingounis and Nicoll, 2008).

It is also worth noting that in addition to the influence of KCNQ channel expression on how neurons respond to stimuli, the basic oscillatory firing properties of neurons *in vivo* is also affected. In mice expressing dominant negative KCNQ2 alleles, the resonance frequency of neurons in the hippocampus is shifted towards lower frequencies (Peters *et al.*, 2005). As KCNQ channel expression is found to be concentrated at sites that control neuronal rhythm and synchronization (Cooper *et al.*, 2001), it is reasonable to hypothesize that the distinct voltage and kinetic properties of these channels are utilized by neurons to conduct complex neuronal processes.

Finally, there is emerging evidence that KCNQ channels also contribute to the slow afterhyperpolarization (sAHP)(Kim *et al.*, 2016; Tzingounis and Nicoll, 2008), which is a calcium induced current whose identity is still under debate. An enticing mechanism proposed by these studies is that calcium influx following AP increases membrane PIP₂ levels through the action of hippocalcin, and subsequently, increased PIP₂ levels shift the voltage-dependence of KCNQ2/3 channels so that they can operate at the more hyperpolarized voltages at which sAHPs take place. If this mechanism holds true, then this is an amazing example of how the multi-modal regulation of KCNQ channels by voltage and PIP₂ can produce temporally distinct but related effects on AP waveforms and neuronal excitability (mediating both mAHP and sAHP after the same depolarizing stimulus).

Speculated roles of M-channels in neuronal circuits

Given knowledge of their widespread expression in the brain and in many different neuron types, the impact of cholinergic neurons on excitability *in vivo*, indirectly through the modulation of KCNQ channels, is likely to play an important role in certain processes. For example, it is

known that increased activity of cholinergic neurons from the forebrain can increase the activity of various cortical circuits; for example, parallel stimulation of cholinergic afferents enhances the sensitivity of direction-sensing neurons of the visual cortex (Delmas and Brown, 2005). Such increases in activity may, in part, be due to the enhanced neuronal excitability following muscarinic receptor activation, and downregulation of M-currents. Alternatively, degradation of the cholinergic neurons, such as in Alzheimer's disease, may lead to cognitive decline due to downstream M-channel-mediated neuronal silencing (Delmas and Brown, 2005). While these physiological processes are likely to be true to a certain extent, there are few studies that have investigated specific roles for KCNQ channels in neuronal circuits *in vivo*.

An example is the examination of the impact of KCNQ channel block in the retrotrapezoid (RTZ) nucleus of rat brain (Hawryluk *et al.*, 2012), a region that is responsible for regulating breathing in response to CO₂ levels. In this study, the authors demonstrate that administering XE-991 into the RTZ nucleus of live rats causes an increase in breathing that is reminiscent of what is observed upon administration of serotonin in this region (Mulkey *et al.*, 2007). Serotonin release from raphe nuclei that innervate this region is thought to regulate breathing in addition to CO₂/pH dependent chemo-sensation. The authors found that KCNQ channel block in the RTZ nucleus blunts its response to serotonin, resulting in reduced serotonin induced phrenic nerve discharge and breathing activity. Based on these findings it is hypothesized that post-synaptic activation of serotonin receptors causes a G_q mediated PIP₂ depletion and subsequent KCNQ channel closure and increased RTZ neuron activity.

Another study revealed the involvement of KCNQ channels in signaling processes regulating motor function in the substantia nigra (Shi *et al.*, 2013). Specifically, it was found that the activation of dopaminergic neurons in this region by the peptide hormone ghrelin, can be

antagonized by KCNQ channel block with XE-991. Inhibition of the PLC-PKC pathway induced by activation of the ghrelin receptor GHS-R1a attenuated the ghrelin response, suggesting that ghrelin produces an inhibition of KCNQ channels through PLC-PKC that leads to neuronal excitation. Interestingly, PKC inhibition alone leads to a complete inhibition of ghrelin effects suggesting that it is phosphorylation, rather than PIP₂ depletion, which leads to KCNQ channel inhibition. In a model of Parkinson's disease where haloperidol induces symptoms of motor impairment, administration of either ghrelin or XE-991 into the substantia nigra provided the same therapeutic effects, suggesting that these mechanisms play a role in the physiology of motor control.

These examples highlight only a few of likely many receptor-mediated pathways that influence KCNQ channel function in order to regulate neuronal excitability to produce specific physiological functions. Numerous studies have been conducted to elucidate the molecular mechanisms of how activation of these pathways lead to functional effects on the ion channel protein. In the next sections, these mechanisms will be discussed.

Mechanism of KCNQ channel regulation by PIP₂

After the identification of KCNQ channels as the muscarine-sensitive K⁺ current, the elucidation of mechanisms involved in receptor mediated channel closure remained elusive for some time. First, the accumulation of evidence demonstrating that M-currents are impacted by receptors that are coupled to the pertussis toxin-insensitive G_q class of G-proteins (Haley *et al.*, 1998; Pfaffinger *et al.*, 1988), suggested that G_q mediated activation of PLC is involved this mechanism. PLC depletes PIP₂ and releases the diffusible second messengers IP₃ and DAG; therefore, subsequent research investigated the role of these messengers in muscarinic-receptor coupled KCNQ current rundown (Beech *et al.*, 1991; Ríó *et al.*, 1999). The general conclusion from these studies was that these messengers are not necessary for coupling muscarinic receptor

activation to KCNQ channel inhibition, leaving the possibility that PIP₂ depletion itself, or direct interactions of these channels with G protein subunits, may be responsible. The emergence of inward rectifying K⁺ channels being gated by PIP₂ and Gβγ subunits (Huang *et al.*, 1998; Shyng and Nichols, 1998), made it seem plausible that similar mechanisms might be involved in the gating of M-channels.

Later experiments showed that recovery of M-currents from muscarinic inhibition can be attenuated by blocking the re-synthesis of PIP₂ by applying nonhydrolyzable ATP analogs or blocking the activity of PI 4- kinases, and that PIP₂ itself can activate these channels (Suh and Hille, 2002; Zhang *et al.*, 2003), providing strong evidence that PIP₂ is indeed the gating modifier coupling muscarinic receptor activation to channel closure. However, these studies did not completely rule out the possibility that PKC activation or a rise in Ca²⁺ was still playing a role. To rule out the contribution of these factors, the Hille lab (Suh *et al.*, 2006) applied a rapamycin-induced enzyme translocation system to rapidly alter PIP₂ levels without affecting intracellular [Ca²⁺] or other second messengers, and demonstrated that PIP₂ depletion itself is sufficient to gate M-channels. Since this study, the emergence of voltage-sensitive phosphatases as a means to deplete PIP₂ with voltage has become an important tool for studying interactions of KCNQ channels with PIP₂. In a study analyzing the kinetics of PIP₂ metabolism and regulation of KCNQ2/3, it was concluded that the mean residence time of PIP₂ with a channel subunit is <10ms and does not limit the rate of current rundown produced by VSP or PLC, which deplete PIP₂ via hydrolysis of the 5' phosphate or by removal of the IP₃ head group, respectively (Falkenburger *et al.*, 2010).

With the establishment that PIP₂ is a critical determinant of KCNQ channel function, numerous studies have investigated how PIP₂ is involved in molecular mechanisms of channel

gating. Despite earlier discussions on the determination of PIP₂-dependent gating of neuronal KCNQs, it is worth mentioning that the importance of PIP₂ in gating KCNQ1 channels also emerged in parallel (Loussouarn *et al.*, 2003; Zaydman and Cui, 2014; Zaydman *et al.*, 2013). In particular, studies of KCNQ1 channel interactions with PIP₂ have been important in revealing the potential aspects of channel gating that may be affected, providing a template for investigation of differences in PIP₂ modulation of other KCNQ channel isoforms.

The general consensus on the effect of PIP₂ on KCNQs is that it is necessary for opening of the gated pore in these channels. The rundown of inside-out patch recordings that is reversible or delayed with exogenous PIP₂ (Loussouarn *et al.*, 2003; Zhang *et al.*, 2003), as well as demonstration that KCNQ2-5 single channel conductances are not impacted by PIP₂ while open probability approaches zero in its absence (Li *et al.*, 2005), suggest that PIP₂ has a role in stabilizing conformations that are necessary for pore opening. While KCNQ channels are voltage-gated, the impact of PIP₂ on the voltage-dependent gating appears to vary depending on KCNQ isoform. Loussouarn *et al.* (2003) show that PIP₂ can shift the voltage-dependent activation of KCNQ1+KCNE1 channels by ~12 mV in the hyperpolarizing direction, but there is little evidence that PIP₂ levels affect the voltage-dependent gating of KCNQ2/3 subunits (Zaydman and Cui, 2014). It is safe to say that while PIP₂ may impact channel voltage sensing, it is not the primary means of channel modulation. Utilizing the voltage clamp fluorometry technique to study bi-directional effects of PIP₂ on the voltage-sensing domain and pore in KCNQ1 channels, Zaydman *et al.* (2013) provide a quantitative model in which PIP₂ allosterically couples the voltage-sensing domain with the pore gate: in the absence of PIP₂ the active VSD is no longer able to influence pore opening, and *vice versa*.

What are the structural determinants of PIP₂ binding and regulation of KCNQ channels? The positioning of negatively charged phosphate groups of PIP₂ in the inner membrane, as well as the fact that the cytosolic domains (S2-S3 linker, S4-S5 linker, C-terminus) of all KCNQ channels are rich with basic residues, many of which are highly conserved, suggest that electrostatic interactions between PIP₂ and these residues may be essential for channel opening. Crystal structures of the PIP₂ binding in inwardly rectifying Kir2.2 and GIRK channels (Hansen *et al.*, 2011; Whorton and MacKinnon, 2011) clearly reveal how such interactions may stabilize conformations leading to the opening of homologous gates in KCNQ channels.

With this notion, several groups have performed experiments using site-directed mutagenesis and chimeric approaches to elucidate how KCNQ channels might interact with PIP₂ (Hernandez *et al.*, 2008; Zaydman *et al.*, 2013; Zhang *et al.*, 2003, 2013; Zhou *et al.*, 2013). The general conclusion that can be drawn from these studies is that there is a distribution of basic residues throughout the cytosolic domains in these channels which are involved in enabling channel-PIP₂ interactions, as well as facilitating the coupling of the VSD and PD. In particular, charges located in the S2-S3 linker, S4-S5 helix/linker region as well as at the proximal C-terminus appear to be critical as singular charge neutralizations at many of these sites results in a significant loss of current expression and PIP₂ affinity (Zaydman *et al.*, 2013; Zhang *et al.*, 2013; Zhou *et al.*, 2013). In KCNQ1, Zaydman *et al.* (2013) identified eight residues in this region that lead to near complete loss of pore function, but a comprehensive scan in KCNQ2/3 has not yet been performed.

In KCNQ2/3 subunits, the region separating the A-B helices in the more distal C-terminus have been implicated in facilitating channel-PIP₂ interactions as neutralization of basic residues here also leads to reduced PIP₂ affinity and channel function (Hernandez *et al.*, 2008). However, combined charge neutralizations in this region have a weaker effect on channel function than the

singular mutations mentioned above, and a more recent study (Aivar *et al.*, 2012) demonstrates that removal of this entire region in KCNQ2 still results in functional channels, albeit with a reduced open probability. Taken together, it seems likely that the primary PIP₂ interaction residues that determine pore opening and coupling lie at the VSD-PD interface defined by the cytosolic regions of the VSD and the proximal C-terminus, and that charged residues in the distal C-terminus may be involved in minor interactions with PIP₂, or more likely, facilitate channel functioning by other binding partners that exert effects via C-terminal interactions.

There is also a wide range of apparent PIP₂ affinity among the different KCNQ subunits. KCNQ3 subunits display di-C8-PIP₂ sensitivity that is an order of magnitude higher than KCNQ2 or KCNQ4 subunits (Li *et al.*, 2005; Telezhkin *et al.*, 2012a). Interestingly, application of PIP₂ to excised patches expressing KCNQ2/3 heteromeric channels clearly shows a biphasic increase in current, which can be explained by channel opening in response to PIP₂ interactions with KCNQ3 subunits at lower concentrations, followed by lower affinity interactions with KCNQ2 enabling maximal channel activation by PIP₂ (Telezhkin *et al.*, 2012a). Single channel analyses of KCNQ2 vs KCNQ3 homomeric channels reveal that the native on-cell open probability is much greater in KCNQ3 vs KCNQ2 (0.9 vs 0.11, respectively)(Li *et al.*, 2004), and application of PIP₂ upon patch excision causes a marked increase of open probability in KCNQ2(Li *et al.*, 2005); however, open probability does not reach unity at saturating levels of PIP₂, suggesting that in addition to differing PIP₂ affinities, the PIP₂-dependence of pore coupling to voltage-dependent activation also differs between KCNQ subtypes. These results are also quite thought provoking, suggesting the hypothesis that variable expression of KCNQ subtypes in different neurons (for example the selective expression of KCNQ5 homomers in CA3 vs CA1 hippocampal neurons(Tzingounis *et*

al., 2010)) may be a method of regulating the impact of PIP₂ on M-currents, thereby fine tuning the effects of receptor mediated excitation.

Finally, another study performed in the Brown lab (Telezhkin *et al.*, 2012b) investigated the structural determinants of PIP₂ that are important for its stabilizing effects on the channels, by analyzing the ability of lipids with varying lipid tail and headgroup composition to open KCNQ2/3 channels in excised patches. This study demonstrates that at a minimum, a lipid tail anchor and one negatively charged phosphate in the headgroup is required for channel activation. A monophosphate presented by a sphingosine or fingolimod lipid headgroup was less effective than PI(4)P. Furthermore, PI(4)P is less potent than PI(4,5)P₂, which is equally potent to PI(3,4,5)P₃. This study supports the notion that PIP₂ is the primarily lipid regulator of these channels, and that the KCNQ channel architecture has evolved to detect and respond to PIP₂ in a manner that is sensitive, but only enough to operate within the range of typical endogenous levels of PIP₂ to enable dynamic regulation.

Regulation by CaM/Ca²⁺ and AKAP5/PKC signalling

An early indication that M-channels can be modulated by cellular processes other than direct hydrolysis of PIP₂ was the observation that bradykinin-induced inhibition of KCNQ2/3 currents can be inhibited by IP₃ receptor block, internal calcium buffering, or depletion of internal calcium stores (Cruzblanca *et al.*, 1998). In 2002, multiple groups released their findings that the C-terminal region of KCNQ2 interacts with calmodulin (CaM) and that two domains that resemble IQ and 1-5-10 CaM binding motifs (now often referred to as helix A and B) are essential for this interaction (Wen and Levitan, 2002; Yus-Nájera *et al.*, 2002)(Fig. 1.2). Furthermore, CaM binding appeared to be independent of Ca²⁺ binding as both WT CaM and Ca²⁺-insensitive CaM₁₂₃₄ interacted equally well (Wen and Levitan, 2002). In this study, co-expression of a CaM binding

peptide inhibited the expression of KCNQ2/3 currents, suggesting that channel interactions with apoCaM are important for channel function (Wen and Levitan, 2002).

Subsequently, it was demonstrated that overexpressing CaM, but not CaM₁₂₃₄, confers profound Ca²⁺ sensitivity to KCNQ2/3 channels expressed in CHO cells (Gamper and Shapiro, 2003). Under these conditions, a rise in intracellular Ca²⁺ fully abolishes KCNQ2/3 currents, suggesting that under normal conditions, there may not be sufficient CaM to interact with overexpressed channel protein to confer Ca²⁺ sensitivity. Alternatively, overexpression of CaM may cause Ca²⁺-bound CaM to predominantly interact with KCNQ2/3 channels and cause channel inhibition. In this study, expression of CaM₁₂₃₄ in SCG neurons prevented the afore-mentioned bradykinin receptor mediated inhibition of neurons, but not muscarinic effects, supporting the hypothesis that bradykinin-induced inhibition results from the PLC-IP₃- Ca²⁺ release pathway.

Why does bradykinin receptor activation, but not muscarinic stimulation operate through this pathway? Delmas and Brown (2005) speculate that it may have to do with the coupled localization of internal IP₃ receptors (and calcium stores) to bradykinin receptors on the cell surface producing a localized rise in Ca²⁺ concentration that is sufficient to modulate KCNQ channels through CaM. Bradykinin-induced rise in intracellular Ca²⁺ has been shown to promote PIP₂ resynthesis through the action of neuronal Ca²⁺-sensor-1 (Gamper *et al.*, 2004), thereby preventing PIP₂ depletion from being the primary mechanism of channel inhibition.

To add to the complexity of the mechanisms regulating receptor mediated M-channel modulation, around the same time, the involvement of AKAP5 (also referred to as AKAP79/150) mediated PKC action on KCNQ channels also emerged (Hoshi *et al.*, 2003). AKAP5 is a scaffold that anchors PKC and KCNQ in close proximity such that muscarinic activation results in phosphorylation of the C-terminus through the PLC-DAG-PKC pathway, and channel inhibition.

This inhibition is likely produced indirectly by inhibiting channel-PIP₂ interactions and making channels more sensitive to PIP₂ depletion, as over-expression of AKAP5 sensitizes KCNQ2-5 channels to muscarinic inhibition (Bal *et al.*, 2010).

Interestingly, the PKC phosphorylation residues identified overlap with CaM-binding in helix B, suggesting an additional mechanism for PKC inhibition of channel-PIP₂ interactions, by displacing CaM or altering channel-CaM interactions. In a recent study it was shown that indeed, PKC phosphorylation, or the S541D ‘pseudo-phosphorylation’ mutation, inhibits channel interactions with CaM (Kosenko *et al.*, 2012), while producing an increased sensitivity to muscarinic inhibition of KNCQ2 currents.

These works investigating the effects of PIP₂, CaM, Ca²⁺, and AKAP5/PKC on receptor mediated inhibition can be integrated to imagine an orchestrated multi-step mechanism of receptor mediated M-current inhibition. Under normal resting conditions, normal KCNQ channel function is enabled in part by its association with apoCaM. Numerous studies have demonstrated that CaM is required for efficient trafficking of KCNQ2/3 (Alaimo *et al.*, 2009; Cavaretta *et al.*, 2014; Devaux *et al.*, 2004; Etxeberria *et al.*, 2008), supporting the notion that CaM binding stabilizes channel assembly and expression. Upon muscarinic receptor activation, PLC activation depletes PIP₂, while simultaneous activation of PKC through DAG disrupts channel-CaM interactions, weakening channel-PIP₂ interactions to magnify the effect of PIP₂ depletion. Essentially, the AKAP/PKC pathway synergizes with the PIP₂ depleting effects of PLC. Alternatively, activation of receptors such as bradykinin can produce channel inhibition in a manner that is independent of PIP₂ and AKAP5/PKC, but dependent on Ca²⁺ and CaM possibly for reasons previously discussed. What is quite fascinating from all these studies is the likelihood that CaM plays a dual role in both

enabling and disabling channel function depending on which receptor-mediated systems are at play.

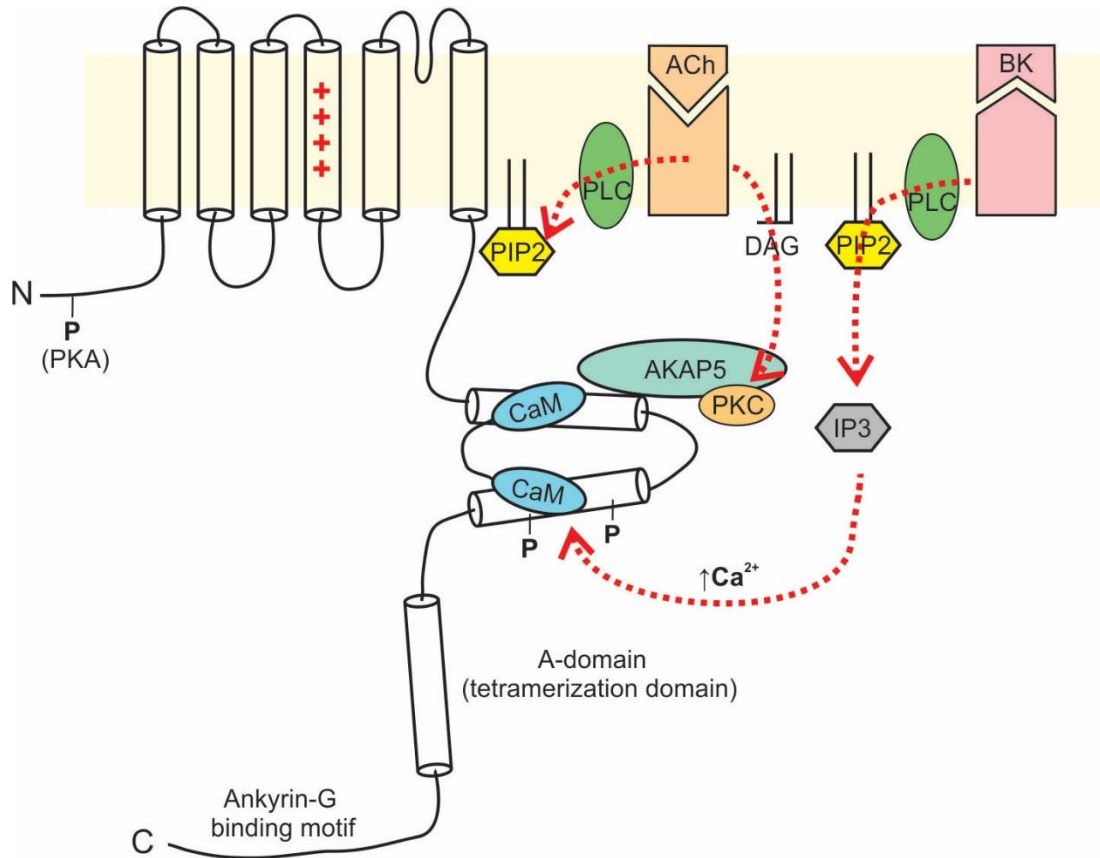


Figure 1.2: Multi-modal regulation of KCNQ2/3 channels. Highlighted in red are the pathways through which channel function can be regulated, such as through changes in membrane voltage (sensed by S4 Arg residues), PLC mediated PIP₂ depletion, activation of AKAP5/PKC mediated C-terminal phosphorylation, and CaM dependent regulation by Ca²⁺ through bradykinin receptor mediated signalling.

Additional regulatory mechanisms

KCNQ channel interactions with PIP₂ have emerged as a central convergence point for a majority of the regulatory mechanisms characterized thus far, but there are a few more accessory binding partners for KCNQ channels that have been identified, and it seems plausible that many more will emerge in future studies. Such proteins include Syntaxin 1A (Etzioni *et al.*, 2011; Regev *et al.*, 2009), the sodium channel auxiliary subunit Nav β 1 (Nguyen *et al.*, 2012), SUMO proteins (Qi *et al.*, 2014), and the β secretase BACE 1 (Hessler *et al.*, 2015).

Syntaxin 1A is a synaptic membrane protein that is involved in the SNARE complex and neurotransmitter release. The demonstration that KCNQ2 channels can localize to presynaptic terminals and regulate the release of neurotransmitters in hippocampal neurons (Martire *et al.*, 2004; Peretz *et al.*, 2007a), was followed by determination that syntaxin 1A can bind to the C-terminus of KCNQ2 (Regev *et al.*, 2009). Interestingly, it appears that syntaxin 1A binds to helix A, which is also known to interact with CaM; as a result there seems to be interplay between CaM and syntaxin 1A effects on channel function, as CaM overexpression attenuates syntaxin-mediated inhibition of KCNQ2 (Etzioni *et al.*, 2011). Furthermore, a sequence of residues present in the N-terminus of KCNQ3 appears to preclude syntaxin 1A action on these subunits. Insertion of these residues in KCNQ2, or deletion from KCNQ3, inhibit or endow syntaxin 1A actions respectively, suggesting that syntaxin 1A binding to the A helix in the C-terminus modulates N- and C-terminal interactions that promote channel closure. The physiological significance of such a mechanism remains unclear, however, it seems plausible that syntaxin 1A that is not involved in vesicle release may promote calcium influx at the presynaptic terminus by inhibiting K⁺ flux through KCNQ2 containing M-channels.

The evidence that the sodium channel auxiliary subunit $\text{Na}_v\beta 1$ regulates KCNQ2, on the other hand, is quite limited, with one study reporting modest effects of $\text{Na}_v\beta 1$ coexpression on slowing the activation kinetics and right-shifting the GV curve of KCNQ2 currents (Nguyen *et al.*, 2012). The small effect observed in this study does not preclude the possibility of an artifact resulting from $\text{Na}_v\beta 1$ overexpression producing an indirect effect on KCNQ2 channels, and it is difficult to appreciate co-IP experiments purporting to demonstrate KCNQ2- $\text{Na}_v\beta 1$ interactions in the absence of substantive functional data.

In contrast, the effect of the β secretase BACE1 has striking effects on KCNQ2, greatly enhancing current expression and shifting voltage dependence of activation by $\sim -20\text{mV}$ (Hessler *et al.*, 2015). These effects of BACE1 were determined following the observation that BACE1 knockout mice display neuronal hyperexcitability due to a loss of XE-991 sensitive currents, which led the authors to hypothesize that BACE1 may be an endogenous auxiliary subunit of M-channels. The proteolytic action of BACE1 is not essential for its modulatory effect; therefore, the authors predict that as a type 1 transmembrane protein like KCNE1 (which regulates cardiac KCNQ1 subunits), BACE1 resides in neuronal membranes and associates with KCNQ2 subunits to enhance their function under normal physiological conditions. BACE1 initially garnered much attention for the discovery of its role in generating amyloid peptides implicated in the progression of Alzheimer's disease (Cai *et al.*, 2001; Luo *et al.*, 2001). It will be interesting to see how this story unfolds in terms of how KCNQ2 channel modulation is involved in the pathophysiology associated with changes in BACE1 expression, or if BACE1 regulation of KCNQ2 channels has any unique function in normal physiology. My interpretation of this study is that under normal conditions, BACE1 effects on KCNQ2 channels are saturated, based on the fact that the discrepancy of M-

current expression between neurons from WT and BACE1 knockout mice is similar to the maximally inducible M-current under heterologous expression.

Finally, another emerging mechanism of KCNQ channel regulation worth noting is covalent modification by small ubiquitin-like modifiers (SUMO). Recent work using a SENP2 knockout mouse model suggest that hyper-SUMOylation of KCNQ2/3 channels causes functional silencing, enhanced neuronal excitation, and, ultimately, death caused by epilepsy similar to what is observed in cases of SUDEP (sudden unexplained death in epilepsy)(Qi *et al.*, 2014). In this study, immunoprecipitation/blot analyses demonstrate modification of hippocampal KCNQ2 channels by SUMO2. They demonstrate that neurons from SENP2 knockout mice have reduced M-current, and are hyper-excitabile. Furthermore, administration of the KCNQ opener retigabine can inhibit this increase in excitability and prevent seizures in SENP2 knockout mice. These findings strongly suggest that in healthy mice, SENP2 expression results in KCNQ2 deSUMOylation and restoration of channel function, allowing neurons to properly regulate excitability.

These examples of both covalent and non-covalent modification of KCNQ channels help to illustrate a general idea regarding the vast molecular toolkit utilized by neurons *in vivo* to regulate M-currents, and in doing so, modulate neuronal excitability. Some mechanisms of regulation clearly have a greater impact on channel function, whereas others have more nuanced effects. Epileptogenesis produced by substantial loss of KCNQ channel function is likely to mask the effect of potential alterations in channel modulation in these nuanced ways, and therefore, advancements in the discriminatory power of neurological assessments in both humans and animal models may help elucidate the physiological importance of some of these processes.

Molecular determinants of subunit assembly, heteromerization, and localization

Unlike ‘canonical’ delayed rectifier K_v channels, which possess N-terminal T1-domain motifs that govern the tetrameric assembly of subunits within subfamilies (Li *et al.*, 1992; Vivienne Shen *et al.*, 1993; Xu *et al.*, 1995), KCNQ channels possess an analogous C-terminal helical domain termed the “A-domain”(consisting of the most distal C-terminal helix, helix D), which guides the assembly of subunit types into both homomeric and heteromeric ion channels (Howard *et al.*, 2007; Schwake *et al.*, 2003, 2006). The generation of chimeras where the A-domain is swapped between KCNQ subtypes confers the ability to generate non-native ion channel configurations (Schwake *et al.*, 2003)(Fig. 1.2). Crystal structures show that the tail region of ~30 residues in the KCNQ4 A-domain can self-assemble to form a tetrameric coiled-coil structure through a network of hydrophobic and electrostatic interactions (Howard *et al.*, 2007). Subtle variation in the amino-acid sequences of the A-domains in different KCNQ subtypes is expected to underlie subtype-specificity of KCNQ channel assembly.

While KCNQ1, 2, 4 and 5 are able to form functional homotetrameric ion channels, KCNQ3 subunits are unique in that they appear to only express with other subtypes, unanimously giving poor current expression when expressed alone in heterologous systems. When co-expressed with KCNQ2 or KCNQ5, KCNQ3 dramatically boosts current expression by an order of magnitude (Lerche *et al.*, 2000; Wang and McKinnon, 1995). Such a massive increase in expression when KCNQ3 is co-expressed with KCNQ2, is enabled through the aforementioned inter-subunit interactions mediated by the A-domain (Schwake *et al.*, 2006). Based on their analyses of the side-chain contacts formed in the coiled-coil KCNQ4 A-domain tail in their crystal structure, Howard *et al.* (2007) proposed that the inability of KCNQ3 to form homotetrameric channels is due to destabilizing electrostatic and steric interactions that occur at the inter-subunit

A-domain interface, which seems plausible given that KCNQ2, 4 and 5 subunits are more homologous to each other at these contact points relative to KCNQ3. However, it was found that mutating a KCNQ3 alanine residue in the pore-helix domain to a threonine residue that is normally present in other KCNQs (as well as other K_v channels at homologous site) confers a profound “rescue” of current, suggesting that KCNQ3 channels are able to form functional channels that are electrically silent due to a non-functional pore (Etxeberria *et al.*, 2004; Gómez-Posada *et al.*, 2010). Further biophysical work has characterized a network of interactions in the pore region of KCNQ3 that is important for ion conduction, without altering channel trafficking to the plasma membrane (Choveau *et al.*, 2012a, 2012b). The study by Gómez-Posada *et al.* (2010) also reports that the A315T mutation enhances surface expression of KCNQ3 channels, and propose that in addition to creating an inactivated pore, the native alanine residue contributes to an overall lack of channel stability that precludes efficient trafficking of channels from the ER to the PM.

Arguably the most unique feature of M-channels, in the context of the family of voltage-gated K^+ channels, is the aforementioned Ankyrin-G binding motif that is present in the distal C-terminus of KCNQ2 and KCNQ3 subunits. The first indication that such a targeting motif might exist was from observations in immunostaining experiments of rat sciatic nerves that KCNQ2/3 localizes to the nodes and axon initial segments, that this axonal targeting follows the expression of Ankyrin-G in developing rats, and that Ankyrin-G and KCNQ2/3 can be co-immunoprecipitated (Devaux *et al.*, 2004). Subsequently, it was demonstrated that this localization is absent in Ankyrin-G knockout mice (Pan *et al.*, 2006), and analysis of the C-terminal sequence of KCNQ2 and KCNQ3 revealed the presence of a motif homologous to the Ankyrin-G binding motif identified in the domain II-III linker of Na_v channels that is required for axonal targeting (Garrido *et al.*, 2003; Pan *et al.*, 2006). This sequence is located at the C-terminus, almost 500 residues from

the S6 helix and distal to the helices involved in CaM binding and subunit assembly described earlier. A more in-depth study has demonstrated that despite having similar Ankyrin-G binding motifs, the C-termini of KCNQ2 and KCNQ3 serve specific roles in channel localization (Chung *et al.*, 2006). In this study, fusion of the C-terminus of KCNQ2 or KCNQ3 to a reporter protein revealed that KCNQ2 subunits enable preferential targeting of channels to axonal membranes versus the dendrites, whereas the KCNQ3 C-terminus contain determinants that enable expression at more distal axonal segments versus the AIS. Interestingly, the determinants of these subunit-specific effects on localization appear to be in proximal regions of the C-terminus, suggesting that while the Ankyrin-G binding domains of these subunits underlie general interactions that are important for nodal and AIS localization, there are other structural determinants that can be utilized by neurons to further enhance the spatial specification of M-current expression.

Mechanisms of BFNC pathogenesis

Over 30 KCNQ2 and KCNQ3 mutations have been identified in cases of BFNC, and considerable work has been done to elucidate mechanisms of disease pathogenesis. Most BFNC mutations are found in KCNQ2, with only 3 disease mutations identified in KCNQ3 thus far (Singh, 2003). Consistent with knockout mice studies discussed previously in which significant loss of KCNQ2 function causes death and/or severe neurological defect, many of these mutations produce only a moderate loss of current expression (Schroeder *et al.*, 1998). Co-expression of the BFNC causing KCNQ2 mutation Y284C (Singh *et al.*, 1998), along with one equivalent of WT KCNQ2 and two equivalents of KCNQ3 (to mimic endogenous conditions), produces a mere 25% loss of currents. Haploinsufficiency, rather than exertion of dominant-negative effects on channel function, appears to be the predominant pathogenic mechanism of BFNC causing mutations; however, there is one exception, in which a dominant negative C-terminal insertion has been identified in a

family of BFNC patients (Singh, 2003). A possible explanation for the unusual tolerability in this family may be genetic variability in other genes controlling neuronal excitability that can offset the deleterious effect of this allele. Most BFNC mutations in both KCNQ2 and KCNQ3 are found either in the pore region or the C-terminus. Experimental evidence shows that BFNC mutations in the C-terminus disrupt the proper trafficking and assembly of channels (Borgatti *et al.*, 2004; Schwake *et al.*, 2000), and promote expedited degradation of channel complexes by exerting destabilizing effects (Soldovieri *et al.*, 2006). These findings are consistent with knowledge that the C-terminus permits inter-subunit interactions essential for channel assembly.

While most BFNC mutations cause loss of current expression with little or no effect on channel gating, two mutations have been identified in the voltage sensing domain of KCNQ2 channels: R207W and R214W (Castaldo *et al.*, 2002; Dedek *et al.*, 2001). Both of these mutations are neutralizations of a S4 helix gating charge involved in voltage-sensing. Channels expressing these mutations have slightly shifted voltage dependence of activation (to more depolarized potentials), but also significantly slower kinetics of activation upon membrane depolarization. Co-expression of mutant subunits along with WT KCNQ3 produces channels that display an intermediate level of delayed kinetics and voltage-sensitivity, which seems to cause M-current suppression sufficient to cause BFNC. Interestingly, patients harboring the R207W mutation also experience lifelong myokymia, which is characterized by involuntary skeletal muscular contractions (Dedek *et al.*, 2001). The R207 residue is located more centrally on the S4 helix compared to the R214 residue, and inhibits channel activation and voltage-sensing to a greater degree upon neutralization; this is the rationale for the more severe clinical manifestation of the R207W mutation.

RETIGABINE AND KCNQ CHANNEL PHARMACOLOGY

Overview of commonly used AED therapies and their mechanisms

Currently there are over thirty AED therapies available for the treatment of epilepsy, with the primary goal of these therapies being to ameliorate seizure frequency and/or severity. The selection of therapy depends on many factors, but usually begins as monotherapy with drug selection based on the seizure type, followed by additional add-on drugs when necessary. Ultimately, the treatment regime becomes highly individualized, but even after poly-therapy, it is estimated that ~30% of patients remain refractory to treatment and continue to experience seizures (Kwan and Brodie, 2000). An Italian clinical study observing the therapeutic regimen of over 1000 patients diagnosed with refractory epilepsy found that almost 80% of patients were receiving at least two AEDs and a third were receiving three or more (Malerba *et al.*, 2010). Paralleling the highly variable etiology of epilepsies and their clinical manifestations, is the unpredictable and varied outcome of receiving AED therapy. Fortunately, approximately half of newly diagnosed epilepsy patients will experience full seizure control with monotherapy, and 70% after adjuvant therapy (Kwan and Brodie, 2000); in short, while many people receive fully adequate therapy, others are forced to play a balancing act that involves avoiding the unwanted side effects associated with additional AEDs, while trying to reduce the numbers of seizures they experience.

Despite the abundance of AEDs, the majority of these drugs operate through only a few known mechanisms: inhibition of sodium or calcium channels, and enhancement of GABA signaling. Sodium channel blockers such as carbamazepine, phenytoin and lamotrigine, are among the most commonly prescribed AEDs. These operate through use-dependent block of sodium channels and possess some interesting features that make them well suited as AEDs. Preferential and slow binding of these drugs to the inactivated state of these channels ensures that they act on

hyperactive neurons that are able to accumulate inactivated sodium channels sensitized to block (Kuo and Bean, 1994; Rogawski and Löscher, 2004). These drugs are proposed to interact with a common binding site consisting of key aromatic residues present in the domain IV S6 helix of Nav channels (Kuo, 1998; Ragsdale *et al.*, 1996). Interestingly, there are reports that in some cases seizures can be paradoxically aggravated by sodium channel blockers like carbamazepine (Lerman, 1986). While the mechanism of AED aggravated seizures is not clear, one proposed mechanism is the inhibition of inhibitory circuits (Rogawski and Löscher, 2004). This seems plausible as numerous mutations in the SCN1A gene (encoding Nav1.1 channels) have been identified in cases of Dravet syndrome (also referred to as SMEI, severe myoclonic epilepsy of infancy) (Claes *et al.*, 2001, 2003), and it has been demonstrated that Nav1.1 channels are selectively expressed in inhibitory interneurons (Yu *et al.*, 2006).

In addition to blocking the activity of sodium currents contributing to neuronal action potential generation, there are reports that phenytoin and valproate can inhibit the late sodium current at concentrations lower than those required for phasic block (Segal and Douglas, 1997; Taverna *et al.*, 1998). This effect is caused by stabilization of the inactivated state of the channels at voltage ranges where a small fraction of channels equilibrate between open and inactivated states. As the late sodium current is implicated in contributing to burst firing of neurons, its inhibition may be an important aspect of how drugs like phenytoin and valproate exert anti-epileptic activity.

Voltage gated calcium channels (VGCC) of both the high voltage activated (HVA, P/Q-, L-, N-, R-type) and low voltage activated (LVA, T-type) also constitute a major target of AEDs. HVA VGCCs are essential regulators of voltage-dependent neurotransmitter release at synapses, and therefore, their inhibition prevents inter-neuronal AP propagation. An example of a widely

used drug in this class is gabapentin, a GABA derivative that was synthesized as a potential GABA receptor agonist (Rogawski and Löscher, 2004) but was instead found to interact with the $\alpha 2\delta$ auxiliary subunits of VGCCs (Gee *et al.*, 1996). Gabapentin binding prevents proper modulation of HVA VGCCs by $\alpha 2\delta$ subunits, leading to a decrease in Ca^{2+} currents and inhibition of neurotransmitter release (Dooley *et al.*, 2000; Sutton *et al.*, 2002). In contrast, levetiracetam is an inhibitor of VGCCs that is more subtype-specific, in that it selectively inhibits N-type calcium channels (Lukyanetz *et al.*, 2002). This also indicates that unlike gabapentin, levetiracetam is likely exerting its effects directly on the channel α -subunit. Unlike the HVA VGCCs that govern neurotransmitter release in the brain, T-type calcium channels activate at lower voltages and are important in controlling neuronal burst firing and oscillations (Perez-Reyes, 2003). This activity is particularly important for thalamic function, and is engaged during thalamo-cortical dysregulation that leads to absence seizures. Ethosuximide is a drug that is particularly effective against absence seizures because it selectively blocks T-type calcium channels (Coulter *et al.*, 1989).

The last major class of AEDs are modulators of GABA signaling. Interestingly, one of the first AEDs ever used was bromide salts, dating back over 150 years (Rogawski and Löscher, 2004), and part of bromide's efficacy lies in its ability to conduct through GABA_A channels, which are more selective for bromide than chloride (Bormann *et al.*, 1987). AEDs such as benzodiazepines (ie. diazepam) and barbiturates (ie. phenobarbital) are positive allosteric regulators of GABA_A receptors, enhancing Cl^- conductance at inhibitory synapses. They are often administered in status epilepticus, a severe form of convulsion in which return to normal consciousness does not occur for five minutes. Other drugs such as vigabatrin and tiagabine impact GABA_A signalling indirectly

by inhibiting GABA breakdown or uptake from inhibitory synapses, respectively (Biase *et al.*, 1991; Suzdak and Jansen, 1995).

Finally, it is noteworthy that while a specific mechanism of action has been ascribed for many of the drugs described, it is clear that many if not most AEDs are “dirty” in the sense that have been shown to act via multiple mechanisms (Rogawski and Löscher, 2004). There is some agreement that these additional targets contribute to many undesirable side effects of AEDs, but what is more difficult to reconcile is which target constitutes the primary mechanism of action of an AED that displays a lack of specificity. Certain drugs such as valproate, which displays a broad spectrum of anti-epileptic activity, are poorly understood relative to other AEDs but more clinically effective and frequently prescribed.

The discovery of retigabine and its development as an AED

The chemical synthesis of retigabine was performed by a German company called ASTA in the early-mid 1990’s after an NIH program evaluating anti-epileptic outcomes of existing drugs revealed that flupirtine (a drug used in Europe as an acute analgesic) displayed anti-convulsant properties (Rostock *et al.*, 1996). Using flupirtine as a template, ASTA generated a compound library and discovered that retigabine, which was referred to as compound D-23129 at the time, displayed greater potency. This initial report on anti-convulsant effects of retigabine revealed protection against both chemically and electrically induced convulsions in mice, and even demonstrated a better protective index than the established AEDs phenytoin and valproate based on the therapeutic versus toxic dose ratios.

Shortly thereafter it was established that retigabine enhances potassium currents in cultured neurons (Rundfeldt, 1997). Based on the nature of the currents elicited by retigabine along with the simultaneous emergence of KCNQ2/3 channels as the correlates of the M-channel that is

mutated in neonatal epilepsies (Charlier *et al.*, 1998; Singh *et al.*, 1998; Wang *et al.*, 1998), several groups went on to express KCNQ2/3 channels heterologously to demonstrate that retigabine is a powerful activator of these channels (Main *et al.*, 2000; Rundfeldt and Netzer, 2000; Wickenden *et al.*, 2000). The mechanistic insights that emerged in these and subsequent studies will be discussed below.

With the establishment that retigabine displays broad anti-epileptic activity in animal models and the determination of a clear therapeutic target, retigabine entered the clinical trial pipeline which resulted in its approval for human use as an adjuvant drug in refractory epilepsy in 2011. In a series of multi-center clinical trials conducted in Europe, in which over 1200 patients with refractory epilepsy were randomized to placebo or varying doses of retigabine, it was demonstrated that retigabine dose-dependently reduces seizure frequency by up to 54.5% (Brodie *et al.*, 2010; French *et al.*, 2011; Porter *et al.*, 2007). However, it was also clear from these studies that retigabine produces many side effects such as dizziness, headache, fatigue, vertigo, confusion and urinary retention, with higher doses causing as much as 26.8% of patients to discontinue their treatments (French *et al.*, 2011). Overall, these trials indicated that while retigabine could produce significant therapeutic effects, it would likely be incorporated into personalized treatment regimes as an adjuvant therapy only in cases where the benefits of seizure reduction outweighed its adverse effects.

Current mechanistic understanding of retigabine action on KCNQ channels

Initial studies revealing the potentiating effects of retigabine on KCNQ2/3 channels demonstrated its ability to accelerate channel activation, slow channel deactivation and shift the voltage dependence of channel opening to more negative potentials (Main *et al.*, 2000; Wickenden *et al.*, 2000). A subsequent study demonstrated that retigabine activates KCNQ2-5 channel

subunits but not KCNQ1, and that muscarinic rundown of KCNQ2/3 currents prevents current potentiation (Tatulian *et al.*, 2001). This study also found that in the presence of retigabine, M-currents are protected against muscarinic induced rundown, suggesting that a common factor governs retigabine induced channel potentiation as well as muscarinic induced inhibition (my results from chapter 4 indicate that this is PIP₂). The same group also performed single channel recordings to show that retigabine does not affect single channel conductance but rather, increases the channel open probability (Tatulian and Brown, 2003).

Based on the previous findings that KCNQ2-5 but not KCNQ1 subunits are sensitive to retigabine, chimeric approaches were utilized to determine channel regions essential for retigabine effects (Schenzer *et al.*, 2005; Wuttke *et al.*, 2005). By inserting transmembrane regions corresponding to KCNQ1 into KCNQ2 or KCNQ3 backgrounds, the authors of these studies demonstrated that the pore region of these channels is essential for retigabine effects, and narrowed down the interaction to a single tryptophan residue in the S5 helix of all retigabine sensitive KCNQ subunits, which, when inserted into the equivalent position in KCNQ1 endows retigabine sensitivity (Schenzer *et al.*, 2005). Additional mutagenesis experiments suggest that while this S5 tryptophan residue (W265 in KCNQ3) is essential for retigabine effects, other residues residing in the pore region of the channel (Leu-272 in S5, Leu-314 in pore loop, Leu-338 in S6 in particular) are also important (Lange *et al.*, 2009). Taken together, the functional data from these experiments reveal that retigabine is likely to bind to the pore through interactions with several residues, although the S5 Trp is the only residue that can be mutated to abolish retigabine effects while preserving channel function.

Scope of thesis investigation

To date, most published investigations of retigabine have been clinically focused, with many reports testing its efficacy in various animal models of disease. Relative to other anti-epileptic drugs, few studies have delved into the topic of understanding the detailed mechanisms of action of retigabine, possibly limited by the experimental approaches that were available. Nevertheless, important aspects of retigabine pharmacology have emerged, such as a general understanding of the retigabine pharmacophore, as well as the biophysical effects caused by retigabine binding. One obvious gap in our knowledge is how retigabine binding to the pore domain exerts such a massive shift in voltage-sensitivity. A recent study demonstrated that under muscarinic receptor mediated inhibition, retigabine loses its ability to potentiate KCNQ2/3 channels unlike the channel opener zinc pyrithione (ZnPy)(Zhou *et al.*, 2013), suggesting that PIP₂ might be an important mediator of retigabine action on these channels.

In recent years, several research groups have successfully employed the voltage-clamp fluorometry technique to measure conformational changes of the voltage-sensing domain in KCNQ1 channels in order to study the effects of PIP₂ and the auxiliary subunit KCNE1 on channel gating and voltage sensing (Barro-Soria *et al.*, 2014; Osteen *et al.*, 2010; Zaydman and Cui, 2014). Inspired by these studies, I began my PhD work by generating a KCNQ3 channel construct amenable for VCF studies and optimizing the fluorescence recording apparatus so that I could perform similar studies on KCNQ3 channels. The main objective of employing this method was to understand how retigabine modulates voltage sensitivity in these channels, and to determine the role that PIP₂ plays in mediating the pharmacology and function of these channels. This work is the topic of the fourth chapter, and was the project that took up most of my time in the lab. As I was gaining momentum on this endeavor, I also had the opportunity to employ unnatural amino

acid mutagenesis to investigate the atomic interactions that underlie retigabine binding to KCNQ3, specifically investigating the role of the crucial S5 residue W265. The results of this study (described in Chapter 3) pinpoint a hydrogen bond interaction that likely occurs between the indole nitrogen of W265 and a carbonyl oxygen group present on retigabine and other derivatives, and represents what is currently the most detailed experimental evaluation of the retigabine pharmacophore. More recently, I have also developed a project aimed at understanding the stoichiometry of retigabine action, which has not been explored previously. Electrophysiological recordings from KCNQ3 concatamers devised to control the stoichiometry of retigabine sensitive subunits surprisingly indicated that that expression of a single retigabine-sensitive subunit can fairly closely replicate the pharmacological sensitivity of wild-type channels. This project comprises a smaller fifth and final research chapter of this thesis. Collectively, the research that is presented here provides fundamental new insights into the binding mechanism of retigabine, the number of retigabine binding events required for a full functional effect, and the detailed mechanism of transduction of retigabine binding to the voltage sensing apparatus of neuronal KCNQ channels.

Chapter 2: Methods

MOLECULAR BIOLOGY

KCNQ2 (human) and KCNQ3 (human) channel cDNAs were propagated and manipulated using the pTLN vector (gifts of Dr M. Taglialatela and Dr T. Jentsch). Introduction of point mutations was accomplished using PCR to combine two fragments each of which contained the mutation in an overlapping region of the sequence ('two-step' PCR method). To accomplish this, we used standard PCR approaches to amplify a 5' fragment and a 3' fragment (using a 'flanking primer' paired with a mutagenic primer). These fragments were then mixed along with the 'flanking primer' pair for a second round of PCR to combine the overlapping fragments. The resulting fragment was then subcloned into the appropriate parent vector using EcoRI and NotI restriction enzymes, and the sequence was verified by Sanger sequencing approaches (Genewiz). Sequences for the flanking primers and the 'forward' mutagenic primers are provided in Table 2.1 ('reverse' mutagenic primers are simply the reverse complement). In all experiments involving homomeric expression of KCNQ3 channels (including *in vivo* nonsense suppression experiments), the Ala315Thr mutation was introduced to enable efficient trafficking of homomeric KCNQ3. KCNQ3 does not efficiently form functional channels; however, the Ala315Thr mutation enables efficient KCNQ3 functional expression without co-injection of KCNQ2 mRNA (throughout the text we refer to KCNQ3[Ala315Thr] as KCNQ3*).

Concatemeric constructs of KCNQ3* were generated by first creating dimers of combinations of KCNQ3* and KCNQ3*[W265F] by subcloning copies of the cDNA sequence into the NheI-XhoI or XhoI-HindIII restriction sites of pcDNA3.1(-). PCR primer design omitted a stop codon from the leading subunit, while preserving a stop codon in the trailing subunit. Sequences of individual inserts were confirmed by Sanger sequencing before combining them by

restriction digestion and ligation, leading to a dimer of the form: NheI-COPY1(no stop)-XhoI-COPY2-STOP-HindIII. A second set of dimers was constructed with one subunit in the NheI-XhoI position (stop codon omitted), and a second subunit cloned in the XhoI-HindIII position but with an engineered NheI site. These second dimers had the form: NheI-COPY1(no stop)-XhoI-COPY2(no stop)-NheI-HindIII. Using an NheI digestion and ligation to combine these dimers, we generated a variety of tetrameric channel combinations of the form: NheI-COPY1(no stop)-XhoI-COPY2(no stop)-NheI-COPY3(no stop)-XhoI-COPY4(no stop)-HindIII, in pcDNA3.1(-).

The plasmid encoding Ci-VSP was kindly provided by Dr Y. Okamura. Complementary RNA was transcribed from the cDNA using the mMessage mMachine Kit (Ambion). Stage V–VI *Xenopus laevis* oocytes were injected with cRNA alone or cRNA plus synthetic tRNA (for nonsense suppression, described below). After injection, oocytes were incubated for 27–72 h at 18 °C before recording.

WESTERN BLOT, ANTIBODIES

Lysates from HEK cells transfected with KCNQ3* channel constructs were separated by gel electrophoresis on 0.7% SDS-PAGE gels, and transferred to nitrocellulose blots using standard protocols. KCNQ3 protein was probed with a rabbit polyclonal antibody (APC-051, Alomone), HRP-conjugated mouse anti-rabbit secondary antibody (ABM), and visualized using ECL reagents and a FluorChem SP Gel Imager.

Primer	Sequence (5' to 3', forward)	Primer	Sequence (5' to 3', forward)
KCNQ2 FF	CCA AGC GCA ACG CCT TCT ACC	Q3 G219C	GTG GGA AAC CAA TGC AAT GTT CTG GCC
KCNQ2 RF	GGC TGG TTT AGT GGT AAC CAG	Q3 N220C	GGA AAC CAA GGC TGT GTT CTG GCC ACC
KCNQ3 FF	GGC GAC GTG GAG CAA GTC ACC	Q3 V221C	GA AAC CAA GGC AAT TGT CTG GCC ACC TCC
KCNQ3 RF	TAA GGC CTC AAA GTC TCC TTG	Q3 L222C	CAA GGC AAT GTT TGT GCC ACC TCC CTG
Q2 W236F	GCT GGT CAC TGC CTT CTA CAT CGG CTT CC	Q3 A223C	GGC AAT GTT CTG TGC ACC TCC CTG CGA AGC
Q3 W265F	GCA AAG AAC TCA TCA CGG CCT TCT ACA T	Q3 T224C	GGC AAT GTT CTG GCC TGC TCC CTG CGA AGC
Q3 W265S	GCA AAG AAC TCA TCA CGG CCT TGT ACA T	Q3 R183A	GGA TGT TGC TGC GCA TAC AAA GGC TGG
Q3 W265T	GC AAA GAA CTC ATC ACG GCC ACG TAC ATC GGT TTC CTG AC	Q3 K185A	GC TGC CGA TAC GCA GGC TGG CGG GGC
Q3 W265Y	GC AAA GAA CTC ATC ACG GCC TAC TAC ATC GGT TTC CTG AC	Q3 R188A R190A	CGA TAC AAA GGC TGG GCG GGC CGA CTG AAG
Q3 W265TAG	GCA AAG AAC TCA TCA CGG CCT AGT ACA T	Q3 R190A	GGC TGG CGG GGC GCA CTG AAG TTT GCC
Q3 T271F	GGT ACA TCG GTT TCC TGT TTC TCA TCC TTT CTT CAT TTC	Q3 K192A	CGG GGC CGA CTG GCG TTT GCC AGG AAG
Q3 T271V	GGT ACA TCG GTT TCC TGG TAC TCA TCC TTT CTT CAT TTC	Q3 R195A	CTG AAG TTT GCC GCG AAG CCC CTG TGC
Q3 L272I	GGT ACA TCG GTT TCC TGA CAA TCA TCC TTT CTT CAT TTC	Q3 K196A	G AAG TTT GCC AGG GCG CCC CTG TGC ATG
Q3 L314A	GGG GCC TGA TCA CAG CGG CCA CCA TTG GCT ATG G	Q3 K248A	GGT GGC ACC TGG GCG CTT CTG GGC TCA G
Q3 L314V	GGG GCC TGA TCA CAG TGG CCA CCA TTG GCT ATG G	Q3 K358A	GGG CTG GCC CTC GCG GTG CAG GAG CAA C
Q3 L338A	GCC GCC ACC TTT TCC GCA ATT GGC GTC TCC TTT TTT GCC	Q3 R364A	CAG GAG CAA CAC GCT CAG AAG CAC TTT G
Q3 L338V	GCC GCC ACC TTT TCC GTA ATT GGC GTC TCC TTT TTT GCC	Q3 H367A	CAC CGT CAG AAG GCC TTT GAG AAA AGG
Q3 G216C	GTG GTT GCT GTG GGA TGT CAA GGC AAT G	Q3 K370A R371A	G AAG CAC TTT GAG GCA GCG AGG AAG CCA GCT GC
Q3 N217C	GTT GCT GTG GGA TGC CAA GGC AAT GTT C	Q3 R372A K373K	GCT CAG CAG CTG GCG CCG CCC TTT TCT CAA AG
Q3 Q218C	GCT GTG GGA AAC TGT GGC AAT GTT CTG	Q3 K370A R371A R372A	C TTT GAG GCA GCG GCG GCG CCA GCT GCT GAG C

Table 2.1: List of Mutagenic Primers. Corresponding reverse complement primers were used in conjunction with flanking primers (FF: forward flanking, RF: reverse flanking) to generate all mutants used.

HARVESTING XENOPUS LAEVIS OOCYTES

Mature female *Xenopus laevis* weighing >100 grams were obtained from the University of Alberta Biology Department or Boreal Science (Ontario), and handled in accordance with the animal care procedures implemented at the University of Alberta or University of British Columbia. Oocyte lobes were harvested and dissected into smaller fragments of ~10-20 oocytes in OR2 solution (82.5 mM NaCl, 2.5 mM KCl, 1 mM MgCl₂, 5 mM HEPES, pH 7.6), and transferred to a collagenase solution consisting of 3 µg/mL of Type IV collagenase (Worthington Biochemical Corporation) in OR2. 1:5 ratio mixtures of oocytes to collagenase solution, not exceeding 25 mL, were placed in 50 mL falcon tubes and placed on a rotator which inverted the tubes at a frequency of 0.5 Hz. We found this step to be crucial, as it enabled thorough exposure of oocytes to the collagenase solution without physically damaging oocytes. Oocytes were checked periodically starting at 2 hours, until a majority of their follicular layers were removed by the collagenase. Subsequently, the collagenase solution was replaced with OR2 and tubes were placed back on the rotator for another 30 minutes, to rinse the oocytes and allow any remaining follicular layers to peel off. Oocytes were sorted and kept in OR3 solution at 18°C until use (500 mL Leibovitz's L-15 Medium, 3.57 g HEPES, 5 mL Glutamine, 5 mL Gentamycin, 500 mL H₂O, pH 7.6, filtered).

UNNATURAL AMINO ACID MUTAGENESIS

Fluorinated Trp derivatives (5-F₁-Trp; 7-F₁-Trp; 5,7-F₂-Trp (F₂-Trp) and 5,6,7-F₃-Trp (F₃-Trp) were purchased from Asis Chem (Watertown, MA) and Sigma-Aldrich (St Louis, MO). The 'Ind' Trp variant was synthesized in-house as described previously (Lacroix *et al.*, 2012). Incorporation of unnatural amino acids into ion channel proteins was carried out as described extensively in prior publications (Beene *et al.*, 2003; Pless *et al.*, 2013a, 2013b). Briefly, unnatural amino acids (aa) were protected with nitroveratryloxycarbonyl and were activated as the

cyanomethyl ester, which were then coupled to the dinucleotide pdCpA (GE Healthcare/Dharmacon, Lafayette, CO). This aminoacyl dinucleotide was subsequently ligated to a modified (G73) *Tetrahymena thermophile* tRNA. The amino-acylated tRNA-aa was deprotected by ultraviolet irradiation immediately before oocyte injection. In a typical experiment, 80 ng of tRNA-aa and 40 ng of KCNQ3 cRNA were injected in a 50 nl volume. In control experiments, the cRNA alone or the cRNA together with a tRNA coupled to pdCpA but without an appended amino acid were injected (these parallel control experiments were conducted every experimental day and the results are described throughout the text).

TWO ELECTRODE VOLTAGE CLAMP

Voltage-clamped potassium currents were recorded in modified Ringer's solution (in mM): 116 NaCl, 2 KCl, 1 MgCl₂, 0.5 CaCl₂, 5 HEPES (pH 7.4) using an OC-725C voltage clamp (Warner, Hamden, CT). Glass microelectrodes were backfilled with 3 M KCl and had resistances of 0.1–1 MΩ. Data were filtered at 5 kHz and digitized at 10 kHz using a Digidata 1440A (Molecular Devices) controlled by the pClamp 10 software (Molecular Devices). Drugs were purchased from Toronto Research Chemicals (retigabine) or Tocris (ML-213, flupirtine, ICA-069673, ICA-110381), stored as 100 mM stocks in dimethylsulphoxide and diluted to working concentrations each experimental day.

VOLTAGE CLAMP FLUOROMETRY

Xenopus laevis oocytes expressing KCNQ3*[Q218C] (abbreviated as Q3*VCF in chapter 5) were incubated in 100 μM Alexa Fluor-488 Maleimide (ThermoFisher Scientific) for 20 minutes in a depolarizing high K⁺ Ringer's solution (in mM): 100 mM KCl., 1 mM MgCl₂, 0.5 mM CaCl₂, 5 mM HEPES (pH7.4). Following labelling, oocytes were thoroughly rinsed in standard Ringer's solution, and kept on ice for prompt use. Fluorometry was simultaneously

performed with a two-electrode voltage clamp on an Olympus IX51 inverted microscope. A PhlatLight LED (Luminus Devices) powered by a DC power supply (F25-12-AG, Bel Power Solutions) served as the light source, and emitting light from the oocyte animal pole was collected and amplified as an electric signal using a PIN040-A photodiode (OSI Optoelectronics) connected to a patch-clamp head unit/amplifier in voltage-clamp mode (Axopatch-1C, Axon instruments).

DATA ANALYSIS

Voltage-dependence of channel activation and normalized fluorescence change was fitted with a standard single component Boltzmann equation of the form $G/G_{\max} = 1/(1+\exp((V-V_{1/2})/k))$, where $V_{1/2}$ is the voltage where channels exhibit half-maximal activation, and k is a slope factor reflecting the voltage range over which an e-fold change is observed. Data in chapter 5 were fitted with a double Boltzmann equation of the form $G/G_{\max} = a[1/(1+\exp((V-V_{1/2a})/k_a))]+(1-a)[1/(1+\exp((V-V_{1/2b})/k_b))]$, where a and b represent the shifted and un-shifted channel populations, respectively. Fluorescence data were low-pass filtered at 20 Hz and adjusted for bleaching by subtracting a linear component fitted to the baseline fluorescence at the beginning and end of each voltage sweep. To minimize the impact of bleaching, only data from cells displaying a $>0.5\%$ maximal ΔF were used for analysis. ΔF values were obtained by dividing the maximal fluorescence change at the end of the test pulse by the baseline fluorescence preceding the test pulse, from single non-averaged sweeps. Statistical tests and significance are described in figure legends throughout the text.

CONSTRUCTION OF MOLECULAR MODEL

The molecular model of KCNQ3 was generated using a homology model of KCNQ3 based on the Kv1.2-2.1 paddle chimera structure (PDB 2R9R)(Long *et al.*, 2007) using the online SWISS-MODEL tool (swissmodel.expasy.org)(Kiefer *et al.*, 2009), fused manually to a KCNQ2/KCNQ3 chimeric C-terminal domain structure (PDB 5J03)(Strulovich *et al.*, 2016), followed by energy minimization (Schrodinger Maestro). A series of docked conformations of PIP₂ were predicted using AutoDock Vina 1.1.2 (Trott and Olson, 2010). We emphasize that this is a preliminary structural model intended to illustrate our hypothesis, and that further development and refinement of the model will be possible as further constraints are collected.

Chapter 3: H-bonding with W265 is Essential for Retigabine Effects

BACKGROUND AND SUMMARY

A conserved tryptophan residue in the pore-forming S5 helix of retigabine-sensitive KCNQ channels (KCNQ2 W236, KCNQ3 W265) is known to be essential for retigabine effects and is absent in the retigabine-resistant cardiac isoform KCNQ1 (Lange *et al.*, 2009; Schenzer *et al.*, 2005). The identification of retigabine as a potent K_v channel opener has led to numerous compound library screens to generate novel analogs with altered subunit specificity and effectiveness (Boehlen *et al.*, 2013; Gao *et al.*, 2010; Peretz *et al.*, 2007a; Xiong *et al.*, 2008; Yu *et al.*, 2011). However, the molecular details that underlie retigabine-KCNQ channel interactions have remained elusive because of the inherent lack of resolution of conventional site-directed mutagenesis techniques.

To overcome these limitations, unnatural amino acid mutagenesis was used to subtly rearrange atoms and electrons in the Trp side chain that form the retigabine binding site. Repositioning of the indole nitrogen atom of KCNQ3 W265 completely abolishes retigabine effects, suggesting that retigabine interaction requires formation of a H-bond with W265. The importance of this H-bond interaction is further illustrated by introduction of fluorinated Trp analogs (with increased H-bonding propensity) at KCNQ3 W265, causing increased drug potency. Using a range of retigabine analogs, the carbonyl oxygen moiety is identified as an electrostatic fingerprint that correlates with drug potency and may act as a H-bond acceptor with KCNQ. These experimental constraints pinpoint specific atoms and chemical forces involved in retigabine interactions, and highlight approaches that may be used to guide rational improvement of existing drugs.

RESULTS

Retigabine modulation of KCNQ channels through an S5 Trp

Retigabine strongly affects voltage-dependent gating of KCNQ2 and KCNQ3* channels (Fig. 3.1a,b) by generating a substantial hyperpolarizing shift of the $V_{1/2}$ of activation by ~40-60 mV (KCNQ3* refers to KCNQ3[Ala315Thr] – see METHODS). These effects have also been demonstrated in KCNQ4 and KCNQ5, but are absent in KCNQ1 due to the absence of an essential Trp residue (Trp 236 in KCNQ2, Fig. 3.1a; Trp 265 in KCNQ3, Fig. 3.1b, Leu246 in KCNQ1)(Lange *et al.*, 2009; Schenzer *et al.*, 2005). This Trp side chain lies in the pore-forming S5 transmembrane segment, near the intracellular voltage-operated gate of the channel. As KCNQ2-5 subunits generally assemble as heteromers in the CNS, we tested the effects of retigabine in oocytes co-injected with KCNQ2 and KCNQ3 and observed large shifts of activation to more negative voltages, although not quite as large as with KCNQ2 or KCNQ3 alone (Fig. 3.1c). Some KCNQ channel activator molecules also cause a marked increase in peak current, however the effects of retigabine on KCNQ3* channels are quite modest (rarely greater than a 15% increase in peak current), and throughout this study we have focused on the large gating shifts observed in these channels.

Heteromeric KCNQ2/3 channels were used to alter the number of available retigabine binding sites, by co-injecting KCNQ2[W236Phe] with WT KCNQ3, or KCNQ3[W265Phe] with WT KCNQ2. Assuming 1:1 stoichiometry of KCNQ2/3 assembly, both conditions are estimated to eliminate roughly half of the retigabine binding sites. Consistent with this, we observed intermediate effects of retigabine with fewer available binding sites, indicating that multiple molecules of the drug must bind for a full effect (Fig. 3.1c). A surprising, currently unexplained observation, was that the retigabine-mediated gating shift in KCNQ2/3 heteromers (~-40 mV) was

noticeably smaller than the shift in KCNQ2 or KCNQ3* homomeric channels. This likely hints that determination of the exact details of stoichiometry and cooperativity of drug binding in heteromeric channels will require alternative experimental approaches. We measured the effects of various mutations at position W265 (in KCNQ3*) or W236 (in KCNQ2) on retigabine sensitivity (Fig. 3.1d). In both KCNQ2 and KCNQ3* channels, only a Trp side-chain present at this position was sufficient to enable a significant activation shift by retigabine, and even conservative mutations to other aromatic side chains (Phe or Tyr, Fig. 3.1a, b, d) cannot replicate the retigabine-mediated gating shift.

We tested whether KCNQ3 position Trp 265 plays a role in regulating channel responses to PIP₂. Using the voltage-sensitive phosphatase Ci-VSP to hydrolyze PIP₂ at depolarized voltages, we pulsed oocytes through a range of prepulse voltages followed by a test pulse to -20 mV to assess channel activity after PIP₂ depletion. We observed similar channel rundown with depolarizing voltage steps in both KCNQ3* and KCNQ3*[W265Phe] channels, indicating that W265 does not significantly influence the effects of anionic phospholipids on channel function (Fig. 3.1e,f). Overall, these findings illustrate that KCNQ3 residue W265 is essential for the effects of retigabine, but does not play a significant role in regulating channel gating by voltage or PIP₂.

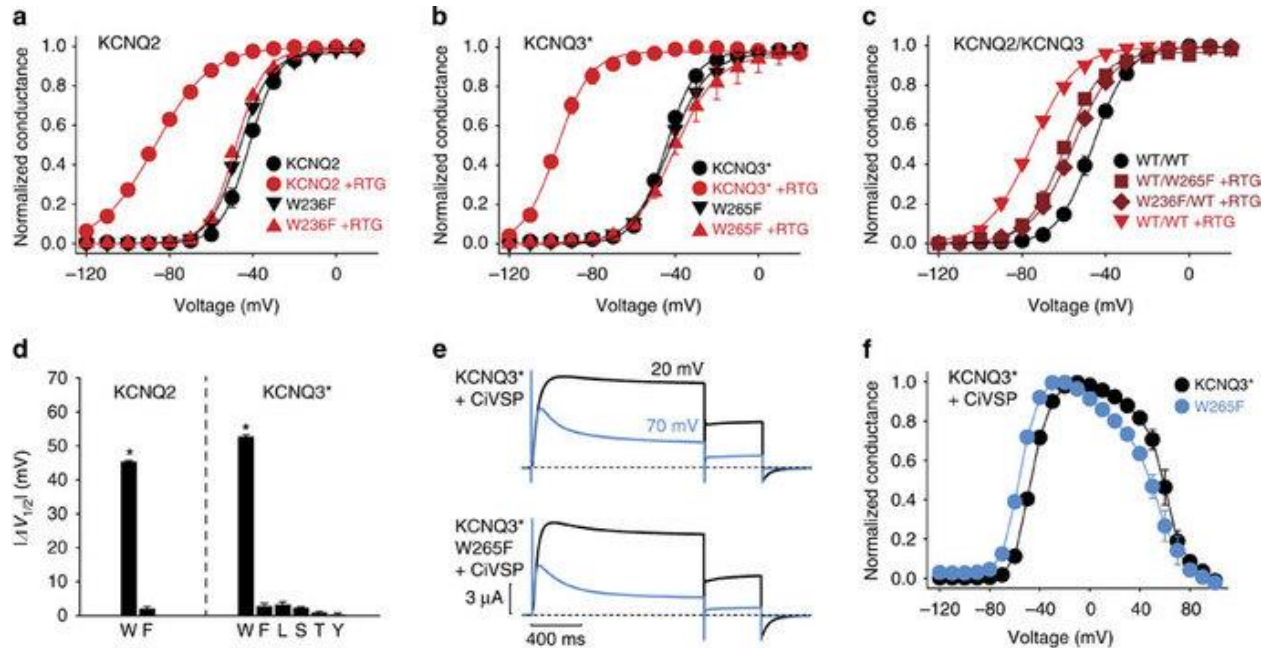


Figure 3.1: Multiple retigabine molecules modulate KCNQ2 and KCNQ3 channel subunits via an S5 Trp side chain. (a,b) Conductance–voltage relationships for (a) KCNQ2 ($n=3$) and KCNQ2[W236Phe] ($n=6$), and (b) KCNQ3* ($n=5$) and KCNQ3*[W265Phe] ($n=3$) homomeric channels along with indicated mutants (retigabine concentration of $100\ \mu\text{M}$). (c) Conductance–voltage relationships for heteromeric combinations of KCNQ2 and KCNQ3 (1:1 ratio of injected mRNA, with or without Trp→Phe mutations as indicated, $n=5$ for each combination), used to generate channels with reduced numbers of retigabine binding sites. (d) Summary of $V_{1/2}$ shifts in saturating $100\ \mu\text{M}$ retigabine for mutations of KCNQ2 W236 and KCNQ3 W265 as indicated (* $P<0.05$ in a paired Student's t -test comparing control versus $100\ \mu\text{M}$ retigabine in each experimental oocyte, $n=3$ – 6 per mutant). Only a Trp at either position is sufficient for retigabine sensitivity. (e) Exemplar currents of KCNQ3* and KCNQ3*[W265Phe] mutant coexpressed with Ci-VSP, illustrating that the Trp side chain responsible for retigabine sensitivity is not required for PIP_2 sensitivity. (f) Summary data of tail current magnitude ($-20\ \text{mV}$) after prepulses to a range of voltages, in oocytes expressing KCNQ3* ($n=5$) or KCNQ3*[W265Phe] ($n=5$) channels, along with Ci-VSP. In all panels, error bars represent \pm s.e.m.

Unnatural amino acid mutagenesis of KCNQ3 channels

In order to investigate the underlying mechanism of retigabine interactions with this essential Trp sidechain, we employed unnatural amino acid mutagenesis to introduce subtly altered Trp variants (Fig. 3.2a). With this method, a stop codon (TAG) is placed in the ion channel gene at a site of interest, and this mRNA is co-injected into *Xenopus laevis* oocytes along with a synthetic amino-acylated tRNA (carrying an unnatural amino acid) that is orthogonal to *Xenopus* tRNA synthetic pathways. When the ribosomal translation machinery encounters the introduced TAG stop codon, the complementary synthetic tRNA (with a CUA anti-codon) enables read-through and incorporation of the appended amino acid into full-length ion channels (Fig. 3.2a).

Among the KCNQ channels we tested, KCNQ3* channels exhibited large currents when expressed as homomeric channels in *Xenopus* oocytes, with a short latency between injection and expression, and were found to be an effective model system for incorporation of unnatural amino acids. KCNQ3* is also a useful model for retigabine binding because it does not possess a second interaction site that is targeted by some other recently studied KCNQ2 activators (see DISCUSSION)(Boehlen *et al.*, 2013; Peretz *et al.*, 2010), and so our results are specifically focused on the retigabine binding site formed by W265. Several criteria illustrate the feasibility and fidelity of the nonsense suppression approach in KCNQ3* channels. Firstly, in the presence of a full-length tRNA lacking a conjugated amino acid (pdCpA control), virtually no ionic currents were observed for several days after injection (Figure 3.2b,d). However, when KCNQ3*[W265TAG] channels were co-injected with Trp-conjugated tRNA, robust currents with WT-like gating were observed, indicating efficient suppression of the introduced TAG stop codon and synthesis of functional channels with WT-like properties (Fig. 3.2b,e). Secondly, although there may be differences in the efficiency of unnatural amino acids at this position, we are

restricting our investigation to homomeric channels (rather than KCNQ2/KCNQ3 heteromers), and to biophysical parameters ($V_{1/2}$, activation kinetics) that are normally independent of channel expression, so differences in expression of channel subtypes should not impact our findings. Lastly, we are confident that the synthetic Trp-tRNA was incorporated in a significant fraction of channel subunits because elicited currents responded to retigabine (Fig. 3.2c, f, g), and only Trp appears to be sufficient for retigabine sensitivity (Fig. 3.1d).

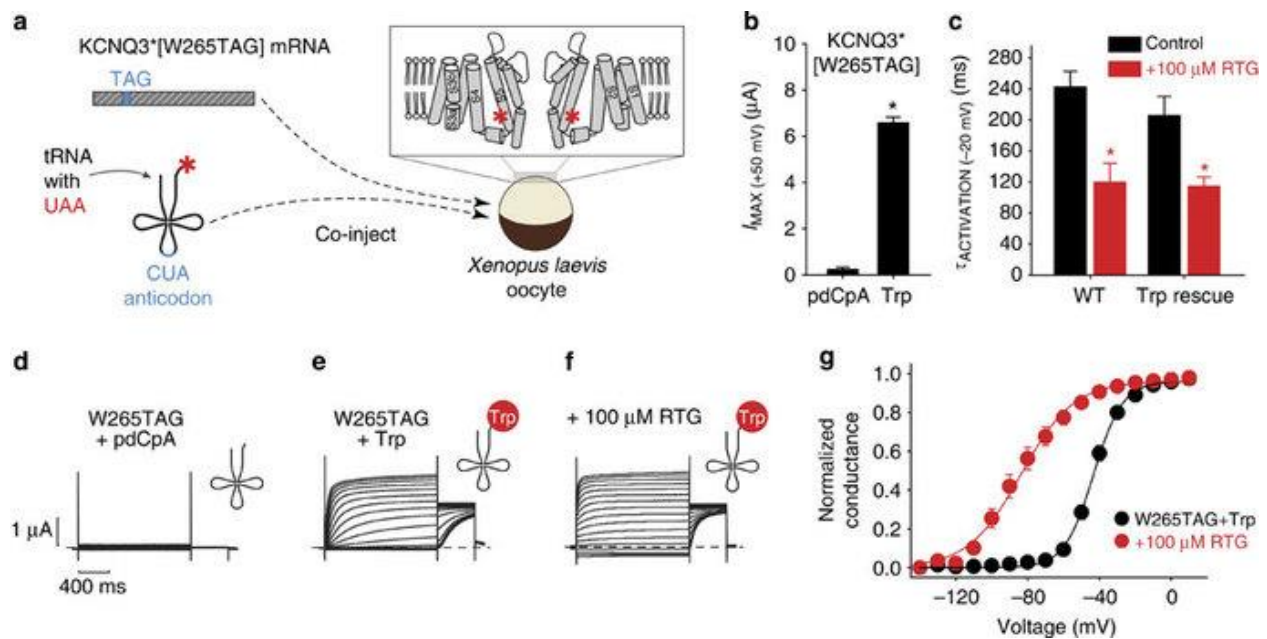


Figure 3.2: Nonsense suppression for amino-acid incorporation in KCNQ3* channels. (a) Schematic diagram of the nonsense suppression method, in which mRNA (with a stop codon at W265) and amino-acylated tRNA are co-injected into *Xenopus* oocytes. Incorporation of the unnatural amino acid enables readthrough of the stop codon and expression of functional channels. (b) Current magnitudes in oocytes injected with KCNQ3*[W265TAG] mRNA and either an unconjugated tRNA (pdCpA; n=5) or tRNA amino-acylated with Trp (n=8, *P<0.05, Student's t-test). (c) Activation kinetics of KCNQ3* (n=5) and KCNQ3*[W265TAG] (n=8) channels rescued with Trp, in the presence or absence of 100 μM retigabine (*P<0.05, Student's t-test). (d-f) Exemplar currents from oocytes injected with KCNQ3*[W265TAG] mRNA, and indicated synthetic tRNAs. (g) Conductance–voltage relationships for Trp-rescued KCNQ3*[W265TAG] (n=8), with retigabine response, illustrating faithful incorporation of the desired side chain at position 265. For KCNQ3* channels $V_{1/2} = -44 \pm 1$ mV, $k = 7.5 \pm 0.5$ mV; for Trp-rescued KCNQ3*[W265TAG] $V_{1/2} = -43 \pm 2$ mV, $k = 7.9 \pm 0.5$ mV. Error bars throughout represent \pm s.e.m.

Loss of retigabine effects after removal of W265 H-bonding

Next, we tested the retigabine sensitivity of KCNQ3* channels synthesized with the 'Ind' amino acid at position 265. This unnatural amino acid side chain ablates the hydrogen bonding capability of Trp by shifting the position of the indole nitrogen atom (Fig. 3.3a) but retains the sterics and identical chemical composition of Trp. KCNQ3*[W265TAG] currents were efficiently rescued with Ind relative to the pdCpA control, yielding relatively large voltage-activated K⁺ currents that closely resembled KCNQ3* (Fig. 3.3b,c). Remarkably, however, this single atom alteration in each of the KCNQ3* subunits entirely abolishes the ability of retigabine to activate KCNQ3* channels (Fig. 3.3d, e). Again, little or no currents were observed from oocytes co-injected with only the pdCpA control tRNA. Notably, Ind channels displayed WT-like gating, indicating that this residue does not play a significant role in conformational stabilization of channel states in the absence of drug. However, given the potent impact of such a minor manipulation, we examined the effects of the W265Ind substitution on channel gating more closely, to rule out the possibility of significant perturbation of channel function. We observed no statistically significant difference in the $V_{1/2}$ or slope of the voltage-dependence of activation of KCNQ3* and KCNQ3*[W265Ind](see Table 3.1). Also, activation kinetics of KCNQ3*[W265Ind] were very similar to channels rescued with Trp at position 265 (Figure 3.3d, e). Lastly, as described earlier, the more disruptive W265Phe mutation did not alter inhibition of KCNQ3* currents by PIP₂ depletion (mediated by Ci-VSP). Thus, this collection of observations support the highly specific effect of the W265Ind substitution on drug interactions (with little disruption of intrinsic channel voltage-dependent gating or lipid regulation), indicating that H-bond formation with W265 is a crucial step for retigabine action.

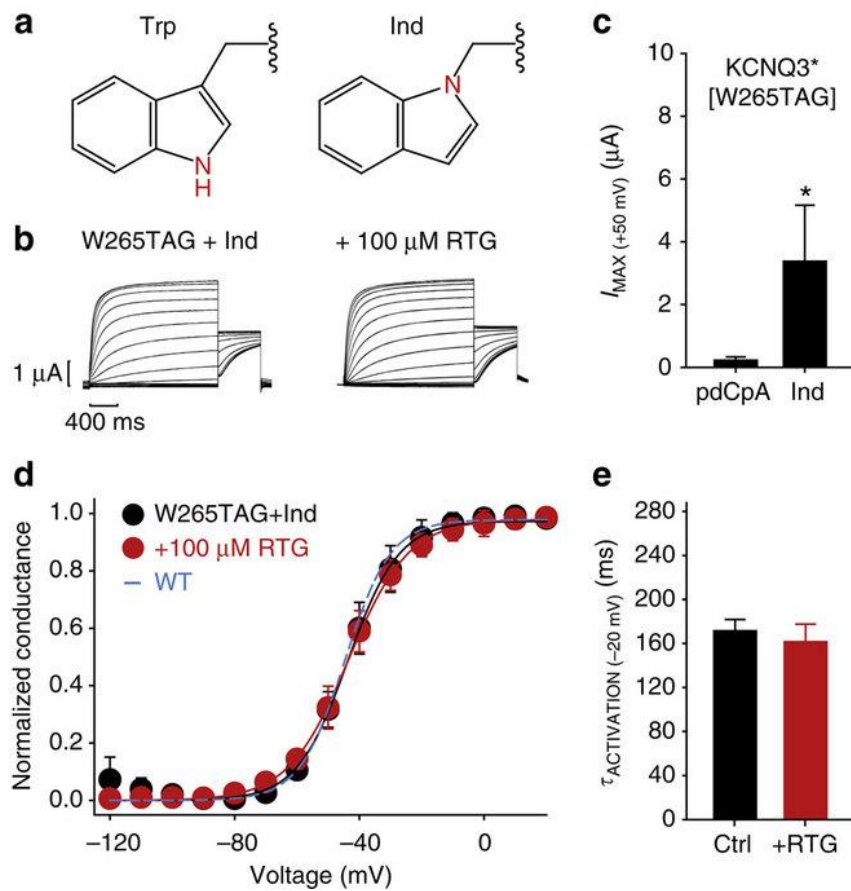


Figure 3.3: The position of the Trp 265 indole nitrogen is essential for retigabine sensitivity. (a) Chemical structures of Trp and Ind side chains, illustrating the subtle change in the position of the indole nitrogen atom. (b) Exemplar currents elicited from a *Xenopus* oocyte with Ind-rescued KCNQ3*[W265TAG] channels illustrating retigabine insensitivity. (c) Current magnitudes in oocytes injected with KCNQ3*[W265TAG] mRNA and either an unconjugated tRNA (pdCpA; n=5) or tRNA amino-acylated with Ind (n=7, *P<0.05, Student's t-test). (d) Conductance–voltage relationships for Ind-rescued KCNQ3*[W265TAG], in the presence and absence of retigabine, illustrating the importance of the correct positioning of the N–H group. For KCNQ3*[W265Trp], $V_{1/2} = -43 \pm 2$ mV, $k = 7.9 \pm 0.5$ mV; for KCNQ3*[W265Ind], $V_{1/2} = -48 \pm 2$ mV, $k = 7.3 \pm 0.6$ mV (no statistical significance, \pm indicates s.e.m). (e) Activation kinetics for KCNQ3*[W265Ind] measured at -20 mV in the presence and absence of 100μ M retigabine (n=7, no statistical significance). In all panels, error bars represent \pm s.e.m.

Construct	$V_{1/2}$	k	n
WT-Trp	-44.4 ± 0.9	7.49 ± 0.5	5
265TAG-Trp	-43.0 ± 1.3	7.93 ± 0.5	12
265TAG-F ₁ -Trp	-37.9 ± 1.1	9.26 ± 0.5	9
265TAG-F ₂ -Trp	-47.6 ± 1.3	9.92 ± 0.8	7
265TAG-F ₃ -Trp	-62.3 ± 2.5	10.89 ± 0.8	12
265TAG-Ind	-47.5 ± 1.2	7.25 ± 0.6	7

Table 3.1: Activation gating parameters for unnatural amino acid substitutions of KCNQ3*[W265TAG] channels. Fitting of conductance-voltage relationships (see Methods) yielded $V_{1/2}$ (voltage where activation is half-maximal) and the slope factor k (voltage range where fractional activation changes e-fold). Data are presented as mean \pm standard error (S.E.M.).

Tuning the strength of the W265-retigabine interaction:

To investigate the possible involvement of other modalities of Trp interactions with the drug, we also examined the consequences of fluorination of W265 on retigabine effects. Trp fluorination is typically used to modify the electrostatic surface potential and test for the effects of cation- π interactions (Fig. 3.4a)(Dougherty, 1996). We were unable to express channels carrying the F₄-Trp side chain (fluorines at ring positions 4,5,6, and 7, as numbered in Fig. 3.4a) but robust current rescue was observed for less fluorinated derivatives such as F₃-Trp (Fig. 3.4b,c). Retigabine potentiation of KCNQ3* channels was retained with F₃-Trp substitution at W265 (Fig. 3.4c-e), a substitution that still potently diminishes the negative electrostatic potential on the face of the side chain (Fig. 3.4a), indicating that a cation- π interaction of W265 with retigabine or some other entity (perhaps another channel residue) is not required for retigabine effects. It is noteworthy that progressive fluorination of W265 caused variable effects on KCNQ3* gating properties (Table 3.1), with F₁-Trp causing a modest depolarizing shift of the activation $V_{1/2}$, while F₃-Trp significantly shifted gating in the hyperpolarizing direction. This lack of an obvious trend also suggests that an endogenous cation- π interaction involving W265 does not contribute significantly to the gating process.

The most interesting outcome of fluoro-Trp substitutions highlights the role of hydrogen bond formation by the indole N-H group. Specifically, fluorination of the Trp side chain significantly increases the polarity of the indole N-H, thereby strengthening the hydrogen bonding propensity of the indole side-chain (Pless *et al.*, 2013b). This is illustrated by the electrostatic surface potentials for Trp and F₃-Trp (note the more polarized electrostatic surface potential of F₃-Trp, highlighted by the blue color around the N-H bond, in the lower right corner as oriented in Fig. 3.4a). Consistent with this, retigabine potency was increased with fluoro-Trp analogs at W265. For instance, in KCNQ3*[W265TAG] channels rescued with Trp (mimicking KCNQ3* channels), 1 μM retigabine elicits very little shift in the voltage-dependence of activation (Fig. 3.4d). However, in channels with F₃-Trp substituted at W265, 1 μM retigabine elicits a much larger response (Fig. 3.4d). Consistent with this effect being attributable to strengthening of the formation of a hydrogen bond by W265, we observed a fluorination-dependent strengthening of the potency of retigabine on KCNQ3* channels, with progressive fluorination shifting the retigabine concentration-response to lower doses (Fig. 3.4f). In addition, we observed a small but significant position-dependent effect of mono-fluorination of W265, in which fluorination of ring position 7 (closer to the indole N-H) increased retigabine effects slightly more than fluorination of ring position 5 (Fig. 3.4f). This is consistent with the fluorine substituent at position 7 having a stronger effect on the polarity of the N-H bond.

Since F₃-Trp incorporation itself caused a hyperpolarizing shift of channel activation even in the absence of retigabine (Fig. 3.4d), a possible alternative explanation for increased retigabine potency with F₃-Trp at position 265 was due to a secondary allosteric effect of stabilization of the channel open state, rather than a direct effect on retigabine binding. Thus, as an additional control experiment, we investigated the effects of another mutation on retigabine sensitivity (Asn220Cys,

located in the extracellular S3-S4 linker, distant from the W265 putative retigabine binding residue). This mutation shifts channel opening to more negative voltages, even more than F₃-Trp substitution at position 265. In the Asn220Cys mutant, no sensitization to retigabine was observed (Fig. 3.4g). That is, 1 μM retigabine was unable to generate a marked gating shift, in contrast to the potent retigabine effects with F₃-Trp substitution at W265 (curve fits for the F₃-Trp substitution are included for comparison, Fig. 3.4g). Also, the retigabine concentration-response for Asn220Cys channels was very similar (albeit shallower) to the KCNQ3* background construct demonstrating that the Asn220Cys mutation *per se* does not inhibit retigabine activation (Fig. 3.4h). These observations suggest that an indirect effect of open state stabilization likely does not account for the increased retigabine potency in F₃-Trp substituted channels.

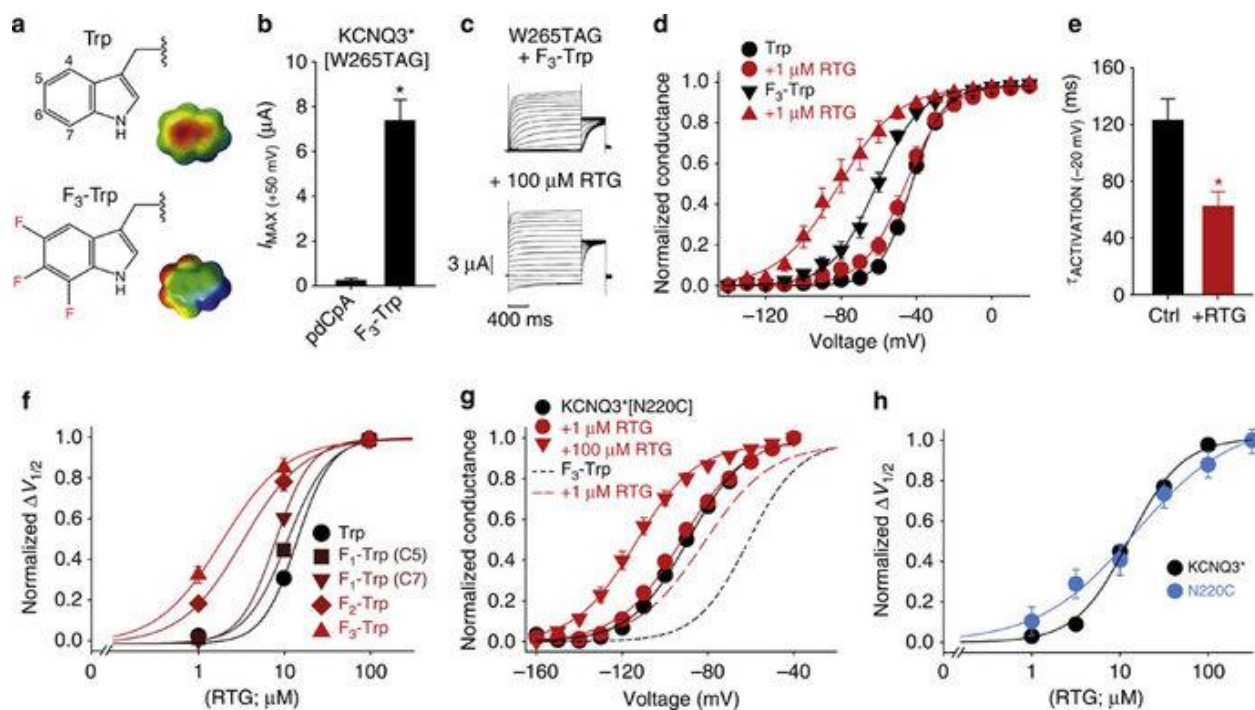


Figure 3.4: The polarity of the W265 indole nitrogen modulates retigabine sensitivity. (a) Chemical structures of Trp (with ring positions labelled) and F₃-Trp, accompanied by colorimetric representations of electrostatic surface potentials. (b) Current magnitudes in oocytes injected with KCNQ3*[W265TAG] mRNA and either an unconjugated tRNA (pdCpA; n=5) or tRNA amino acylated with F₃-Trp (n=12, *P<0.05, Student's t-test). (c) Exemplar currents from F₃-Trp-rescued KCNQ3*[W265TAG] channels in the presence and absence of retigabine. (d) Conductance–voltage relationships illustrating the effects of 1 μM retigabine on Trp-rescued (n=12) and F₃-Trp-rescued KCNQ3*[W265TAG] (n=12) channels. (e) Activation kinetics (–20 mV) for F₃-Trp-rescued channels (n=3), in the presence and absence of 100 μM retigabine (*P<0.05, Student's t-test). (f) Concentration–response curves for retigabine effects on numerous fluoro-Trp analogues (n=9–12 per Trp analogue) substituted at position W265, illustrating enhanced retigabine potency with increased fluorination. (g) Conductance–voltage relationships with indicated retigabine concentrations on a KCNQ3 mutant (Asn220Cys, n=4) with an intrinsic hyperpolarizing shift in gating. Conductance–voltage relationships for F₃-Trp substituted at W265TAG are shown for comparison. (h) Concentration–response curves for retigabine effects on KCNQ3* (n=5) and KCNQ3*[Asn220Cys] (n=4) channels. In all panels, error bars represent ± s.e.m.

Relative contributions of putative drug binding residues:

Given the dramatic effects of the W265Ind substitution, we sought to clarify the contributions of other residues reported to play a role in retigabine binding. Using a chimeric approach between KCNQ1 and KCNQ3, previous work identified KCNQ3 residues Thr271 (S5 helix), Leu272 (S5 helix), Leu314 (pore helix), and Leu338 (S6 helix) as important contributors to a putative retigabine binding pocket (Lange *et al.*, 2009). We generated several mutations at each of these positions in KCNQ3* and tested retigabine effects over a broad range of concentrations (Fig. 3.5a, b). We observed that all functional mutants at these positions retained a large retigabine-mediated gating shift (Fig. 3.5b), although reduced potency was reflected by a shift to higher drug concentrations in many cases. Moreover, many of these mutations caused intrinsic shifts in channel gating in the absence of retigabine (Fig. 3.5a). Previous reports have suggested that many of these mutations strongly diminish retigabine action, but our application of a wider range of concentrations illustrates that while potency of the drug is weakened, strong gating shifts can still occur in these mutants. These data indicate that contacts with Thr271, Leu272, Leu314, and L338 make measurable contributions to retigabine binding affinity. However, the W265Ind substitution abolishes any response to retigabine at experimentally achievable concentrations. Thus, W265Ind remains the most structurally subtle, yet most disruptive mutation we have identified in terms of retigabine sensitivity, and highlights the potential importance of H-bonding with the W265 side chain.

We next used a previously published molecular model of the retigabine binding site to investigate alternative binding modes of the drug (Lange *et al.*, 2009). In the published model ('original' in Fig. 3.5c) there are no obvious H-bond acceptors in the vicinity of the W265 side chain. There are also no apparent H-bond interactions with the Thr271 side chain. However, this

putative binding site can accommodate altered orientations (eg. ‘flip’ in Fig. 3.5c) in which the drug occupies a similar space (see ‘overlay’ panel illustrating both binding models in Fig. 3.5c), but orients the carbamate moiety of retigabine in close proximity to Trp 265. A rotameric shift of W265 enables a close interaction between the indole N-H and a carbamate oxygen atom of retigabine. Using molecular dynamics simulations (of 12 retigabine binding sites starting in a ‘flip’ orientation, for 10 ns each), we measured the mean distance between the retigabine carbamate oxygen and indole N-H group at the end of the simulations as $4.0 \pm \text{s.e.m. } 0.5 \text{ \AA}$ (4 binding sites were measured between 2-3 Å, 3 sites between 3-4 Å, and 5 sites were >5 Å), consistent with the possible formation of a hydrogen bond in this region.

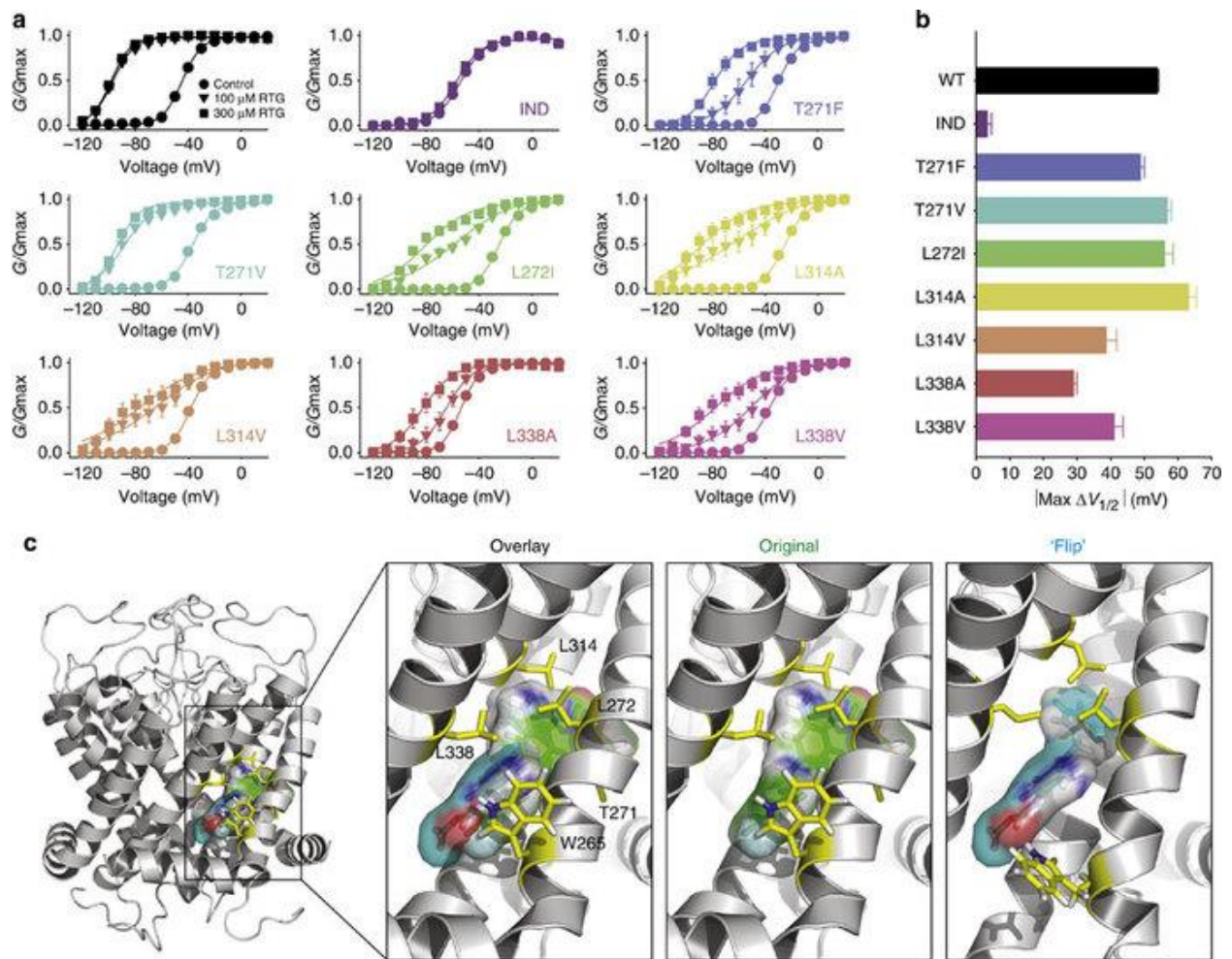


Figure 3.5: Detailed characterization of secondary retigabine binding residues and alternative binding site orientations. (a) Conductance–voltage relationships were gathered for the indicated KCNQ3* mutant channels (n=4–6 per mutant), in 0, 100 or 300 μ M retigabine. (b) Maximal $\Delta V_{1/2}$ in 300 μ M retigabine measured in each mutant channel. Error bars in a,b represent s.e.m. (c) retigabine was docked into a molecular model of the pore-forming domain of KCNQ3. Two orientations are shown with the carbamate group in either the vicinity of Leu314 (‘original’ model) or W265 (‘flip’ model). The two binding models are superimposed in the ‘overlay’, showing the similar space occupied by both drug orientations.

Identification of a likely H-bond acceptor in retigabine:

We further investigated the mechanism of hydrogen bonding with W265 by seeking potential hydrogen bond acceptors in the retigabine molecule, a task facilitated by the availability of numerous retigabine analogs. We first considered the analog ML-213 because it has a simplified chemical scaffold compared to retigabine and a reduced number of possible hydrogen bond acceptors (Fig. 3.6a,b). We found that ML-213 is a more potent activator of KCNQ3* compared to retigabine ($EC_{50} = 3.6 \pm \text{s.e.m. } 0.2 \mu\text{M}$ versus $11.6 \pm \text{s.e.m. } 0.4 \mu\text{M}$, respectively, Fig. 3.6c). We have also included the calculated electrostatic surface potentials for retigabine and ML-213, illustrating that the negative surface potential around the carbonyl oxygen is more pronounced for ML-213 (red protrusion, Fig. 3.6a, b).

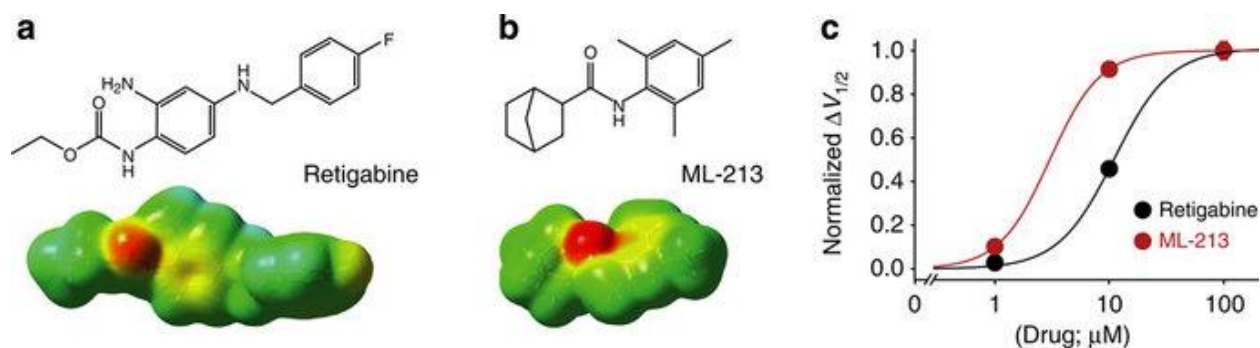


Figure 3.6: ML-213 exhibits a stronger electrostatic surface potential and higher potency than retigabine for KCNQ3* activation. (a,b) Chemical structures and electrostatic surface potentials for retigabine and ML-213. Note the increased negative surface potential in the vicinity of the carbonyl oxygen atom in ML-213. The scale for electrostatic surface potential representation is red: -80 kcal, yellow: 0 kcal, blue: $+80$ kcal. (c) Concentration–response curves for retigabine and ML-213 ($n=5$) effects on KCNQ3* channels ($n=5$). Error bars represent \pm s.e.m.

Expanding on these observations, we examined a spectrum of KCNQ channel activators with varying potency in KCNQ3* channels (Fig. 3.7). We have depicted all of the drugs tested and colorimetric representations of their calculated electrostatic surface potentials, along with the observed EC₅₀ for the shift of V_{1/2} of activation of KCNQ3*[W265TAG] channels (rescued with Trp, F₃-Trp, or Ind). For all drugs tested, effects were abolished by the W265Ind substitution, indicating a common mechanism via hydrogen bond formation with W265. Also, F₃-Trp substitution at W265 generally resulted in higher drug potency, although this effect was not as pronounced with the less polar analogs ICA-110381 and ICA-069673. Importantly, all of the activator compounds contain a carbonyl oxygen (either in the carbamate moiety of retigabine and flupirtine, or in the amide linker in ML-213 or the ICA compounds), and it is noteworthy that the strength of the negative surface potential correlates well with the potency of the drug for KCNQ3* activation – drugs with a weaker electrostatic surface potential trend towards weaker potency on KCNQ3* channels (Fig. 3.7). The ICA compounds are less potent activators of KCNQ3* channels within our typical experimental concentration range (up to 300 μM), and notably ICA-110381 caused considerably more activation in F₃-Trp substituted channels, demonstrating that effects of an otherwise weak channel activator can be strengthened by targeting the chemical properties of W265. Taken together, these findings illustrate the importance of the hydrogen bonding propensity of W265, likely involved in the formation of a hydrogen bond with a carbonyl oxygen present in retigabine and its analogs.

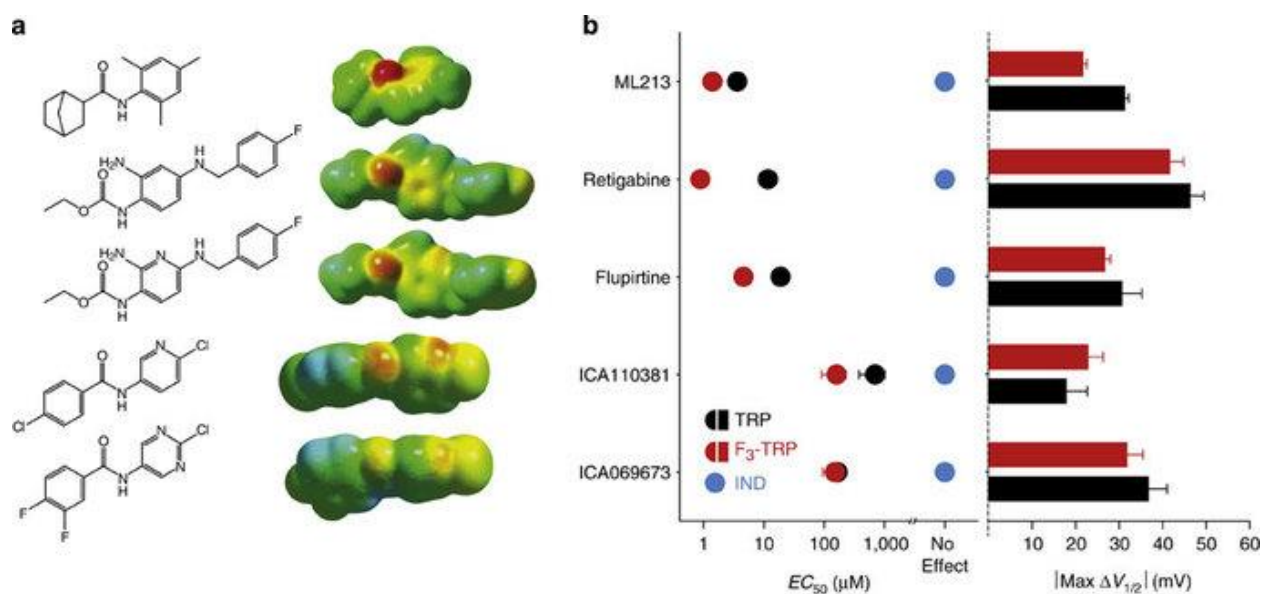


Figure 3.7: Effects of retigabine analogues correlate with electrostatic surface potential. (a) Chemical structures and electrostatic surface potentials for a series of retigabine analogues. All structures and surface potential maps have been aligned on the basis of the location of the conserved amide-ester bond—note the gradient of the intensity of the negative surface potential around the carbonyl oxygen atom (scaling is the same as in Fig.6). (b) Summary illustrating the EC_{50} of each drug on Trp-rescued, F_3 -Trp-rescued and Ind-rescued KCNQ3*[W265TAG] channels ($n=4-9$ per data point), and the maximal efficacy ($\Delta V_{1/2}$) of each drug in F_3 -Trp and Trp-rescued channels (effects on Ind-rescued channels are minimal and thus have been omitted). Error bars represent \pm s.e.m.

DISCUSSION

At the outset of our study, chimeric studies with the retigabine-insensitive KCNQ1 channel had identified the importance of a Trp residue (KCNQ3 W265) in the pore-forming region, near the presumed cytoplasmic channel gate. Retigabine interactions with this site had been rationalized as generic hydrophobic interactions with this conserved Trp residue (also present in KCNQ2, 4 and 5)(Lange *et al.*, 2009; Schenzer *et al.*, 2005).

Although most often considered to be hydrophobic, Trp side chains can deploy diverse chemical forces in ligand interactions (Burley and Petsko, 1985), and these require specialized chemical-scale approaches to be distinguished (Beene *et al.*, 2003). There is growing recognition of the general importance of electrostatic cation– π interactions with all aromatic side chains (Beene *et al.*, 2003; Gallivan and Dougherty, 1999). In addition, both Trp and Tyr side chains can act as H-bond donors. Unnatural amino-acid mutagenesis approaches allow us to parse out atomistic modes of interaction, and also hopefully mitigate the possibility of gross structural perturbations that might arise using conventional mutagenesis. By engineering KCNQ3 channels to include subtle Trp variants at position 265, our study identifies the very atoms required for retigabine effects and, further, the chemical forces involved in forming a direct interaction with retigabine. Surprisingly, our findings indicate that the critical property of W265 for retigabine activation, rather than hydrophobicity, is the ability to H-bond. Repositioning of the indole nitrogen atom to remove Trp H-bonding abolished the effects of retigabine and all analogues tested (Figs 3.3 and 3.7). Moreover, a Trp analogue (F₃-Trp) with altered electrostatics but intact/enhanced H-bonding ability enhances retigabine potency (Figs 3.4 and 3.7). A valuable future direction for these experiments will be to develop an independent measure of drug binding, to distinguish whether the H-bond interaction (disrupted by the W265Ind mutation) is essential for

drug binding, or couples drug binding to a later step involved in channel potentiation. Nevertheless, these observations highlight a rarely investigated mode of drug interactions with Trp, as Trp residues in a binding pocket are often presumed to indicate a hydrophobic site. Our findings illustrate the importance of detailed investigation of the underlying chemistry of these binding sites to better understand mechanisms of drug action.

By demonstrating the effects of H-bond strength on a range of KCNQ3 activators, our findings suggest the importance of a carbonyl oxygen (usually in a carbamate or amide moiety) for the formation of a negative electrostatic surface potential to act as a H-bond acceptor. Previous screens of compound libraries have investigated important physicochemical features important for drug activity on KCNQ2–5 channels. Several studies have reported the importance of an amide bond (or a carbonyl oxygen) as an essential element of the pharmacophore, although the relationship between this functional group and the H-bonding propensity of W265 has not been recognized (Miceli *et al.*, 2008; Wu *et al.*, 2004). Notably, KCNQ activators with marked structural diversity appear to act through W265 (several examples are shown in Fig. 3.8), and these share the common feature of a carbonyl oxygen that we suggest acts as an essential hydrogen bond acceptor. Supporting this notion, our findings illustrate that ML-213 is an effective KCNQ3 activator, correlated with its strong surface potential relative to other drugs tested. In the context of understanding drug interactions with ion channels and other receptors, these observations illustrate the importance of investigating specific chemical forces that enable drug interactions with aromatic side chains known to contribute to binding sites in other ion channels (for example, voltage-gated Na⁺ channels, human ether-a-go-go related gene product (hERG))(Mitcheson *et al.*, 2000). These insights could guide rational ‘tuning’ of the properties of certain functional groups to alter drug properties in desirable ways.

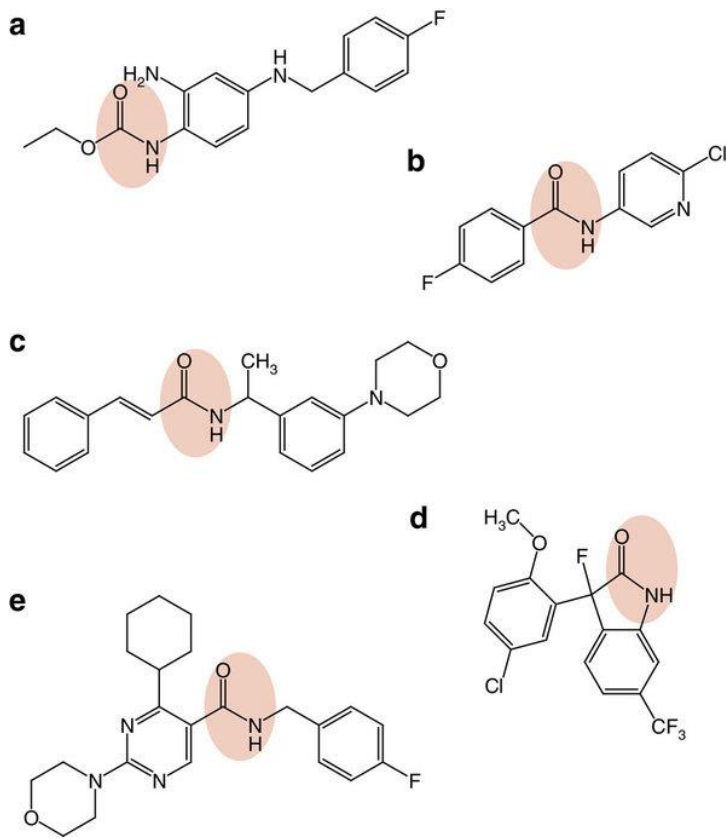


Figure 3.8: Diverse structures of KCNQ openers. Multiple structures of KCNQ channel openers are presented to highlight the overall features of an amide group flanked by various ring structures. Our findings highlight the importance of the amide carbonyl for interaction with KCNQ3 W265 and likely equivalent positions in KCNQ2, 4 and 5. Drugs depicted are (a) retigabine, (b) ztz-240 (Gao *et al.*, 2010), (c) acrylamide (s)-1, (d) BMS-204352 and (e) an unnamed experimental drug (Wu and Dworetzky, 2005).

On the basis of the magnitude of the retigabine-induced shift of the conductance–voltage relationship, saturating effects of retigabine are estimated to stabilize channel opening by $\sim 6 \text{ kcal mol}^{-1}$ (calculated as $\Delta G = \Delta(zFV_{1/2})$). As a comparison, formation of a H-bond between a carbonyl and amino groups (N-H: O=C) is generally quite weak, on the order of 2 kcal mol^{-1} . A tetrameric KCNQ channel likely contains four potential retigabine binding sites, and our characterization of heteromeric channels with fewer binding sites (Fig. 3.1c) indicates that multiple sites may be occupied in saturating retigabine concentrations. Thus, the energetics of the full

retigabine-mediated gating shift can be reasonably attributed to multiple retigabine molecules interacting with W265 via a H-bond. Although not as prominent as the W265 indole nitrogen, other residues also make additional measurable contributions to the overall energy of retigabine binding (Fig. 3.5). It should also be noted that cooperativity between retigabine binding sites has not been investigated in detail, and so it is not known how multiple retigabine binding events may interact and influence channel function. Investigation of libraries of retigabine analogues has highlighted that variable aromatic ring substituents can alter the apparent affinity, maximal effect and subunit specificity (Gao *et al.*, 2010; Wu and Dworetzky, 2005). For example, many ring substituents (such as halogenation) alter the polarity of the carbonyl oxygen and thereby alter drug interactions with W265. In addition, it seems likely that diverse flanking structures (potentially by interacting with the auxiliary retigabine binding residues investigated in Fig. 3.5) could influence the orientation of the carbonyl oxygen relative to W265.

A final noteworthy detail is that, although our findings delineate an atomic basis for the retigabine interaction with KCNQ3 W265 (and analogous residues in KCNQ2,4,5), there is significant evidence for additional interaction sites that enable potentiation of certain KCNQ subunits. For example, the ICA compounds tested (and other related compounds such as ztz-240), along with a family of diclofenac derivatives, have been reported to influence KCNQ2 channels independent of the conserved S5 Trp residue and exhibit dramatically stronger effects in KCNQ2 relative to KCNQ3 (Boehlen *et al.*, 2013; Gao *et al.*, 2010; Peretz *et al.*, 2007b, 2010). In addition, unrelated KCNQ openers such as zinc pyrithione do not appear to depend on the hydrogen bond interaction that we have identified in this study (Xiong *et al.*, 2007). Therefore, ongoing examination of drug binding to different KCNQ channel subtypes may help to reveal additional sites for KCNQ potentiation.

In conclusion, we have used unnatural amino-acid mutagenesis and available retigabine analogues to localize the effects of retigabine binding to a single H-bond interaction with KCNQ3 W265. These findings highlight an unusual mode of drug interaction with a Trp side chain, and demonstrate the importance of careful investigation of the mechanism of drug interactions to guide rational modification of therapeutic compounds.

Chapter 4: PIP₂ Modulates Functional Coupling and Pharmacology of KCNQ3 Channels

BACKGROUND AND SUMMARY

Previous studies have demonstrated that retigabine stabilizes the open state of KCNQ2-5 channels, reflected in a marked shift (~30-60 mV) of the voltage dependence of channel activation to more negative potentials, and in many cases an increase of maximal open probability (Main *et al.*, 2000; Rundfeldt and Netzer, 2000; Tatulian and Brown, 2003; Wickenden *et al.*, 2000). The retigabine binding site has been characterized in several reports (Kim *et al.*, 2015; Lange *et al.*, 2009; Schwake *et al.*, 2006; Wuttke *et al.*, 2005), highlighting the importance of a binding pocket within the pore domain (PD) anchored by a critical hydrogen bond interaction between the drug and an S5 tryptophan residue that is conserved in retigabine-sensitive KCNQ channels (KCNQ2-5).

KCNQ channel:PIP₂ interactions are essential for channel activity, and have also been highlighted as important modulators of pharmacological sensitivity to certain KCNQ activators. Retigabine effects on KCNQ channels rely on the presence of sufficient PIP₂, while certain other activators such as Zn-pyrithione can rescue KCNQ currents in the nominal absence of PIP₂. Overall, the interactions between KCNQ activators, the KCNQ channel voltage-sensing apparatus, and the essential phospholipid PIP₂, have not been investigated and are poorly understood.

To elucidate how the pore-delimited retigabine binding site results in modulation of voltage-sensing, we used voltage clamp fluorometry (VCF) to track conformational changes of the voltage sensing domains in KCNQ3 channels in response to voltage, retigabine, and PIP₂. Ionic conductance and voltage sensor fluorescence closely overlap under basal PIP₂ conditions, suggesting a tight coupling between the VSD and PD in KCNQ3 channels. Retigabine stabilizes

the conducting conformation of the pore and activated conformation of the voltage sensors, but these effects are attenuated upon PIP₂ hydrolysis by Ci-VSP, revealing a critical role of VSD-PD coupling in retigabine effects. We identify an essential PIP₂ interaction motif below the S6 helix that is likely to mediate VSD-PD coupling and enables the transduction of retigabine binding to altered voltage sensor function. Taken together, the data suggest a mechanism whereby retigabine binding to KCNQ channels at the VSD-PD interface results in dynamic regulation of VSD and PD conformations that is PIP₂ dependent.

RESULTS

Voltage clamp fluorometry of KCNQ3 channels

The VCF approach requires introduction of a fluorophore in a region that undergoes voltage-dependent conformational changes (Fig. 4.1B, bottom). In order to generate a useful KCNQ3* construct for VCF, we tested a series of cysteine mutants throughout the extracellular S3-S4 linker (Fig. 4.1A). This region was highly sensitive to mutation, with several mutants generating ~100mV hyperpolarizing shifts in channel gating (Fig. 4.1A), although we have not explored these large gating effects any further. The KCNQ3*[G219C] and [Q218C] mutations were nearly indistinguishable from KCNQ3* channels in terms of their voltage dependence (Fig. 4.1A) and retigabine response. G219C is homologous to the mutation successfully used in several reports of VCF studies of KCNQ1 (Barro-Soria *et al.*, 2014; Osteen *et al.*, 2010; Zaydman *et al.*, 2013). Both the Q218C and G219C sites reported fluorescence changes upon labelling, but the most robust signals were obtained from channels with Q218C (labelled with Alexa Fluor 488-maleimide, Fig. 4.1B). This construct was used throughout the study and is abbreviated as Q3*VCF in all figures and remaining text.

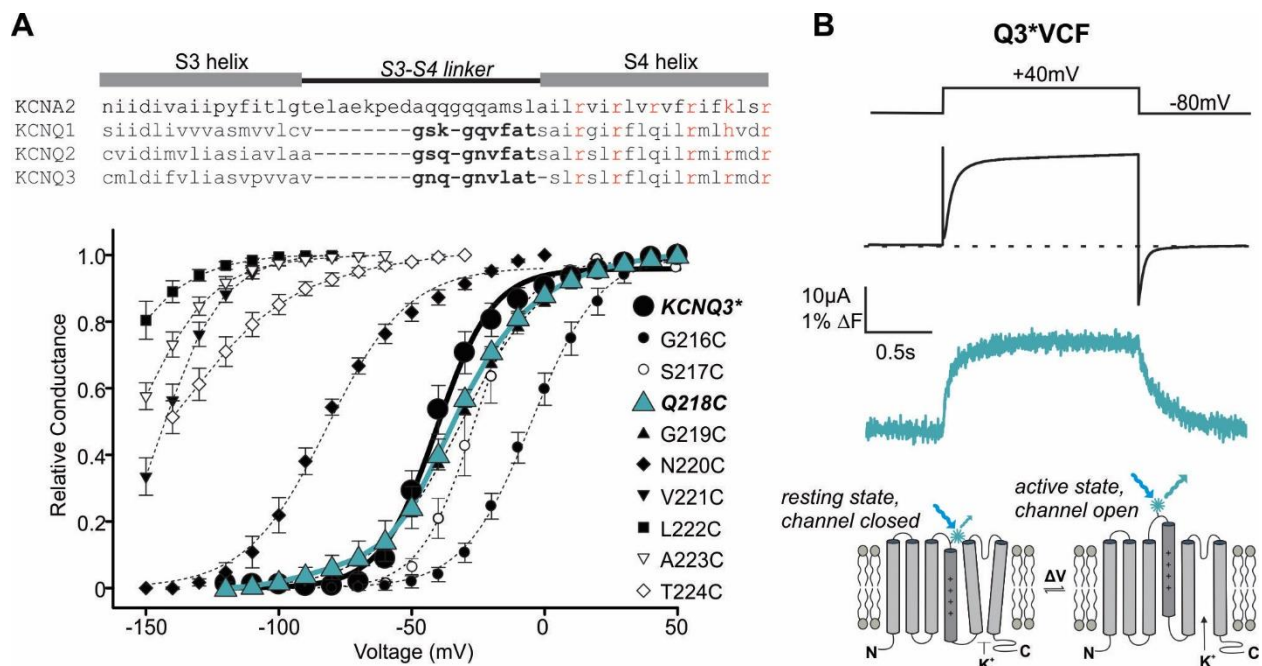


Figure 4.1: Cysteine mutagenesis of KCNQ3* S3-S4 linker residues and identification of Q218C as the ideal position for fluorophore labelling. (A) Cysteine mutations of putative S3-S4 linker residues impact channel voltage-sensing ($n=3-4$ for all mutants) (B) Ionic (black) and fluorescence (green) trace from a *Xenopus laevis* oocyte expressing KCNQ3*[218C] (abbreviated as Q3*VCF in text and all figures), labelled with Alexa-488 maleimide and depolarized to +40mV. Bottom: cartoon illustration of the VCF technique. Error bars represent s.e.m, and * denotes $P<0.5$ using paired or non-paired Student's t-tests, in all figures.

Close coupling of the KCNQ3 voltage sensor and pore

Fluorescence-voltage relationships of Q3*VCF were generated by holding oocytes at a depolarized potential (+20 mV) and stepping to a range of hyperpolarizing potentials. This was required because the strongly shifted voltage-dependence of activation in KCNQ3 in retigabine required long interpulse intervals at very negative voltages to achieve a stable fluorescence baseline, leading to technical difficulties with recording. We observed a direct overlap in the voltage dependence of the fluorescence change and conductance (Fig. 4.2A). This close coupling of the pore and voltage sensor persists in the presence of saturating RTG, as both pore gating and fluorescence are shifted equally to hyperpolarized potentials by approximately 60 mV (Fig. 4.2A, E, note that the absolute $V_{1/2}$ reported here differs somewhat from typical experiments because of

the altered voltage step protocol that was needed). RTG is known to decelerate channel closure, and we demonstrate that it also strongly decelerates the kinetics of voltage sensor deactivation (Fig. 4.2B), and modestly accelerates activation (Fig. 4.2C). Unexpectedly, we also observed that RTG increases the magnitude of the fluorescence signal (ΔF) in response to a given depolarization (Fig. 4.2F). Overall, these findings demonstrate that RTG binding to the pore alters the voltage sensor equilibrium, and this conformational coupling can be detected with VCF. As an important control, all effects of RTG on fluorescence and currents are abolished when the RTG binding site is disrupted by the W265F mutation (Fig. 4.2D-F), demonstrating the requirement for RTG binding to the channel pore.

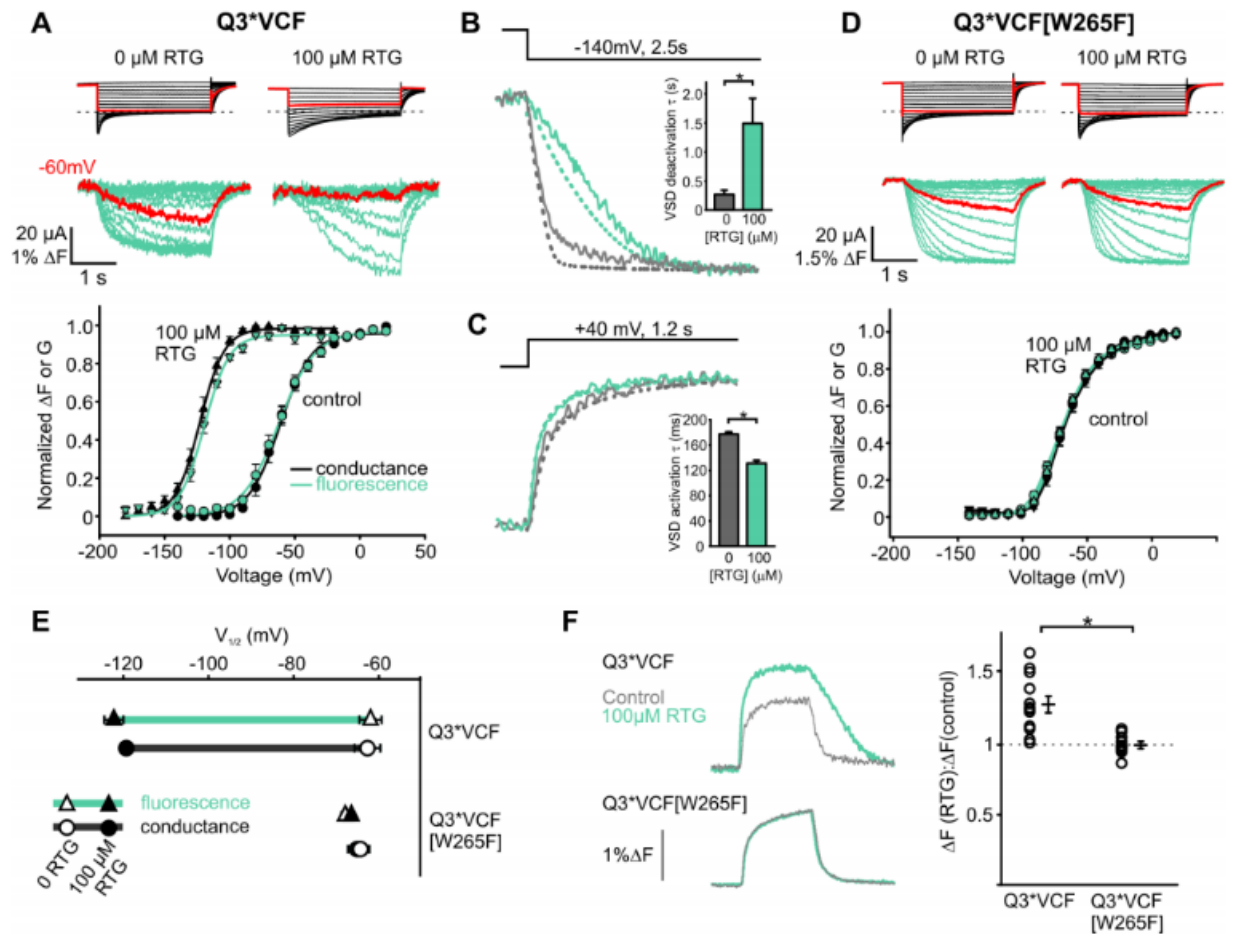


Figure 4.2: Characterization of retigabine effects on Q3*VCF fluorescence. (A) Oocytes were clamped at a holding potential of +20mV/-20mV and hyperpolarized in -10 mV steps to -140mV/-180mV for 3 seconds in control/100μM RTG, respectively. Sample current (black) and fluorescence (green) traces (top) and normalized ΔF or G (tail currents) are displayed (bottom) (n=6 or 5, ctrl/RTG). (B and C) Sample fluorescence sweeps and summary of deactivation kinetics at -140mV (τ : 254.2 \pm 23.6 ms in control and 1436 \pm 177.2 ms in RTG, n=9 each) and activation kinetics at +40mV (τ : 177.5 \pm 3.4 ms in control and 131.2 \pm 4.6 ms in RTG, n=5 each) in the presence (green) or absence (grey) of 100μM RTG. (D) Same protocols were used as in (A) to assess RTG effects on Q3*VCF [W265F] (n=7 or 8, ctrl/RTG). (E) Summary of $V_{1/2}$ values (ΔF and G) for Q3*VCF and Q3*VCF[265F] \pm 100 μ M RTG (Q3*VCF: 62.0 \pm 2.6 mV and -62.71 \pm 3.0 mV for ΔF and G in control, respectively, -122.2 \pm 2.2 mV and -119.3 \pm 1.4 mV for ΔF and G in 100μM RTG; Q3*VCF[W265F]: -65.12 \pm 2.1 mV and -67.9 \pm 1.7 mV for ΔF and G in control, -64.4 \pm 2.1 mV and -67.2 \pm 1.5 mV for ΔF and G in 100 μ M RTG). (F) Fluorescence sweeps and $\Delta F(\text{RTG})/\Delta F(\text{control})$ summary data from depolarizations to +40mV from -140mV in the presence (green) or absence (grey) of 100μM RTG for Q3*VCF(1.28 \pm 0.06, n=12) and Q3*VCF[W265F](1.00 \pm 0.02, n=11)

PIP₂ influences pore coupling and VSD movement

The membrane phospholipid PIP₂ is an essential co-factor and regulator of KCNQ channels. PIP₂ is required for pore opening, and its hydrolysis underlies G_q-coupled receptor-mediated channel inhibition (Suh *et al.*, 2006; Zhang *et al.*, 2003). Recent investigations of KCNQ1 suggest this requirement reflects PIP₂-dependent conformational coupling of the VSD and PD (Zaydman and Cui, 2014; Zaydman *et al.*, 2013). Therefore, we reasoned that PIP₂-dependent coupling might also influence transduction of RTG binding from the pore to the voltage sensor. To evaluate the influence of PIP₂, we co-expressed Q3*VCF with the voltage-sensitive phosphatase Ci-VSP, allowing time-resolved control of PIP₂ levels using depolarization to activate the phosphatase (Murata *et al.*, 2005). At depolarized potentials that activate Ci-VSP, we observed a fluorescence deflection that persists even as pore closure is induced by PIP₂ depletion (Fig. 4.3A). A subsequent identical depolarization produces a similar fluorescence change but little current, illustrating that PIP₂ is not required for voltage sensor movement, as the voltage sensor appears to operate independently of the pore in the absence of PIP₂ (Figure 4.3A).

There are important quantitative differences in voltage sensor fluorescence signals after PIP₂ depletion. There is a pronounced increase in the magnitude of the fluorescence signal that occurs simultaneously with PIP₂ depletion (Figure 4.3B). This is not immediately obvious in Figure 4.3A because the Ci-VSP mediated PIP₂ depletion is occurring on approximately the same time scale as activation of current and fluorescence. However, in oocytes with slower current rundown kinetics, there is a clear correlation between the time course of current decay and a second phase of fluorescence unquenching at +100 mV where Ci-VSP becomes activated (Figure 4.3B, see also 4.3E). To confirm that this unusual behavior was due to PIP₂ depletion, we performed the same protocol in the absence of Ci-VSP (Fig. 4.3C), and observed that depolarizations to +100

mV compared to +20mV elicited fluorescence signals with a much smaller increase in magnitude, and lacking the unquenching phase (Fig. 4.3B-D). Although perhaps not ideal, even more convincing evidence of this effect came from non-uniformly voltage clamped oocytes, where artefactual irregular kinetics of current decay closely overlap with kinetics of fluorescence unquenching (Figure 4.3E,F).

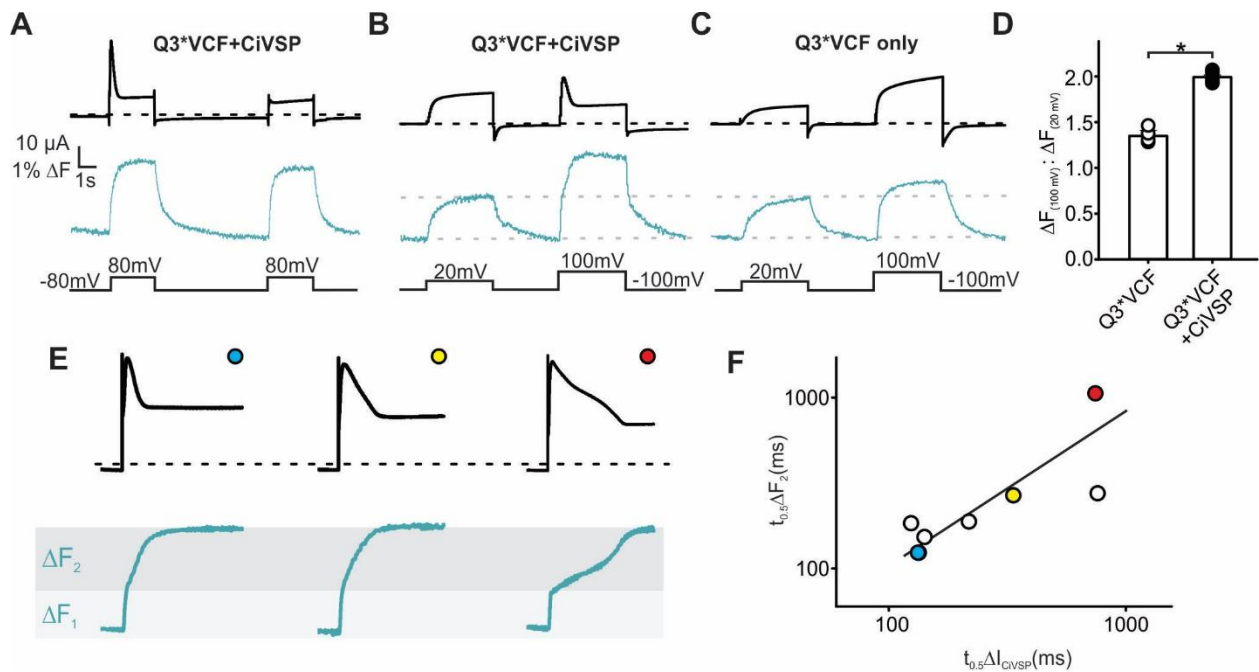


Figure 4.3: PIP₂ depletion alters Q3*VCF fluorescence. (A) Sample trace from an oocyte expressing Q3*VCF + Ci-VSP, highlighting the effects of PIP₂ depletion on current (black) and fluorescence (green). (B and C) When Ci-VSP is present, PIP₂ depletion at highly depolarized potentials produces a significant increase in ΔF . (D) Summary of ΔF (+100mV)/ ΔF (+20mV) for Q3*VCF and Q3*VCF + Ci-VSP (1.35 ± 0.05 and 1.99 ± 0.02 , respectively, n=4 and 5). (E) Sample current and fluorescence traces from oocytes expressing Q3*VCF + Ci-VSP displaying variable kinetics of PIP₂ rundown at +100mV. (F) Time to half maximal Ci-VSP induced current rundown plotted against time to half maximal increase in secondary fluorescence component ΔF_2 for several oocytes (n=8).

Lastly, we performed a triple pulse protocol comprising two depolarizations to +20 mV, separated by a depolarization to +100 mV (to deplete PIP₂). In this experiment, PIP₂ depletion consistently facilitates the fluorescence signal in the second +20 mV depolarization (Fig. 4.4A, B). A final important observation, revisited later, is that PIP₂ depletion causes acceleration of voltage sensor deactivation (Fig. 4.4C), while activation kinetics are largely unchanged. Taken together, these results highlight that PIP₂ enables pore opening in response to voltage sensor movement, and influences the dynamics and conformations experienced by the VSD.

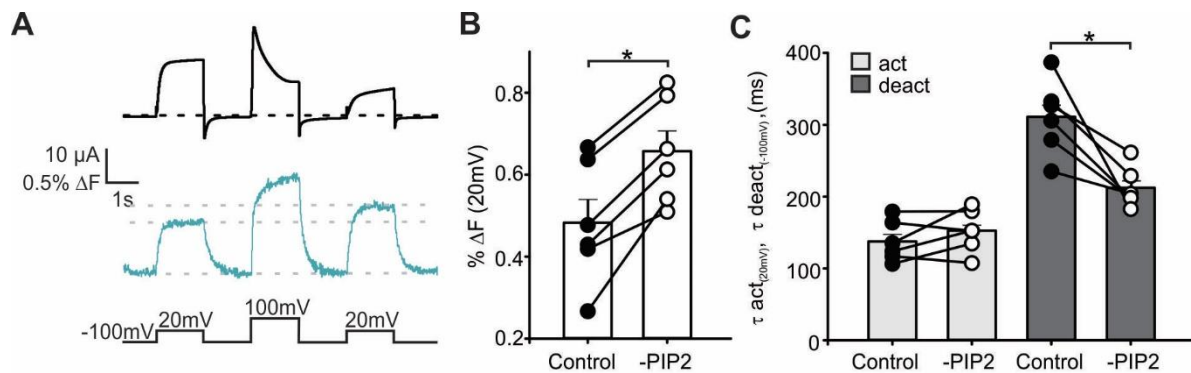


Figure 4.4: PIP₂ depletion produces a voltage independent increase Q3*VCF fluorescence and acceleration of deactivation kinetics. (A) A triple-pulse protocol was applied to assess the impact of PIP₂ depletion on ΔF magnitude and kinetics. (B) Summary graph displaying the increase in ΔF magnitude at +20mV after a PIP₂ depleting +100mV pulse, including paired data points from individual oocytes (0.48 ± 0.06 % ΔF pre-rundown, 0.66 ± 0.05 % ΔF post-rundown). (C) Kinetics of activation and deactivation at +20mV before and after PIP₂ depleting pulse (τ_{act} : 137.7 ± 11.6 ms in control, 152.8 ± 12.2 ms in RTG; τ_{deact} : 311.2 ± 21.1 ms in control, 212.4 ± 11.6 ms in RTG).

Retigabine protects channels from Ci-VSP mediated rundown

We next examined how PIP₂ influences transduction of RTG binding to changes in voltage sensing. We began by using Ci-VSP co-expression to deplete PIP₂ and observed that the effects of Ci-VSP are considerably weakened in the presence of RTG (Fig. 4.5A). In this experiment, voltage pulses between -140mV and +100mV were delivered, followed by a test pulse to -20 mV to observe the extent of PIP₂ depletion after different pre-pulse voltages. In control conditions, this yields a characteristic bell-shaped relationship, reflecting channel activation at modest depolarizations (insufficient to activate Ci-VSP), and strong inhibition of current at positive voltages where Ci-VSP becomes active. In the presence of RTG, channel activation is observed at more negative voltages, as expected (due to the RTG-mediated shift in channel activation). More importantly, there is prominent protection against current rundown at positive voltages (Figure 4.5A), which is reminiscent of previously reported protective effects of RTG against M1 receptor-mediated current rundown (Tatulian *et al.*, 2001). The rundown of current after pulsing to +60mV is attenuated by $54.6 \pm 6.5\%$ in the presence of RTG (Fig. 4.5E, black line). This effect is absent in the W265F mutant (Fig. 4.5B), demonstrating that RTG does not directly inhibit Ci-VSP activity, but instead appears to strengthen channel-PIP₂ interaction, leading to ‘protection’ of channel-associated PIP₂.

We exploited the RTG ‘protection’ effect to investigate reciprocal influences of PIP₂, RTG, and potential PIP₂-interacting residues. The cytoplasmic side of KCNQ channels has a high density of basic residues that may be involved in PIP₂ interaction, especially in the S2-S3 linker and the proximal C-terminus immediately following the S6 helix (Fig. 4.5E, F, G). We performed a charge neutralization scan by mutating positively charged residues to alanine on the Q3*VCF background (Fig. 4.5C-E). In addition to multiple alanine point mutations, we modified a cluster of consecutive

basic residues (“KRRK motif”) in the proximal KCNQ3 C-terminus. For this charge cluster we generated constructs expressing double alanine substitutions, along with a construct in which all four residues were neutralized (termed S6-AARK, S6-KRAA, S6-AAAA). Relative to KCNQ1, there is a slightly higher number of charged side chains in the S2-S3 and C-termini of KCNQ2 and KCNQ3 (Figure 4.5F, G), with notable differences in the “KRRK” cluster.

We reasoned that mutation of residues important for channel:PIP₂ interactions might alter RTG protection against Ci-VSP mediated rundown, potentially by reducing the association time between channels and PIP₂. In the absence of RTG, most mutants exhibited similar sensitivity to Ci-VSP mediated rundown (Fig. 4.5C). However, we observed a range of RTG-mediated protection in these mutants. Most significantly, multiple mutations in the proximal C-terminus abolished RTG-induced protection from Ci-VSP (Fig. 4.5C, D, and E). Currents from the K248A, R364A, H367A, S6-AARK and S6-KRAA mutants were nearly completely inhibited by Ci-VSP at +60mV, even in the presence of RTG (Fig. 4.5E). An interesting exception in this region was the K358A mutant, which was insensitive to Ci-VSP in both the presence and absence of RTG (Fig. 4.5E). The protection effect is retained to varying degrees for all S2-S3 mutants, with R190A and K192A exhibiting slightly weaker protection against Ci-VSP-mediated rundown (Figure 4.5E).

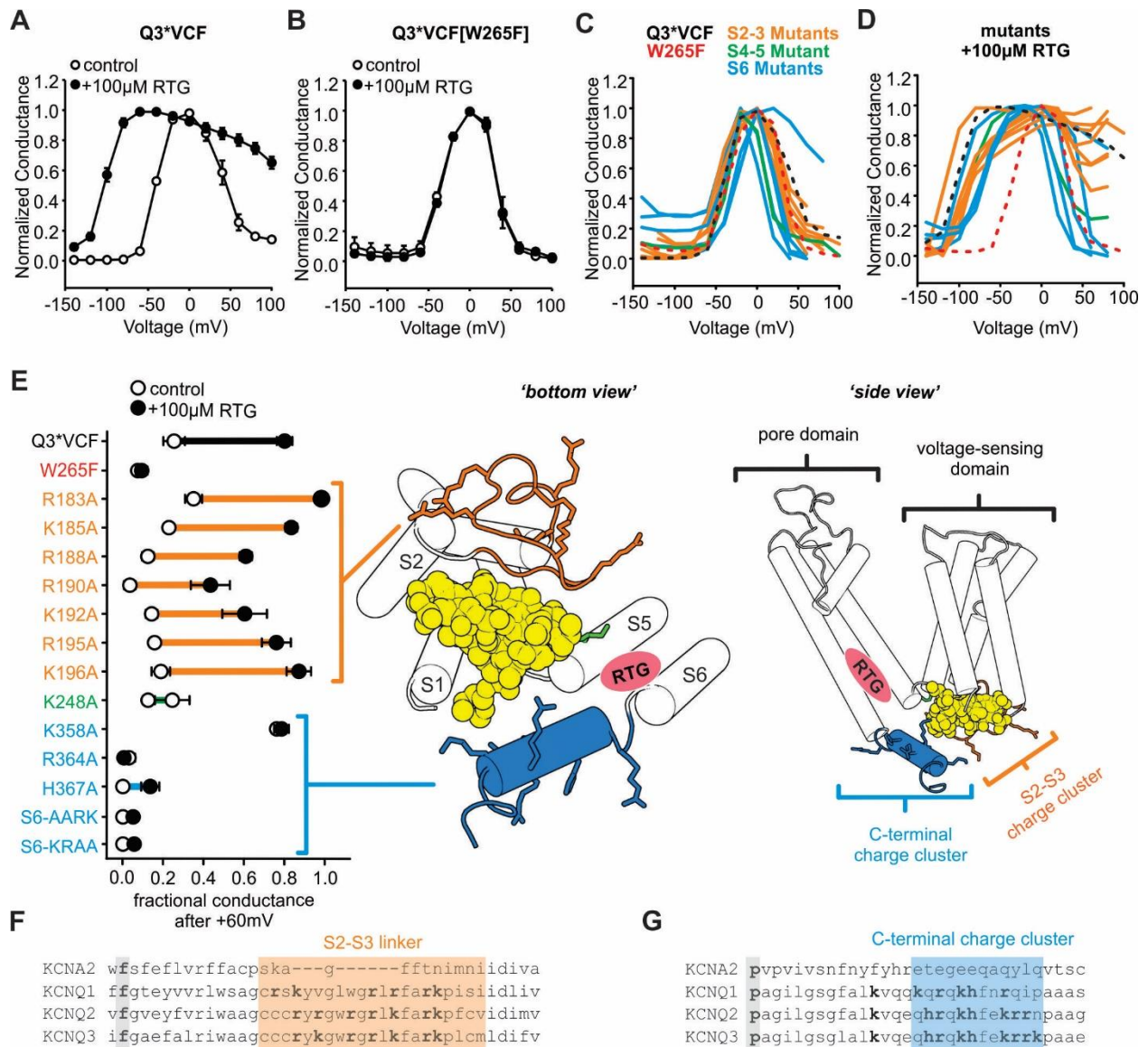


Figure 4.5: RTG induced strengthening of channel PIP₂ interactions relies on C-terminal basic residues. (A and B) Summary GV curves obtained from oocytes co-expressing Ci-VSP with Q3*VCF (A) or Q3*VCF[W265F](B), in the presence (filled circles) or absence of 100 μ M RTG (n=6 and n=5, respectively). (C and D) Summary GV curves obtained from channels expressing various mutations (shown in E and color coded by region) on the background of Q3*VCF and co-expressed with Ci-VSP, in the presence (D) or absence (C) of 100 μ M RTG (n=4 - 6 for all constructs). (E) Summary of Ci-VSP induced current rundown at +60mV, highlighting the necessity of C-terminal residues in enabling RTG mediated PIP₂ rundown protection. (E, right) Illustrations highlight the positions of cytosolic basic residues. (F and G) Sequence alignments highlighting the conservation of poly-basic motif in the S2-S3 linker (F) and C-termini (G) of KCNQ1-3 channels.

More conventional characterization of these charge neutralization mutants was consistent with the RTG protection assay. Neutralization of S2-S3 linker charges had modest effects on current expression, $V_{1/2}$ of activation, or response to 100 μM RTG (Fig. 4.6A, B). In contrast, mutation of K248 (S4-S5 linker) and the majority of basic residues in the proximal C-terminus had profound effects: all except K358A led to $>50\%$ reduction in currents, with K248A, R364A, S6-AARK and S6-AAAA causing $>85\%$ reduction in currents (Fig. 4.6A). The S6-AAAA mutation was the most disruptive, as currents were undetectable in the absence of RTG, although 100 μM RTG rescued a small amount of ionic current and enabled the collection of conductance-voltage relationships (Fig. 4.6B). With the exception of K358A, all proximal C-terminus mutants attenuated (but did not abolish) the RTG-induced shift in $V_{1/2}$ of activation.

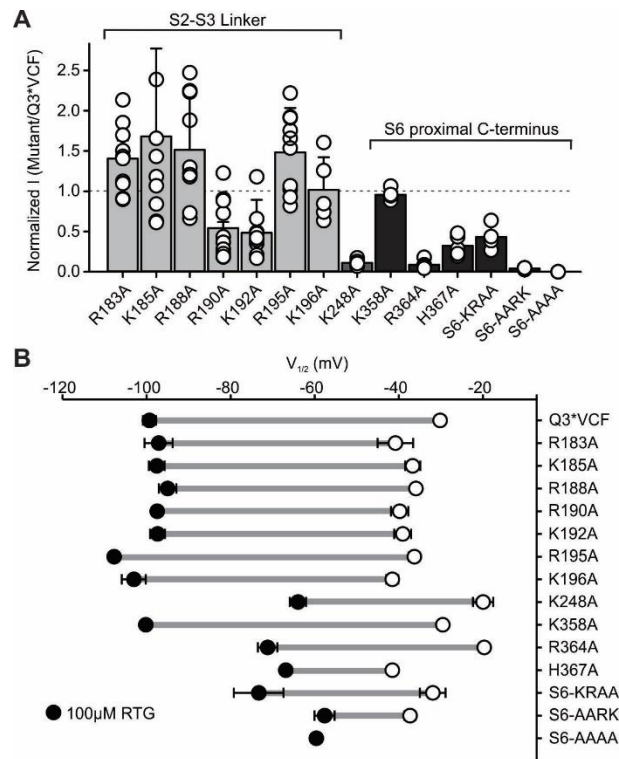


Figure 4.6: Functional characterization of Q3*VCF charge neutralization mutants. (A) Summary of current expression levels one or two days after injection for all mutants normalized to Q3*VCF ($n=4-10$). (B) Activation $V_{1/2}$ values for all constructs in the presence or absence of 100 μM RTG ($n=4$).

Structural basis for PIP₂-mediated VSD:PD coupling

Overall, the charge neutralization scan highlights the importance of charged residues in the proximal C-terminus for channel function and suggest this region is important for normal transduction of RTG binding to altered VSD function. Based on molecular models of KCNQ3, we suggest a possible structural basis for the observed effects (Fig. 4.5E). The rich density of positively charged sidechains on the intracellular surface forms a favorable environment for interaction of negatively charged PIP₂ headgroups (a population of docked PIP₂ headgroup conformations are illustrated as a yellow density in Figure 4.5E). We modeled the proximal C-terminus as a helical extension of the S6 helix in a molecular model of open KCNQ3, based on a fragment of the structure of a chimeric KCNQ2/3 proximal C-terminus (Strulovich *et al.*, 2016). We speculate that these C-terminal positive charges require interaction with a resident PIP₂ molecule residing on the intracellular face of the channel, near the VSD/PD interface – with the PIP₂ headgroup ‘sandwiched’ between the S2-S3 linker charges and the C-terminus. Although this is a hypothetical model, and we do not know the specific orientation of the C-terminal extension of S6, a requirement for something resembling the proposed configuration would account for both poor efficiency of channel opening in C-terminal mutants (Fig. 4.6) or PIP₂ depletion (Figs. 4.3,4.5). Moreover, stabilization of this configuration by RTG would account for the protection of PIP₂ against Ci-VSP rundown, and the loss of protection after neutralization of critical C-terminal residues. We introduce the model here to provide context and interpretation for results that follow.

The C-terminus is essential for normal pore-VSD coupling

We investigated this potential model and the role of the C-terminus in the transduction of RTG effects in more detail using VCF. Despite the extremely small currents detectable from mutations in the KRRK cluster, mutant channels generated robust voltage-dependent fluorescence signals that were consistently much larger than signals from Q3*VCF (Fig. 4.7A). These observations suggest that the mutants express very well at the cell surface but are likely hampered by weak VSD-pore coupling. We also observed marked RTG enhancement of currents in these mutants (Fig. 4.7C), suggesting that there is a ‘reserve’ of channels with dysfunctional pores that can be rescued by RTG.

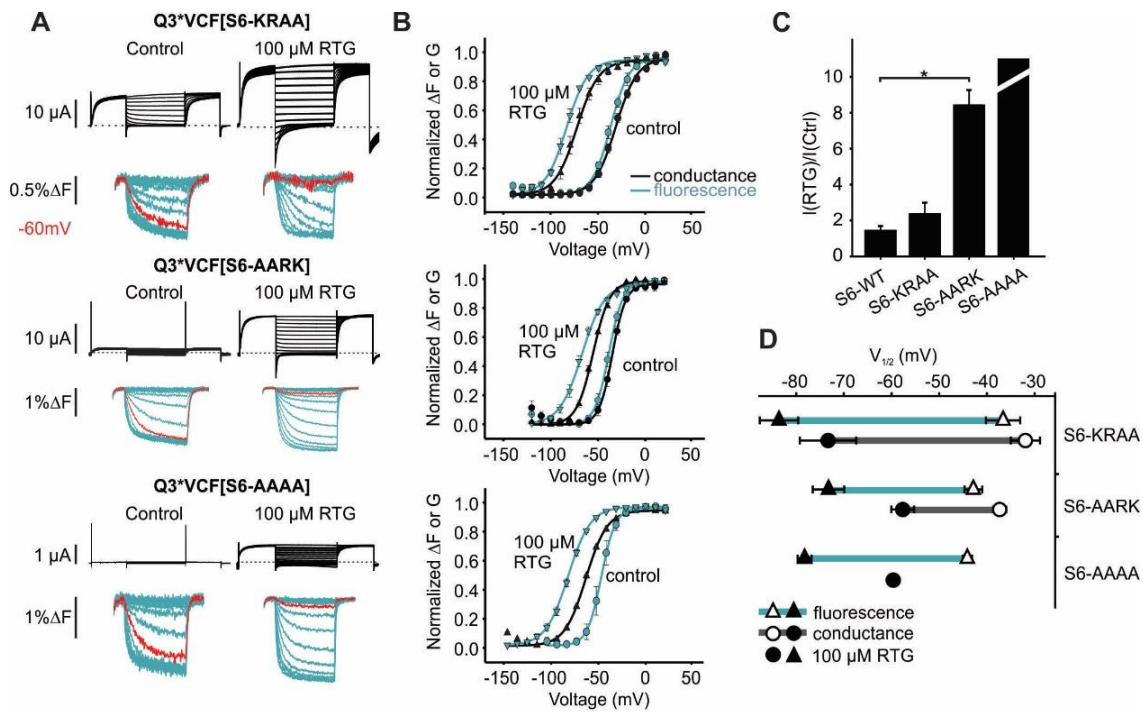


Figure 4.7: RTG effects on the VSD are partially mediated by C-terminal residues involved in VSD-PD coupling. (A) Sample recordings of current (black) and fluorescence (green) obtained from Q3*VCF with charge neutralizations in their S6-KRRK motifs. -60mV sweeps (red) highlight RTG induced shifts in the voltage dependence of ΔF , which remain even as pore function is progressively lost. (B) Summary graphs of the voltage and RTG dependence of ΔF and G for mutants shown in A ($n=4-10$). (C) Summary of RTG induced enhancement of current at +20mV for S6-WT (1.4 ± 0.3), S6-KRAA (2.3 ± 0.6), S6-AARK (8.4 ± 0.9), and S6-AAAA (immeasurable due to absence of currents in 0RTG) ($n=4-10$). (D) $V_{1/2}$ values for ΔF and G , highlighting the RTG mediated shift in fluorescence (green lines).

There were two pronounced differences in the effects of RTG on the C-terminal mutant channels. Firstly, the RTG-mediated shift of the conductance-voltage relationship was weakened relative to Q3*VCF channels (Fig. 4.7B, D), and this effect correlated with the impact of mutations on overall channel function (KRAA channels were more strongly shifted than AARK channels). However, the voltage-dependent shift of the fluorescence-voltage relationship was less perturbed, resulting in a dissociation of FV and GV that was very pronounced in the presence of RTG (Fig. 4.7B, D). Secondly, KRRK mutants markedly altered the kinetic effects of RTG (Fig. 4.8). In Q3*VCF channels, RTG application causes dramatic deceleration of fluorescence deactivation (Figs. 4.2B, 4.8A), and generally leads to the appearance of sigmoidal kinetics (loss of exponential decay kinetics). In the C-terminal mutants, this RTG-mediated effect is attenuated or lost entirely (in S6-AARK or AAAA mutants), suggesting that pore binding of RTG is no longer transduced normally to the VSD (Fig. 4.8A and B). Also, the accelerated deactivation kinetics closely resemble the accelerated deactivation caused by PIP₂ depletion (Fig. 4.4C, Fig. 4.8B). In the context of the structural model described earlier (Fig. 4.5E), these findings are consistent with PIP₂-dependent ‘bridging’ of the open conformation of the C-terminus and active voltage sensor being required for RTG to exert its dramatic effect on voltage sensor deactivation (as PIP₂ depletion or C-terminal mutants abolish the effect). In contrast, RTG-mediated acceleration of the activation kinetics is weakly affected in C-terminal mutants or after PIP₂ depletion (Fig. 4.8C, D).

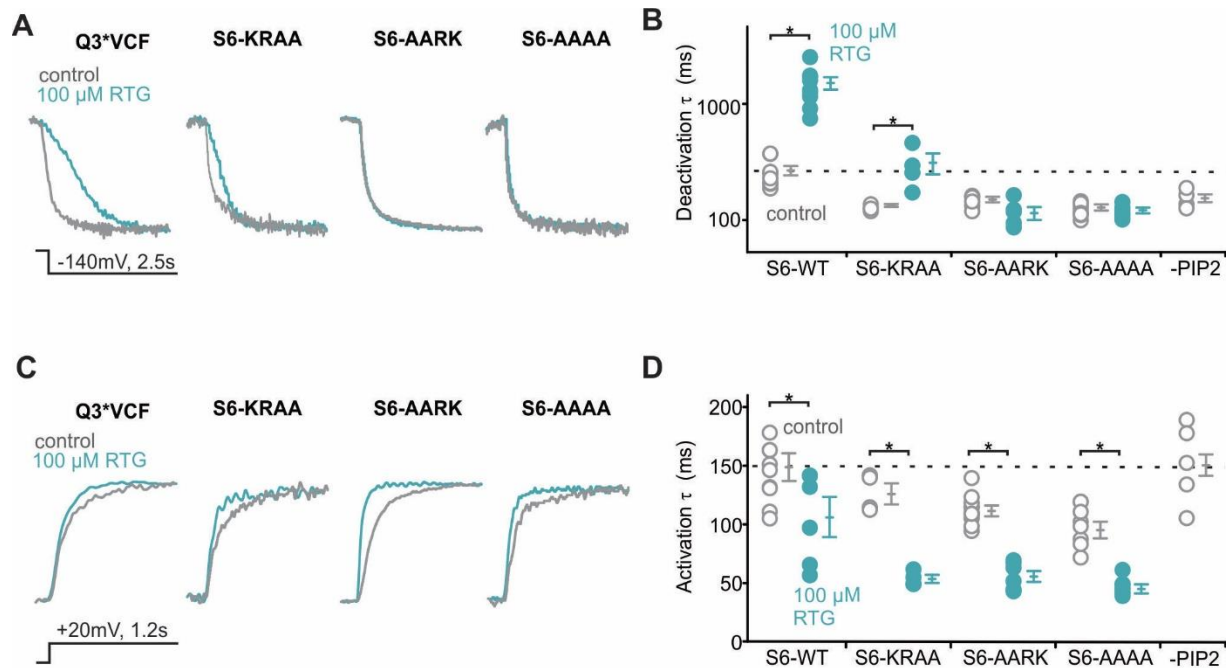


Figure 4.8. S6-KRRK mutations abolish RTG effects on Q3*VCF fluorescence deactivation, but not activation. (A and C) Representative sweeps displaying the impact of RTG (green) on the deactivation (A) and activation kinetics (C) of fluorescence at -140mV and +20mV, respectively. (B and D) Summary of kinetics values (single exponential τ , $n=4-10$).

Residual PIP₂-independent coupling of retigabine effects

Mutations in the KRRK cluster cause attenuated RTG sensitivity, and exert several additional related effects: low efficiency of pore opening, and weakened PIP₂ ‘protection’ that we interpret as a reflection of destabilized PIP₂ binding. However, these mutations do not completely uncouple effects of RTG on the voltage sensor, which still exhibits significant RTG-mediated shifts (Fig. 4.7B, D). In order to distinguish the possibility of some persistent PIP₂-mediated coupling of RTG effects (eg. incomplete effects of the C-terminal mutations) or an alternative mechanism of coupling, we exploited the increased susceptibility of KRRK mutants to Ci-VSP mediated PIP₂ rundown. Specifically, we used the Q3*VCF[S6-AARK] mutant, which expresses a small amount of current that can report Ci-VSP induced PIP₂-depletion, together with a robust

fluorescence signal, affording more confidence that channel:PIP₂ interactions could be abolished in this channel even in the presence of RTG (Fig. 4.5).

With Ci-VSP co-expression, we recorded the voltage-dependence of Q3*VCF[S6-AARK] fluorescence using a holding potential of +80mV (for sustained Ci-VSP activation), to test the voltage sensor effects of RTG with maximal PIP₂ depletion (Fig. 4.9A). Thus far, this appears to be the most efficient and complete method of PIP₂ depletion that we have been able to devise. There are no detectable KCNQ3 currents in the presence or absence of RTG, despite very pronounced fluorescence signals, indicating that the Ci-VSP is functioning properly. The data demonstrate that even in the absence of PIP₂, RTG stabilizes VSD activation leading to a -31.1 ± 1.9 mV hyperpolarizing shift in the FV relationship (Fig. 4.9B), similar to the shift observed without Ci-VSP co-expression (Fig. 4.7D, -30.4 ± 3.8 mV).

These findings are consistent with the kinetic effects of PIP₂ depletion and C-terminal perturbations in different RTG conditions. Abolishing the putative C-terminal/PIP₂ interactions leads to accelerated deactivation, but more importantly, wholly abolishes the effects of RTG on voltage sensor deactivation – drug binding in the pore no longer appears to immobilize the activated conformation of the voltage sensor. However, under conditions that strongly reduce channel:PIP₂ interactions, effects of RTG on voltage sensor activation appear mostly intact (Fig. 4.8C,D). Taken together these data suggest that RTG has dichotomous effects on voltage sensor deactivation (mediated by a C-terminal interaction with PIP₂) and activation (mediated by a PIP₂-independent mechanism).

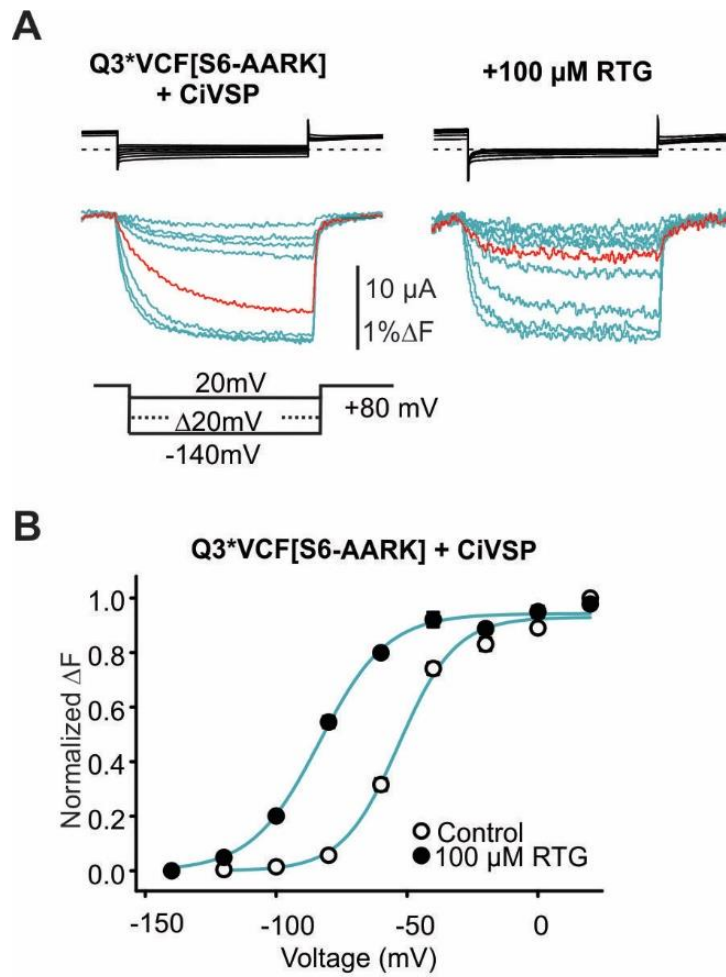


Figure 4.9: RTG activates the VSD in ‘PIP₂-less’ Q3*VCF [S6-AARK] channels. (A) Effects of RTG on the voltage dependence of Δ F from Q3*VCF [S6-AARK] was assessed under PIP₂ depleted conditions. (B) Summary of FV relationships \pm RTG, highlighting the RTG induced shift in the absence of PIP₂ ($V_{1/2} = -53.1 \pm 0.8$ mV in control and -84.2 ± 1.1 mV in 100 μ M RTG, $n=4$).

DISCUSSION

Retigabine is a powerful opener of neuronal KCNQ channels, with a well-defined binding site in the channel pore. However, mechanisms that couple the pore to the voltage sensing domain, and link retigabine binding to altered voltage sensitivity are poorly understood. Previous investigations of voltage-sensing in KCNQ channels have focused primarily on KCNQ1, demonstrating that VSD movements in KCNQ1 are dynamically regulated by association with auxiliary subunits such as KCNE1/3 and by PIP₂, which affect not only the VSD response to voltage, but also coupling of VSD movements to opening of the pore gate (Barro-Soria *et al.*, 2014, 2015; Osteen *et al.*, 2010; Ruscic *et al.*, 2013; Zaydman *et al.*, 2013). Although neuronal KCNQ channels like KCNQ3 share this requirement for PIP₂, their unique sensitivity to retigabine has enabled novel insights into structural motifs that govern the interplay between voltage-sensing, pharmacology, and regulation by PIP₂.

We have demonstrated that retigabine shifts the voltage-dependence of Q3*VCF fluorescence in parallel with channel conductance, directly demonstrating drug-mediated stabilization of the activated voltage-sensor. At ambient PIP₂ levels, voltage-dependence of KCNQ3 activation was modulated over a wide range with retigabine, and close coupling of pore and voltage sensor was retained (Fig. 4.2A). This close coupling resembles observations made in KCNQ1 in the absence of KCNE1 (Osteen *et al.*, 2010). PIP₂ depletion resulted in significant changes of voltage sensor dynamics and coupling that we describe colloquially as ‘unhinging’ of the voltage sensor from the pore.

One obvious feature of the ‘unhinged’ voltage sensor was a dramatic change in the magnitude of the fluorescence signal (Fig. 4.3). We suggest that this effect reflects the adoption of novel VSD conformations once the constraints imposed by PIP₂-dependent pore coupling are

removed. Given that the extracellular environment around the fluorescent tag has not been manipulated in these experiments, it seems reasonable to infer that the much larger fluorescence signals after PIP₂ depletion indicate a significant change in VSD conformation when uncoupled from the pore. It is noteworthy that KCNQ1 channels (tagged at the equivalent position) exhibit much larger fluorescence changes than we have observed in KCNQ3. Although not yet tested directly, one interesting possibility is that this is due to the lack of the critical KRRK cluster present in KCNQ2-5 (and possibly the smaller number of S2-S3 basic residues) that appears to constrain voltage sensor movement (Figs. 4.3, 4.5).

A second feature of the ‘unhinged’ PIP₂-depleted voltage sensor is altered deactivation kinetics of the voltage sensor fluorescence. This feature is particularly prominent in the series of ‘KRRK’ neutralizations (Figs. 4.7, 4.8), as voltage-sensor deactivation becomes accelerated in correlation with loss of channel function. Moreover, deactivation of the ‘unhinged’ voltage sensor appears wholly insensitive to RTG, unlike the dramatic deceleration of deactivation in Q3*VCF. A previous study reported that PIP₂ depletion prevents RTG activation of KCNQ3 channels (Zhang *et al.*, 2013). We were thus surprised to find that despite our best efforts to deplete PIP₂ and ‘unhinge’ the voltage sensor, RTG was still able to induce a substantial hyperpolarizing shift of the VSD (Fig. 4.9). The persistent RTG-mediated shift appears to be due primarily to an effect on VSD activation kinetics, but not deactivation, implying that RTG binding to the pore is communicated in multiple distinct ways to the VSD. Our findings seem to indicate separable PIP₂-dependent and PIP₂-independent modes of coupling between the KCNQ pore and voltage sensors, which specifically affect deactivation or activation, respectively (Figs. 4.8,4.9).

The convergent effects of KRRK mutations and PIP₂ depletion on channel function, voltage-sensor deactivation, and weakened PIP₂ protection, can be rationalized with a model as

shown (Fig. 4.5E). We suggest that the proximal C-terminus and S2-S3 linker can interact with PIP₂, with the lipid ‘sandwiched’ between these motifs. This creates a PIP₂-mediated physical association between the C-terminus (adjacent to the S6 gate) and the VSD. When PIP₂ is abundant, these reciprocal interactions between the VSD, PIP₂, and pore, may be reflected in the close coupling of the FV and GV relationships observed under basal conditions. An intuitive explanation is that when the C-terminus is closely engaged with the voltage sensor (via PIP₂), mutual constraints on their motions cause them to operate with similar voltage-dependence. Perturbation of either of these putative partners (KRRK mutations, or PIP₂ depletion) leads to dissociation of the FV and GV, which is especially apparent in RTG (Fig. 4.7). The influence of retigabine towards stabilizing the engaged C-terminus:PIP₂:VSD arrangement also seems to emerge in the protection of PIP₂ against Ci-VSP mediated degradation. As mentioned, this mirrors earlier characterizations of retigabine demonstrating protection against M1 receptor-mediated rundown. These types of observation may have important implications related to drug mechanism, suggesting that in addition to silencing neurons through the activation of KCNQ channels, RTG is likely to blunt the sensitivity of neurons to endogenous receptor-mediated pathways that operate through PLC mediated PIP₂ hydrolysis.

A prediction of our structural model is that S2-S3 linker mutations might also abolish PIP₂-dependent pore:sensor coupling. We did not observe dramatic effects of S2-S3 linker mutations, although certain mutants, such as R190A, exhibited both weaker PIP₂ protection and less overall current (Fig. 4.5, Fig. 4.6). These residues are good candidates for deeper investigation in the future, although we suspect that there may be considerable redundancy of positively charged S2-S3 positions contributing to PIP₂ interactions, as there are 8 charged residues in a relatively short ~20 amino acid loop. Previous work has proposed that the S4-S5 linker also contributes to channel-

PIP₂ interactions in KCNQ2 and KCNQ3 (Zhang *et al.*, 2013; Zhou *et al.*, 2013). This is supported by our observation that introduction of the S4-S5 linker K248A mutation produced a significant inhibitory effect on channel function and RTG sensitivity in our study.

Collectively, our data indicate that structural changes that occur at the VSD-PD interface upon VSD activation orient PIP₂ molecules to interact with a cluster of basic residues below the S6 helix in the proximal C-terminus to enable pore opening. When RTG binds to the channels, it exerts bi-directional effects on the VSD and PD, simultaneously promoting VSD activation, while strengthening PIP₂ dependent VSD-PD coupling to promote pore activation and further enhance voltage sensitivity.

Chapter 5: Functional Stoichiometry of Retigabine Binding in KCNQ3

Channels

BACKGROUND AND SUMMARY

In this study we have investigated the functional stoichiometry of retigabine actions by manipulating the number of available retigabine binding sites in concatameric KCNQ3* channels. We demonstrate that in the presence of intermediate retigabine concentrations, channels exhibit biphasic conductance-voltage relationships. This behavior suggests that retigabine can exert its effects in a nearly ‘all-or-none’ manner, with channels exhibiting either fully shifted or unshifted behavior. Supporting this notion, we find in concatameric channels containing defined numbers of retigabine sensitive subunits that only a single binding site is required for a nearly maximal retigabine effect, and can recapitulate the apparent ‘all-or-none’ features of retigabine regulation observed in KCNQ3. Taken together these data suggest that a single retigabine binding event can generate a large shift of the KCNQ3 conductance-voltage relationship, and that retigabine-mediated shifts of the KCNQ conductance-voltage relationship may reflect concentration-dependent accumulation of channels in a shifted gating mode.

RESULTS

Biphasic conductance-voltage relationships at intermediate retigabine concentrations

KCNQ2-5 channels exhibit a pronounced hyperpolarizing shift of the voltage-dependence of activation in the presence of saturating concentrations of retigabine. In addition to the pore domain-delimited binding site for retigabine, there are also several reports suggesting an alternative binding site for certain KCNQ openers in the voltage sensing domain (Wang *et al.*, 2017). This alternative site appears to be absent or only weakly effective in KCNQ3 channels, thus making them a good model to investigate retigabine interactions and effects via the conserved pore

site. Although reports vary slightly in terms of the magnitude of this shift, we routinely observe large shifts of ~60 mV in saturating concentrations of retigabine (100-300 μ M) for KCNQ3* (KCNQ3* in figures and remaining text) channels expressed in *Xenopus laevis* oocytes.

In ongoing experiments investigating KCNQ channel openers, we frequently observed a shallow slope of the conductance-voltage relationship at intermediate concentrations of retigabine, when compared to control or saturating conditions. We investigated this phenomenon in more detail with closely spaced voltage intervals, and observed prominent ‘splitting’ of the conductance-voltage relationship. This is apparent in Fig. 5.1A (3 μ M retigabine), in which tail current magnitudes are closely spaced after prepulses to intermediate voltages, leading to a plateau between -80 mV and -50 mV in the conductance-voltage relationship (Fig. 5.1B). This biphasic conductance-voltage relationship is well fit with a sum of two Boltzmann functions (Table 5.1). There is a dose-dependent increase in the contribution of the shifted component of the conductance-voltage relationship, with the ‘left-shifted’ component becoming more prominent with increasing retigabine concentrations (Fig. 5.2A). Using the magnitude of the shifted fraction, we calculated an EC₅₀ of 4.4 μ M with a Hill coefficient close to 1 (Fig. 5.2B). There is a modest increase in the magnitude of the V_{1/2} of the shifted component, from -93 mV at 1 and 3 μ M retigabine, to -103 mV at saturating concentrations (Table 5.1). In addition, the ‘right-shifted’ component was best fit with a V_{1/2} of -41 mV in control conditions, and progressed to more hyperpolarized V_{1/2} values at higher concentrations. At the highest retigabine concentrations, we could not confidently generate fit parameters for the ‘unshifted’ component, and so we have only reported parameters for a single component Boltzmann.

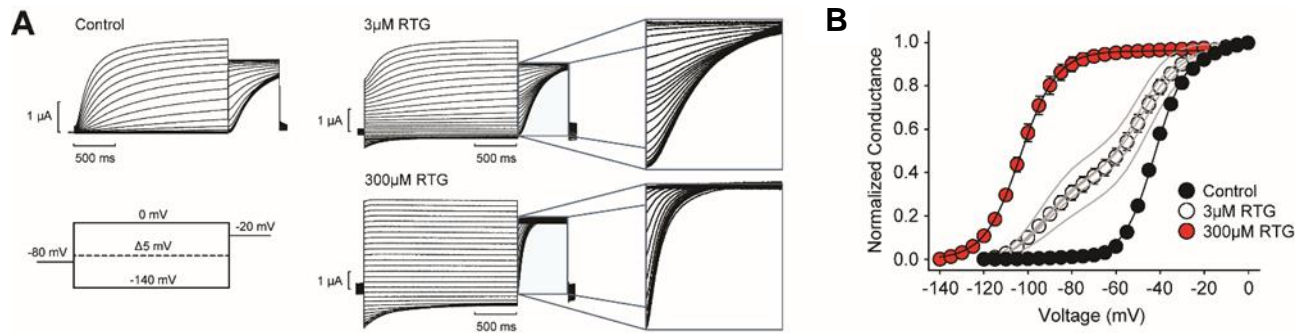


Figure 5.1: A biphasic conductance-voltage relationship emerges at intermediate RTG concentrations. (A) Two-electrode voltage clamp recordings from *Xenopus laevis* oocytes expressing KCNQ3* in Ringer's solution containing 0, 3 μM , and 300 μM RTG using the voltage-step protocol shown. Highlighted in the expansions are the biphasic tail currents evident in 3 μM RTG (B) Summary of GV relationships in different RTG concentrations. Grey lines represent fits of data from individual oocytes in 3 μM RTG, and circles represent averages.

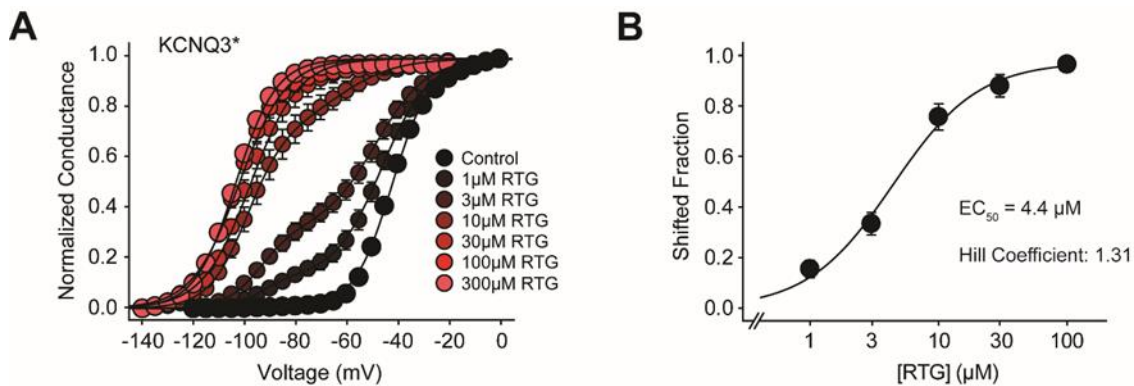


Figure 5.2: Conductance-voltage relationships for KCNQ3* in different RTG concentrations. (A) Summary of normalized tail current recordings from multiple oocytes. Notice the biphasic nature of GV curves at intermediate RTG concentrations. (B) The shifted fraction a at different RTG concentrations was fit with a Hill equation.

RTG Concentration (μM)	Shifted Component, a	$V_{1/2a}$ (mV)	$V_{1/2b}$ (mV)	k_a	k_b	n
0	-	-	-41.8 ± 0.7	-	7.6 ± 0.2	5
1	0.12	-93.3 ± 0.7	-46.0 ± 1.1	5.9 ± 0.4	9.2 ± 0.3	5
3	0.32	-93.5 ± 0.3	-48.3 ± 1.2	6.9 ± 0.1	9.9 ± 0.6	5
10	0.72	-98.8 ± 0.7	-62.0 ± 1.7	7.6 ± 0.2	11.4 ± 0.5	5
30	1	-97.4 ± 2.4	-	9.4 ± 1.3	-	5
100	1	-103.3 ± 0.8	-	7.9 ± 0.7	-	5
300	1	-102.0 ± 1.5	-	9.2 ± 0.8	-	5

Table 5.1: Values for double-Boltzmann fits of recordings from KCNQ3* in different RTG concentrations. The shifted component a , represents the fraction of the total current fit with the hyperpolarized component. The un-shifted component $b= 1-a$. Values for k_a and k_b represent the slope factor for respective fits. In concentrations $>10\mu$ M RTG, the un-shifted component was unresolved, and thus, data was fit to a single shifted component.

Generation of a tetrameric KCNQ3* construct

The retigabine-induced biphasic conductance-voltage relationships suggest that retigabine acts roughly in an ‘all-or-none’ manner, reminiscent of recently reported effects of gamma-subunits of BK channels (Gonzalez-Perez *et al.*, 2015). That is, altered drug concentrations appear to govern the ratio of channels in ‘shifted’ and ‘unshifted’ modes, rather than progressively shifting the $V_{1/2}$ to more hyperpolarized voltages. As described for BK channel modulation by gamma-subunits, there can be numerous stoichiometric channel:modulator configurations that generate an apparent ‘all-or-none’ effect. Experiments with homomeric KCNQ3* do not definitively demonstrate the number of retigabine molecules required to induce the ‘shifted’ gating mode in KCNQ3*, and also do not demonstrate whether varying numbers of retigabine-sensitive subunits within a channel generate differential gating shifts. In order to investigate the stoichiometry of retigabine effects, we generated concatenated KCNQ3 channel constructs with varying numbers of retigabine-sensitive subunits (containing varying numbers carrying the W265Phe mutant, which

abolishes the retigabine effect (Wuttke *et al.*, 2005)). Throughout the study, W refers to a wild-type W265-containing subunit, and F refers to a W265Phe mutant subunit (so for example, ‘WWFF’ contains two WT subunits, and two W265Phe subunits). We confirmed that our plasmids encoded expression of full-length tetramers using Western blots (Fig. 5.3A), and also confirmed that concatemeric channel generation did not alter the conductance-voltage relationship or other general gating properties relative to channels generated from assembly of four identical KCNQ3* monomers (Fig. 5.3B, C). It should be noted that we had difficulties using the KCNQ3 antibody on lysates from *Xenopus laevis* oocytes, so Western blots were carried out using lysates from transfected HEK293 cells (using the same pcDNA3.1(-) construct that was used to generate mRNA for oocyte recordings, Fig. 5.3A).

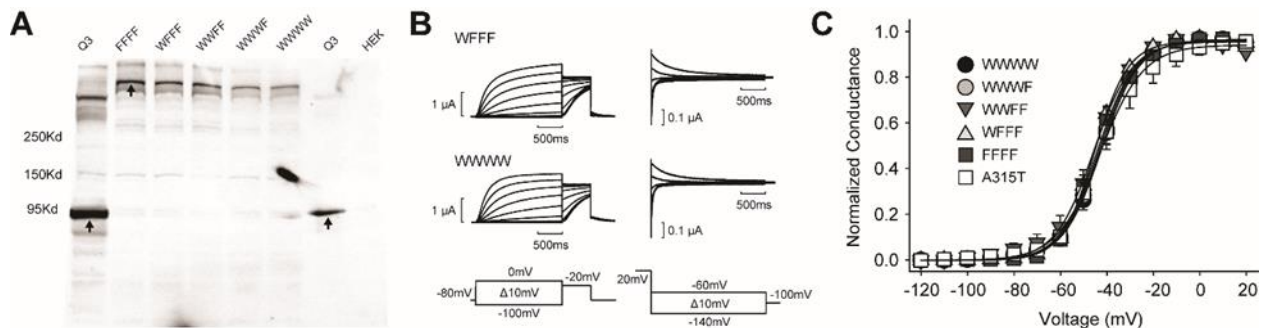


Figure 5.3: Generation of KCNQ3* concatamers with variable stoichiometry of RTG sensitive subunits. (A) Western blots obtained from HEK cells expressing tetrameric constructs show generation of KCNQ3 protein that is four-fold greater in size compared to control. (B and C) Representative traces and summary data displaying intact functional properties of KCNQ3* tetramer constructs, indistinguishable from control (A315T monomer).

A single sensitive subunit encodes a large retigabine effect:

We characterized the maximal retigabine response (maximum $\Delta V_{1/2}$) and sensitivity of concatameric KCNQ3 channels with 1, 2, 3, or 4 retigabine sensitive subunits. Channels with one sensitive subunit (‘WFFF’) exhibited a maximal retigabine-induced gating shifts of -92 ± 1 mV,

in comparison to the WWWW tetramer (-103 +/- 2 mV)(Fig. 5.4A, B). Channels with intermediate numbers of retigabine binding sites exhibited intermediate effects, but it is apparent that the bulk of the maximal retigabine effect can be accounted for by drug binding to a single subunit. It is also noteworthy that the ‘single-site’ WFFF tetramer could partially reproduce the biphasic conductance-voltage relationships observed in KCNQ3* homomeric channels or the WWWW tetramer. This observation is consistent with the notion that a single retigabine binding event is sufficient to nearly completely shift the voltage-dependence of channel gating. It is also noteworthy that the maximally shifted $V_{1/2}$ measured in the WFFF tetramer (-92 mV) is equal to the shifted $V_{1/2}$ component measured at low retigabine concentrations (eg. 3 μ M) in either KCNQ3* channels (-93 mV), or WWWW tetramers (-93 mV). Although perhaps coincidental, this similar effect may suggest that the shifted component observed in KCNQ3 in low retigabine concentrations corresponds to a fraction of channels that have predominantly bound a single retigabine molecule.

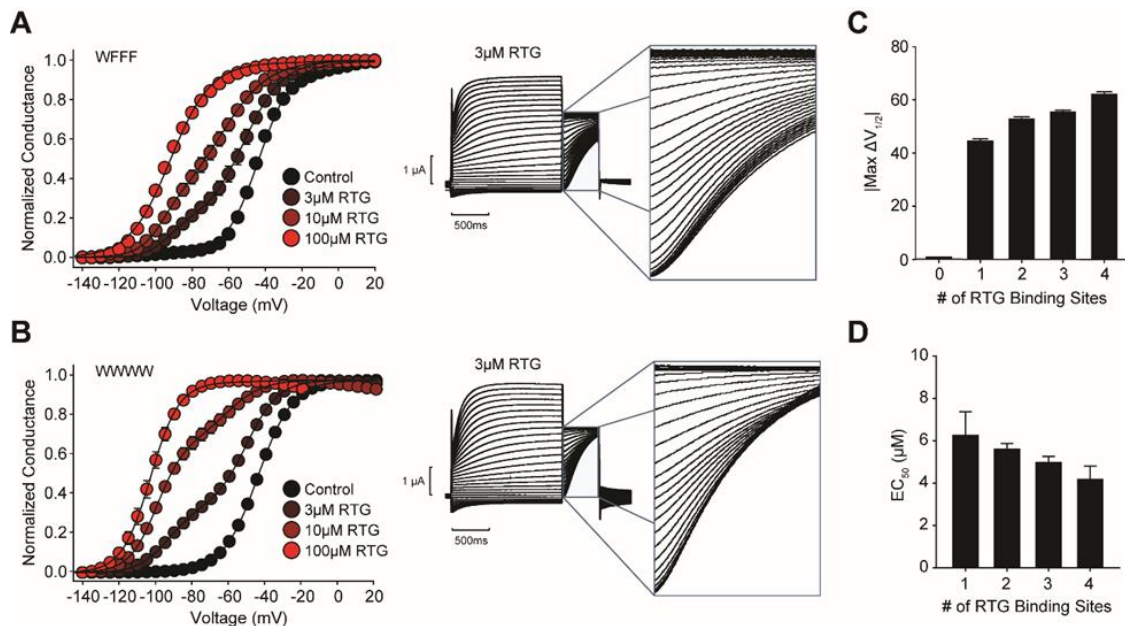


Figure 5.4: A single RTG-sensitive subunit encodes a large RTG effect. (A and B) Summary GV curves obtained from WFFF (A) and WWWW (B) expressed in oocytes and incubated in various RTG concentrations, and representative recordings illustrating the presence of a biphasic tail at intermediate drug concentrations. (C and D) Summary data of the maximal RTG-induced shift in $V_{1/2}$ for different constructs(C), as well as the EC_{50} values (D).

The retigabine-induced gating shift is reflected in changes in both the activation (accelerated) and deactivation (decelerated) kinetics of KCNQ3*. We compared the saturating effects of retigabine on channel gating kinetics in the series of KCNQ3* tetrameric channel constructs, over a range of voltages (Fig. 5.5). Overall, activation kinetics are accelerated similarly whether channels have a full complement of four retigabine sensitive subunits, or just a single subunit (Fig. 5.5B). Similarly, deactivation kinetics are decelerated by retigabine by a comparable extent whether there is one or four sensitive subunits (Fig. 5.5C). These findings are consistent with the effects observed on the conductance-voltage relationship, suggesting that a single retigabine binding event can account for a large component of the maximal retigabine effect.

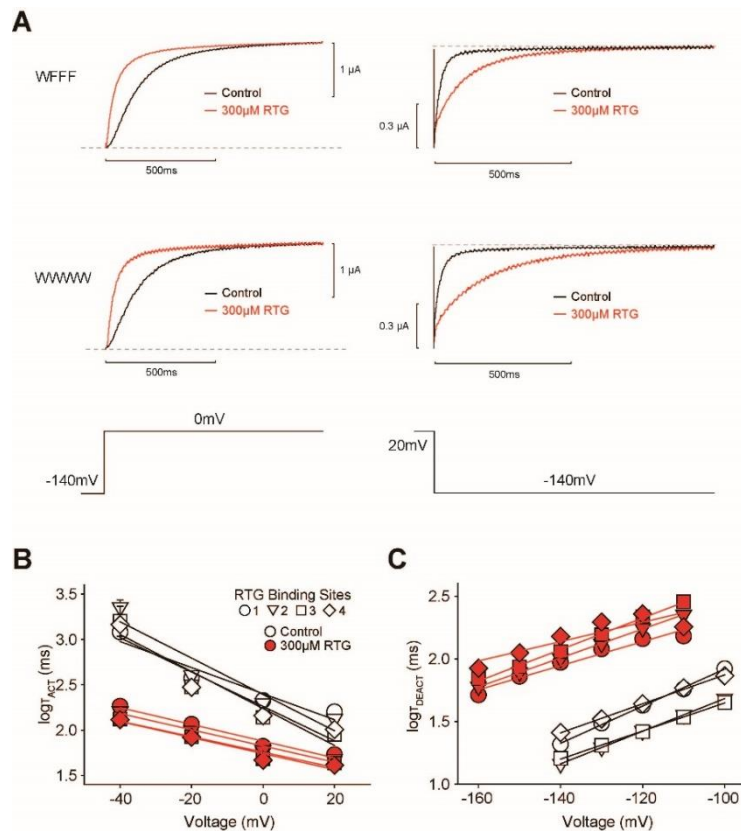


Figure 5.5: Effects of RTG on the activation and deactivation kinetics of KCNQ3* tetramers. (A) Sample activation (left) and deactivation (right) traces obtained at 0mV and -140mV, respectively, in the presence (red) or absence (black) of a saturating concentration of RTG. (B and C) Summary of kinetic data for all constructs ($\log\tau_{act}$, $\log\tau_{deact}$). Notice that kinetic effects of RTG are already pronounced in channels with a single RTG-sensitive subunit.

Auxiliary retigabine binding residue mutations produce pronounced biphasic features

Previous reports identified multiple residues in KCNQ2 or KCNQ3 channels that influence retigabine sensitivity (Fig. 5.6A), albeit less strong than mutations of W265 (or W236 in KCNQ2), which seems to be absolutely essential for retigabine sensitivity (Lange *et al.*, 2009; Schenzer *et al.*, 2005). With the recognition of the unique effects of retigabine on the KCNQ3* conductance-voltage relationship, we also examined the retigabine sensitivity of certain ‘auxiliary’ binding site mutations in more detail. As previously reported, some of these residues (L314A, L272I) exhibit a modest depolarizing shift of channel activation relative to KCNQ3* in control conditions, but retain a similar $V_{1/2}$ in saturating retigabine concentrations. Thus the maximal retigabine-mediated gating shift in these mutant channels can be very large, and the biphasic nature of the conductance-voltage relationship is extremely pronounced (Fig. 5.6B,C). Retigabine effects on these auxiliary binding site mutants exhibits a similar progression of the magnitude of shifted and unshifted components, although higher retigabine concentrations are required than for KCNQ3* channels (consistent with the notion of these amino acids contributing to retigabine binding).

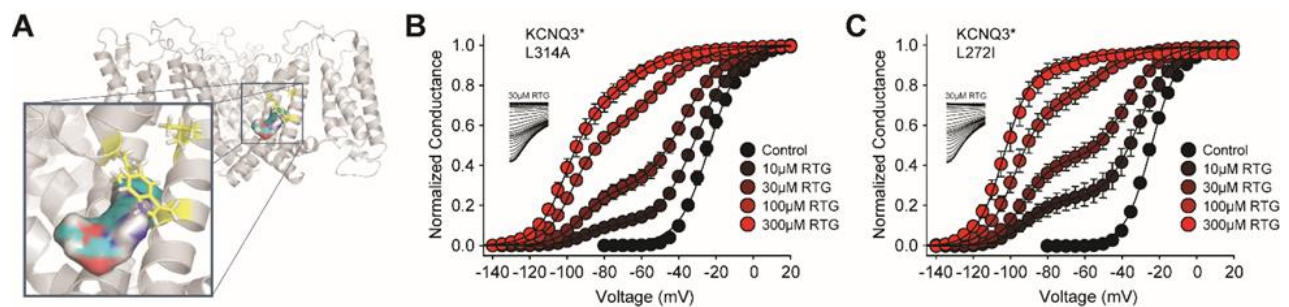


Figure 5.6: Super-shifted RTG-binding site mutants highlight all-or-none shift. (A) Illustration highlighting the positioning of L314 and L272 in close proximity to W265 in the RTG binding site (residues highlighted in yellow). (B and C) Summary GV curves obtained from KCNQ3*[L314A] and KCNQ3*[L272I] channels in different RTG concentrations. Inset displays sample tail current recordings in 30µM RTG, clearly highlighting the two components.

DISCUSSION

Retigabine interaction with KCNQ2-5 potassium channels significantly alters the voltage-dependence of channel activation (Schenzer *et al.*, 2005; Wuttke *et al.*, 2005). In the presence of saturating concentrations of retigabine, the voltage-dependence of these channels is shifted in the hyperpolarizing direction, causing channels to remain open in the normal range of neuronal resting membrane potentials. This hyperpolarizing effect is thought to underlie the therapeutic benefit of retigabine in diseases of membrane excitability like epilepsy. However, unlike other classes of anti-epileptic drugs such as use-dependent Na_v channel blockers, there is only a rudimentary understanding of the fundamental mechanisms of action of retigabine and other KCNQ channel openers.

Using homomeric KCNQ3 channels as a model system, we investigated the number of retigabine-sensitive subunits that are required for a full retigabine response. To this end, we generated concatenated tetrameric subunits, and varied the number of channel subunits carrying the W265Phe mutation previously shown to abolish retigabine sensitivity. It should be noted that KCNQ3*[W265Phe] mutant channels exhibit no response to the highest experimentally manageable concentrations of retigabine, and are presumed to abolish binding, although no direct investigation of retigabine binding to WT or mutant channels has been reported. Due to this uncertainty we have chosen to refer to the number of retigabine-sensitive subunits, rather than the number of retigabine binding sites.

The presence of a single retigabine sensitive subunit was sufficient to reproduce most of the maximal retigabine response observed in homomeric KCNQ3* channels (Fig. 5.4). The biphasic properties of the conductance voltage relationship observed for KCNQ3* (Fig. 5.1) persisted in the WFFF concatenated tetramer, although the components of the GV were less

obviously dissociated. The kinetic effects of retigabine (acceleration of channel activation, deceleration of channel closure) were also consistent between the WFFF and WWWW concatemeric channels. All of these data suggest that a single retigabine binding event is sufficient to generate nearly the maximal retigabine gating effect. We are uncertain why the biphasic nature of the conductance voltage relationship is less apparent in the WFFF tetramer. One possible contributing factor is that the maximal gating shift in this channel (~50 mV) is smaller than observed in WWWW channels (~60 mV), and this may have impacted our ability to resolve distinct components of the conductance-voltage relationship. This is especially true at intermediate retigabine concentrations, because the depolarized component of the conductance-voltage relationship progressively shifts to negative voltages, rather than remaining constant at ~-40 mV, thus making the two components of the GV less obvious. Although we do not have a good explanation for this progressive drift of the fitted $V_{1/2}$ of the depolarized component, it is unlikely to be due to a concentration-dependent population of channels with few (i.e. 1 or 2) molecules of retigabine bound, because the WFFF tetramer would then be predicted to exhibit two consistent and clearly defined components. Given that additional residues contribute to retigabine binding in the pore (and the unknown nature of how they cooperate between subunits), there may be unrecognized effects of retigabine interactions with W265Phe mutant subunits.

We were especially intrigued by the dramatic biphasic response to retigabine that could be engineered in ‘supershifted’ channels carrying auxiliary binding site mutations. Firstly, retigabine appears able to fully overcome the destabilization of channel opening caused by certain mutations, rather than making a constant energetic contribution to intrinsic open state stability of the mutant channel. This may be important in disease-causing loss-of-function KCNQ2 or KCNQ3 mutations linked to epilepsies, and whether retigabine might be an effective therapeutic in some of these

cases. Secondly, the biphasic nature of voltage-sensitivity in the presence of retigabine may influence how one considers dosing effects of the drug in clinical conditions. A drug causing a progressive hyperpolarizing shift of channel activation while maintaining a steep voltage-dependence might be expected to have a steep concentration dependence over which the drug becomes effective at a given voltage. In contrast, a gradual shift in the fraction of shifted/'potentiated' channels at a given voltage might broaden the range over which the drug can have a biological effect.

Lastly, it is important to consider what fundamental mechanism might underlie the biphasic nature of the conductance-voltage relationship in the presence of retigabine. In the case of gamma-subunit regulation of BK channels, random assembly of BK channels with different numbers of auxiliary subunits is presumed to govern the division of channels into populations with distinct gating properties (Gonzalez-Perez *et al.*, 2015). However, in the case of a small molecule, one might expect channel:drug interactions to be more transient. In order to clearly divide available channels into distinct populations, we presume that slow binding and unbinding kinetics of retigabine (relative to the time scale of the experimental voltage pulses) are important to generate this feature in the data. Although detailed characterization of the kinetic features of retigabine:KCNQ channel interactions is an ongoing project, our preliminary findings suggest that this condition is indeed met, with retigabine unbinding normally happening with a time constant of several seconds in rapid perfusion switching experiments.

Chapter 6: General Discussion and Conclusions

IMPLICATIONS FOR DRUG DEVELOPMENT

The key finding highlighted in work presented in chapter 3 was the identification of a H-bond interaction that is likely to occur between W265 in the S5 pore-forming helix of KCNQ3 (and likely KCNQ2, 4, and 5) and a carbonyl oxygen present on most KCNQ2-5 activating compounds. We manipulated the H-bonding propensity of the Trp side chain by rearranging the position of the indole nitrogen, and by weakening the polarity of the N-H moiety through introduction of fluorinated Trp residues. These manipulations either completely ablated channel sensitivity to retigabine (Fig. 3.3) or strengthened the potency of retigabine (Figs. 3.4 and 3.7) and all analogues tested. Despite clear effects of these subtle perturbations on channel pharmacology assessed through electrophysiology, our prediction that W265 is responsible for forming a direct interaction with retigabine is still an assumption, as we have not directly assessed drug binding. This assumption is supported by our observation that the H-bond accepting propensity of retigabine analogues correlates with the negative electrostatic surface potential surrounding their carbonyl oxygen atoms (Fig 3.7).

Our results do not rule out the possibility that H-bonding between W265 and another side chain or regulatory co-factor, determines the structure of the retigabine binding site or is responsible for downstream transduction of retigabine effects upon binding. The same can be said about other residues in the pore domain which we have demonstrated to be important for retigabine effects; however, the positioning of all of these residues in close proximity to W265 make it seem likely that collectively these residues contribute to the formation of a retigabine binding pocket. The indole substitution at W265 is the most subtle yet functionally disruptive mutation for retigabine sensitivity, suggesting that residues in which mutagenesis is less consequential may be

involved in orienting the drug molecule so that this crucial H-bond can be formed. Another possible interpretation of our results is that H-bond formation between W265 and the carbonyl oxygen of retigabine is a prerequisite for drug action as it provides the minimum energy required to allow engagement of the drug in the channel activation process. A recent paper demonstrates that the potency of retigabine can be increased by modifying either of the two phenyl rings of retigabine through fluorination or other small chemical modifications (Kumar *et al.*, 2016). The impact of these alterations mirrors the effects of mutating residues other than W265 on retigabine potency, and demonstrate that while W265 is the most important residue for retigabine effects (and we presume, binding), it is not the sole determinant of potency.

Our observation that the negative electrostatic surface potential of retigabine and its analogues correlates with their potency for activating KCNQ3 has important implications for the design of novel compounds. The carbonyl oxygen in the retigabine molecule is a constituent of a carbamate moiety, flanked by nitrogen and oxygen atoms that can reduce its H-bond accepting capabilities. An appropriate set of follow-up experiments to test our hypothesis would be to experiment with a series of retigabine analogues which are subtly altered at this region: for example, a reasonable prediction might be that replacing the carbamate group with an amide or a simple carbonyl flanked by carbon atoms might enhance retigabine potency. Consistent with this prediction is our data indicating that ML213, which possesses an amide instead of a carbamate, is clearly more potent than retigabine. However, it is important to point out that with ML213, the maximal drug induced shift or efficacy is also reduced, suggesting that the overall architecture of the drug molecule is an important determinant in the magnitude of drug-induced channel stabilization in the active state. Therefore, an exciting possibility is that more subtle manipulations

around the carbamate group of retigabine may result in a compound with greater potency while maintaining efficacy.

Another recent paper demonstrated that adding a propargyl group to the phenyl-group linker region of retigabine enhanced its efficacy in a mouse model of epilepsy, by producing a more favorable brain-plasma distribution without altering the drug potency (Zhou *et al.*, 2015). This finding is consistent with our work suggesting that the distal carbamate region is a critical determinant of drug binding, and demonstrates that tolerable chemical modifications of the body of the drug molecule can lead to improvements in pharmacokinetics without impacting drug potency and efficacy. As more studies emerge revealing specific structure/function properties of drug action, our findings can be incorporated into an effective synthesis strategy to develop more effective therapeutics, a task that will become increasingly more important as KCNQ channel openers are evaluated as therapies in conditions other than epilepsy.

It is important to recognize the emerging concept that KCNQ channels can be regulated through multiple distinct binding sites. W265 is present in the retigabine sensitive KCNQs (2-5); however, certain isoforms such as KCNQ2 can be powerfully activated by drugs that appear to act through interactions with the channel VSDs (Boehlen *et al.*, 2013; Peretz *et al.*, 2010; Wang *et al.*, 2017). The most straightforward evidence for this is that although W236 (the W265 equivalent residue in KCNQ2) is required for retigabine action, there are numerous compounds that do not rely on this residue to exert powerful channel activating effects in KCNQ2. While our study adds to the existing knowledge of the retigabine binding site in the pore domain, there is a relative disparity in our knowledge of the determinants of drug binding and regulation on the VSDs. As future research reveals distinct characteristics of these binding sites, the subtype specificity of drugs that act through VSDs may enable specific targeting of KCNQ subtypes in different diseases,

and to possibly generate therapeutic schemes in which both sites are targeted simultaneously with different compounds to achieve maximum potency, with lower doses and possibly fewer side effects.

Q3*VCF REVEALS IMPORTANT FEATURES OF KCNQ3 CHANNEL BIOPHYSICS

Employing VCF to study conformations of the voltage sensing apparatus in KCNQ3 has been fruitful in illuminating the mechanism of retigabine-induced shift in channel voltage sensing, as well as structural features underlying channel regulation by PIP₂. The journey of successfully applying VCF on KCNQ3 was a challenging one, which involved the generation of many mutant constructs and constantly modifying the experimental procedures as well as the recording equipment in order to obtain satisfactory fluorescence signals with adequate signal:noise. The results from our cysteine substitutions in the S3-S4 linker of these channels indicate that the voltage sensing equilibrium of these channels is regulated by the precise amino acid composition of this extracellular loop. Despite drastic effects of some of these mutations, the Q218C mutation preserved WT-like channel function, and importantly, enabled us to conduct VCF experiments. Interestingly, despite trying to obtain fluorescence from many of the other cysteine mutants, I was only able to succeed with Q218C and G219C, residues which had been used for VCF in KCNQ1 channels by several groups (Barro-Soria *et al.*, 2014; Osteen *et al.*, 2010). Thus it seems likely that there is both sequence and conformational homology between KCNQ1 and KCNQ3 that enable these sites to report state dependent fluorescence changes when labelled with fluorophores. Labelling of residue V221 also enables VCF in KCNQ1, however, I suspect that the hyperpolarizing shift produced by this mutation precluded this construct from utilized for detailed investigations of how KCNE1 regulates voltage-sensor function in these channels. However, this

finding is consistent with our results in KCNQ3 that residues on the S3-S4 are important determinants of channel voltage sensitivity.

There are both similarities and significant qualitative differences in voltage sensor functions revealed by VCF experimentation in KCNQ3 compared to KCNQ1. Similar to KCNQ1 in the absence of KCNE1, the voltage dependence of fluorescence in KCNQ3 overlaps with the voltage dependence of ionic conduction, indicating tight coupling between VSD activation and pore opening in these channels. These findings are quite distinct from VCF reports conducted on *Shaker* potassium channels (Cha and Bezanilla, 1997; Kalstrup and Blunck, 2013; Mannuzzu *et al.*, 1996), which demonstrate voltage-dependent fluorescence changes and gating charge movements occurring at voltages hyperpolarized to pore opening, consistent with models in which movements of the voltage sensors precede a pore opening step (Schoppa and Sigworth, 1998; Zagotta *et al.*, 1994).

Experimental data indicating the presence of sub-maximal conducting states in KCNQ1 (Werry *et al.*, 2013) lend support to a model in which independent movements of the four voltage-sensors contribute to partial pore opening events to produce the overlap in FV and GV relationships for KCNQ1. However, single channel studies performed in KCNQ2/3 have not revealed the presence of such conduction states, making it difficult to rationalize such a mechanism for our experimental observations (Li *et al.*, 2004; Schwake *et al.*, 2000). Furthermore, our data cannot rule out the possibility that the fluorescence change obtained from Q3*VCF is a reflection of concerted rearrangements of the voltage sensing domains in the latter stages of the channel activation process coupled to pore opening, excluding independent movements preceding these motions.

In KCNQ1, VCF has revealed some fundamental channel regulatory mechanisms by endogenous auxiliary subunits such as KCNE1 and KCNE3 (Barro-Soria *et al.*, 2014, 2015). The presence of KCNE1 uncouples pore opening from the initial voltage-sensor activation step, imposing a requirement for additional conformational changes at more depolarized potentials to enable pore opening, leading to the hallmark features of cardiac IKs current. In contrast, KCNE3 can associate with KCNQ1 to lock the VSDs in the activated state, leading to persistent pore opening at physiological voltage ranges. At present, there is no evidence that KCNE1 or KCNE3 contribute to functional regulation of neuronal KCNQ2/3 channels. There is some evidence that KCNE2 may regulate neuronal KCNQs, however, the effects of KCNE2 co-expression on KCNQ2/3 function are extremely modest in comparison to the effects of KCNE1/3 on KCNQ1, reported as a small ~5mV depolarizing shift in channel activation (Tinel *et al.*, 2000). Other major endogenous regulators of KCNQ2/3 discussed in the introductory chapter such as AKAP5 and Calmodulin, exert their effects on channel open probability through indirectly modulating channel interactions with PIP₂. Thus, it will be interesting to see if novel endogenous regulators of KCNQ2/3 emerge that can modulate channel function via directly altering channel voltage sensing properties akin to the regulation of KCNQ1.

Perhaps the most obvious distinction to be made regarding KCNQ3 VCF in relation to KCNQ1 is that PIP₂ depletion leads to a dramatic increase in fluorescence report, which has not been reported in KCNQ1 (Zaydman *et al.*, 2013). Previous work has established that the KCNQ subtypes differ significantly in their PIP₂ sensitivities and maximal open probabilities. KCNQ3 has a PIP₂ sensitivity an order of magnitude greater than other KCNQs (Li *et al.*, 2005), and this increase in PIP₂ sensitivity correlates with channel open probability, with KCNQ3 having an open probability near unity at saturating voltages. In the presence of normal PIP₂ levels, most of the

KCNQ3 VSDs are coupled to an open pore at depolarized potentials; however, upon Ci-VSP induced PIP₂ rundown, uncoupling of the VSDs from the pore is likely to alter its conformation, and this appears to manifest as a dramatic alteration of the fluorescence report. In channels such as KCNQ1 (without KCNE1) where the PIP₂-dependent coupling between the activated VSDs and open pore are weaker (resulting in a lower open probability), it might be expected that even under normal PIP₂ levels, a majority of VSDs are uncoupled from the pore. This seems to be a reasonable interpretation for why PIP₂ depletion does not alter the fluorescence report from KCNQ1, and is supported by our experimental data from the low-open probability Q3*VCF mutants with disrupted proximal C-terminus charges. In the Q3*VCF S6-AARK mutant, PIP₂ depletion causes a much smaller increase in fluorescence, indicating that weak VSD-PD coupling prior to PIP₂ depletion attenuates the impact of PIP₂ depletion on VSD conformations.

This interesting divergence in the regulation of KCNQ channels by PIP₂ and KCNE subunits is likely a reflection of their unique physiological roles. Although KCNQ1 channels must associate with PIP₂ in order to function, their primary functions in the heart, ear, and gut require association with KCNE1 and KCNE3 subunits, which drastically alter their functional properties. In contrast, KCNQ2/3 channels are regulated through numerous signaling pathways (as discussed in the introductory chapter) that converge to modulate PIP₂-channel interactions and control neuronal excitability. Thus, it is hardly surprising that they have evolved an exquisite sensitivity to levels of PIP₂. An intriguing hypothesis is that the conformational heterogeneity of KCNQ channels is not only important for their regulation by diverse endogenous regulators, but also underlies the ‘drugability’ of these channels. The ability to adopt various open conformations occupying a vast energetic landscape may increase the probability that a small molecule can associate with certain states to stabilize channel opening.

MECHANISM OF RETIGABINE INDUCED CHANNEL ACTIVATION

By utilizing VCF in conjunction with various methods of disrupting channel:PIP₂ interactions, our study has elucidated the relationship between channel regulation by PIP₂ and activation by retigabine. Prior work has hinted that PIP₂ plays an important role in mediating retigabine effects, as PIP₂ depletion precludes retigabine-induced pore opening, but not all activators (eg. zinc pyrithione) are affected (Xiong *et al.*, 2007; Zhou *et al.*, 2013). By using VCF to measure retigabine effects on the VSD in the absence of PIP₂, we demonstrate that PIP₂ is not essential for retigabine binding as retigabine is still able to stabilize VSD activation. However, PIP₂ is critical for VSD-PD coupling and pore activation, and through a comprehensive mutagenic scan of cytosolic basic residues, our data suggest that this may be due to interactions between PIP₂ at the VSD-PD interface, and a PIP₂ interaction motif located below the S6 helix of the channel. The observation that retigabine protects channels against PIP₂ rundown supports a model in which the retigabine bound activated state of the channel has a strengthened affinity for PIP₂. Since retigabine stabilizes the activated VSDs in the absence of PIP₂, it is conceivable that when PIP₂ is present, its orientation and interaction with important structural elements of the channel is altered.

To support this model of drug action and to distinguish it from drugs that activate the VSDs directly, it would be interesting to perform the Ci-VSP PIP₂ depletion assay using drugs that target the VSDs. If strengthened PIP₂ dependent VSD-PD coupling is not a primary mechanism of a particular drug, then a reasonable hypothesis would be that Ci-VSP could effectively deplete current in the presence of the drug, despite its ability to promote channel activation by increasing voltage sensitivity. Currently, while there are several known drugs that act through a W236 independent binding site in KCNQ2, such drugs have not been identified for KCNQ3. Therefore this set of experiments can be performed using KCNQ2 channels, for example, by comparing the

effects of retigabine versus ICA-069673, a drug shown to act via an alternative binding site in the VSD (Wang *et al.*, 2017), on Ci-VSP induced current rundown.

STOICHIOMETRY OF RETIGABINE EFFECTS

When we began investigating retigabine action on KCNQ3* channels, we initially attributed the shallowing of the GV curve at intermediate retigabine concentrations to the consequence of averaging recordings from multiple oocytes exposed to drug concentrations in the steep range of the retigabine dose response curve. Typically, the test potentials in our GV protocols were applied in 10mV increments, and therefore, it was difficult to resolve the biphasic nature of the GV curve which became evident when 5mV steps were used. This observation led to our hypothesis that an all-or-none response to retigabine divided channels into two distinct populations: those experiencing a full shift, and a population of unshifted channels.

To test this hypothesis we generated concatemeric constructs with variable numbers of retigabine sensitive subunits and found that channels expressing a single retigabine sensitive subunit recapitulated to a large extent, the retigabine induced shift in voltage-dependence and kinetics observed in WT channels. The characteristic biphasic GV curve at intermediate retigabine levels is present in the WFFF construct, as well as a shift in $V_{1/2}$ of activation $\sim 70\%$ of that observed in 'WWWW' tetramers and homotetrameric KCNQ3* channels. While the possibility exists that the tetramers are not expressing as we expect, and that WFFF expression may result in the expression of channels with more than one retigabine sensitive subunit, there is a clear difference in their pharmacological sensitivity that suggests that the WFFF and WWWW constructs are forming distinct channels. Channels formed by the WFFF construct have a reduced shift in saturating retigabine concentrations, which is similar to the shifted component of the biphasic GV at low retigabine concentrations in WWWW and KCNQ3*. This is likely a reflection

of the majority of shifted channels interacting with retigabine through a single subunit at lower concentrations. Taken together, the data from our KCNQ3 concatamer experiments suggests that in homomeric KCNQ3 channels, the interaction between retigabine and one subunit within the tetrameric complex is sufficient to stabilize channel opening to a great extent, and that subsequent retigabine molecules exert marginal stabilizing effects on channel activation.

At this point, we can only speculate on the mechanistic basis of this effect. However, it would be a reasonable hypothesis that the retigabine-sensitive gating process in a single subunit of these channels is coupled to gating transitions of neighboring subunits. There exist the possibility that the C-terminal motif that we identified to be crucial for channel gating and retigabine effects are actually interacting with the VSDs/PIP₂ of adjacent subunits. To test this, expression of KCNQ3*[S6-AARK] with Q3*VCF[W265F], ideally as a dimeric construct, may abolish retigabine effects on fluorescence. A recent structure resolved in the MacKinnon lab (Whicher and MacKinnon, 2016) revealed that the S4-S5 linker in EAG1 potassium channels interact with the S6 helix of adjacent subunits, as a result of a non-domain swapped configuration of the VSDs and PDs. A unifying mechanism underlying the ability of a single retigabine-sensitive subunit to exert a dominant functional effect, as well as the tight coupling of fluorescence report and pore gating in Q3*VCF, could involve a mechanism where the VSD-PD coupling in KCNQ3 channels occur between domains of adjacent subunits. I think that this presents quite a fascinating avenue for future studies using the constructs and methods established in the work presented in this thesis.

LIMITATIONS AND OUTLOOK ON FUTURE EXPERIMENTS

The primarily limitation in the conclusions drawn from our studies is the use of a KCNQ3* construct that enables functional expression of homomeric KCNQ3 channels. As discussed in the

introductory chapter, M-currents in physiological settings are most abundantly expressed as KCNQ2/3 heteromers and there is very little evidence for a functional role of KCNQ3 homomeric channels. However, without the robust expression of this construct in *Xenopus laevis* oocytes, few of our studies would have been possible. The incorporation of unnatural amino acids via the nonsense suppression technique is inherently inefficient and requires the use of constructs that enable a robust baseline of expression (with short latency) prior to introducing the amber stop codon. For VCF studies, we normally only observe fluorescence changes for Q3*VCF at current expression levels exceeding 20 μ A, and for KCNQ2 and KCNQ2/3 expression, these levels are attainable only several days after injection at which time point a majority of the oocytes have deteriorated and are no longer useful to perform reliable experiments, let alone expose them to the harsh conditions necessary for fluorescent labelling. Based on the expectation that concatameric subunits will also be less efficient at expressing, we generated our tetramers using the same construct, however, currently we have succeeded in generating and expressing KCNQ2 concatamers in mammalian cell lines, and we are subjecting them to similar experimental protocols to understand the subunit stoichiometry of retigabine effects.

As mentioned in the introduction, there is some conflicting evidence regarding the inability of KCNQ3 channels to form functional homomeric channels. In my assessment of the literature, I am inclined to believe that the KCNQ3 homomeric channels can be formed, but inefficiently when compared to co-expression with KCNQ2. In this sense, KCNQ3 trafficking to the membrane is similar to KCNQ2, the expression of which is substantially boosted by KCNQ3 co-injection. I believe the main reason underlying a lack of current expression from KCNQ3 WT subunits is that the presence of the Ala residue at position 315 causes the selectivity filter to be in a non-conducting conformation, and by replacing this residue with a Thr, we are rescuing the ability of these channels

to conduct ions. It is likely that co-expression with WT KCNQ2 rescues pore functionality due to the presence of a Thr at the equivalent position, and it would be interesting to test this hypothesis by generating KCNQ3 WT – KCNQ3* dimeric or tetrameric constructs. Given some clear functional difference between KCNQ2 and KCNQ3 such as their difference in PIP₂ sensitivity, and evidence for a physiological role of KCNQ2 homomers, I think that evolutionarily, KCNQ3 evolved to modulate M-channel functionality by titrating the relative abundance of KCNQ3 subunits within M-channel complexes, and that the presence of the Ala315 residue prevents KCNQ3 channels from being electrically functional on their own.

In accepting the limitations of using the KCNQ3* construct in our studies, as a model M-channel construct, some aspects of our conclusions are subject to more scrutiny than others. In both homomeric and heteromeric channels composed of KCNQ2 and KCNQ3 subunits, we have demonstrated that there is an absolute requirement for a Trp residue at positions 236 and 265, respectively. Thus, our interpretation of our results employing unnatural amino acid mutagenesis of W265 in KCNQ3* can reasonably be extended to native KCNQ2/3 M-channels. When it comes to our interpretation of the mechanism of retigabine-induced channel activation and enhanced voltage sensitivity, this is where we have to be more careful. In Chapter 3, we demonstrated that the retigabine sensitivity of KCNQ2[W236F] co-expressed with WT KCNQ3 is intermediate between WT M-channels and KCNQ2[W236F]:KCNQ3[W265F] channels. This is somewhat at odds with our concatamer study in which a single retigabine sensitive subunit is sufficient to reproduce most of the pharmacological sensitivity in KCNQ3. At this point, we can conclude that either there is a difference in the stoichiometry of retigabine effects between KCNQ3 and KCNQ2/3 channels, or that there are artefactual effects resulting from our concatamers or experimental protocols. The retigabine-induced shift in KCNQ2/3 is significantly less than in

KCNQ2 or KCNQ3* homotetramers, making it more difficult to resolve a biphasic response to retigabine. However, at that time I was not fully aware of the biphasic nature of retigabine sensitivity of KCNQ3* and thus did not carefully assess KCNQ2/3 channels for similar effects using 5mV recording steps. Furthermore, over the course of our studies we have refined our methods of applying solutions of different retigabine concentrations to oocytes, favoring a method of incubating eggs to allow for more consistent equilibration of drug levels between different batches of oocytes. It should not be difficult for us to more accurately resolve these distinctions in future repeat experiments, and along with our data from KCNQ2 tetramers, we should be able to determine if there is indeed a subtype specificity to the stoichiometry of retigabine effects.

In terms of our proposed mechanism of VSD-PD coupling and the role of PIP₂ in retigabine sensitivity of KCNQ3 inferred from our VCF data, it is possible that there are mechanistic differences in native KCNQ2/3 channels. Probably the most convincing argument against this possibility is that the most salient features of our model, such as involvement of the cluster of positively charged residues below the S6 helix, the S2-3 and S4-5 linkers, and the absolute requirement of PIP₂ for retigabine effects on pore opening, are features that are also prominent in KCNQ2 subunits. In the future, I believe it will be possible to perform VCF from KCNQ2/3 heteromeric channels. By selectively recording fluorescence from either KCNQ2 or KCNQ3 VSDs, along with varying combinations of retigabine sensitive subunits and selective mutagenic perturbations, a more detailed understanding of VSD-PD coupling and pharmacology in native channel constructs could be obtained.

SUMMARY

The work presented in this thesis expands our understanding of neuronal KCNQ channel pharmacology at the molecular level. Using unnatural amino acid mutagenesis, we revealed that a Trp residue previously established as essential for retigabine effects is likely interacting with retigabine and its related analogs through H-bonding between the indole N-H and a carbonyl oxygen present in these drugs. Future endeavors developing novel KCNQ channel activators can apply this knowledge to fine tune the potency of novel compounds devoid of effects on unknown targets, and establish library screens in which the importance of this interaction is recognized, increasing efficiency. VCF has proven to be effective at not only illuminating the mechanism of retigabine induced enhancement of channel voltage sensitivity, but also revealing basic structure-function properties of KCNQ channels, particularly highlighting the central role of PIP₂. Finally, our studies using concatamers provides insight into the stoichiometry of retigabine action on KCNQ channels, and highlights the need for further experimentation to resolve how the function and pharmacology of M-channels is affected by its subunit composition.

References

Abel, H.J., Lee, J.C.F., Callaway, J.C., and Foehring, R.C. (2004). Relationships between intracellular calcium and afterhyperpolarizations in neocortical pyramidal neurons. *J. Neurophysiol.* *91*, 324–335.

Aivar, P., Fernández-Orth, J., Gomis-Perez, C., Alberdi, A., Alaimo, A., Rodríguez, M.S., Giraldez, T., Miranda, P., Areso, P., and Villarroel, A. (2012). Surface expression and subunit specific control of steady protein levels by the K_v7.2 helix a-b linker. *PLOS ONE* *7*, e47263.

Akasu, T., Hirai, K., and Koketsu, K. (1983). Modulatory actions of ATP on membrane potentials of bullfrog sympathetic ganglion cells. *Brain Res.* *258*, 313–317.

Alaimo, A., Gómez-Posada, J.C., Aivar, P., Etxeberria, A., Rodriguez-Alfaro, J.A., Areso, P., and Villarroel, A. (2009). Calmodulin activation limits the rate of KCNQ2 K⁺ channel exit from the endoplasmic reticulum. *J. Biol. Chem.* *284*, 20668–20675.

Bal, M., Zhang, J., Hernandez, C.C., Zaika, O., and Shapiro, M.S. (2010). Ca²⁺/calmodulin disrupts akap79/150 interactions with KCNQ (m-type) K⁺ channels. *J. Neurosci.* *30*, 2311–2323.

Barhanin, J., Lesage, F., Guillemare, E., Fink, M., Lazdunski, M., and Romey, G. (1996). K_vLQT1 and IsK (minK) proteins associate to form the IKS cardiac potassium current. *Nature* *384*, 78–80.

Barro-Soria, R., Rebolledo, S., Liin, S.I., Perez, M.E., Sampson, K.J., Kass, R.S., and Larsson, H.P. (2014). KCNE1 divides the voltage sensor movement in KCNQ1/KCNE1 channels into two steps. *Nat. Commun.* *5*, 3750.

Barro-Soria, R., Perez, M.E., and Larsson, H.P. (2015). KCNE3 acts by promoting voltage sensor activation in KCNQ1. *Proc. Natl. Acad. Sci.* *112*, E7286–E7292.

Beech, D.J., Bernheim, L., Mathie, A., and Hille, B. (1991). Intracellular Ca²⁺ buffers disrupt muscarinic suppression of Ca²⁺ current and M current in rat sympathetic neurons. *Proc. Natl. Acad. Sci.* *88*, 652–656.

Beene, D.L., Dougherty, D.A., and Lester, H.A. (2003). Unnatural amino acid mutagenesis in mapping ion channel function. *Curr. Opin. Neurobiol.* *13*, 264–270.

Biase, D.D., Barra, D., Bossa, F., Pucci, P., and John, R.A. (1991). Chemistry of the inactivation of 4-aminobutyrate aminotransferase by the antiepileptic drug vigabatrin. *J. Biol. Chem.* *266*, 20056–20061.

Biervert, C., Schroeder, B.C., Kubisch, C., Berkovic, S.F., Propping, P., Jentsch, T.J., and Steinlein, O.K. (1998). A potassium channel mutation in neonatal human epilepsy. *Science* *279*, 403–406.

Boehlen, A., Schwake, M., Dost, R., Kunert, A., Fidzinski, P., Heinemann, U., and Gebhardt, C. (2013). The new KCNQ2 activator 4-Chlor-N-(6-chlor-pyridin-3-yl)-benzamid displays anticonvulsant potential. *Br. J. Pharmacol.* *168*, 1182–1200.

- Borgatti, R., Zucca, C., Cavallini, A., Ferrario, M., Panzeri, C., Castaldo, P., Soldovieri, M.V., Baschiroto, C., Bresolin, N., Bernardina, B.D., et al. (2004). A novel mutation in KCNQ2 associated with BFNC, drug resistant epilepsy, and mental retardation. *Neurology* 63, 57–65.
- Bormann, J., Hamill, O.P., and Sakmann, B. (1987). Mechanism of anion permeation through channels gated by glycine and gamma-aminobutyric acid in mouse cultured spinal neurones. *J. Physiol.* 385, 243–286.
- Brodie, M.J., Lerche, H., Gil-Nagel, A., Elger, C., Hall, S., Shin, P., Nohria, V., Mansbach, H., and On behalf of the RESTORE 2 Study Group (2010). Efficacy and safety of adjunctive ezogabine (retigabine) in refractory partial epilepsy. *Neurology* 75, 1817–1824.
- Brown, D.A., and Adams, P.R. (1980). Muscarinic suppression of a novel voltage-sensitive K⁺ current in a vertebrate neurone. *Nature* 283, 673–676.
- Brown, D.A., and Passmore, G.M. (2009). Neural KCNQ (K_v7) channels. *Br. J. Pharmacol.* 156, 1185–1195.
- Burley, S.K., and Petsko, G.A. (1985). Aromatic-aromatic interaction: a mechanism of protein structure stabilization. *Science* 229, 23–28.
- Cai, H., Wang, Y., McCarthy, D., Wen, H., Borchelt, D.R., Price, D.L., and Wong, P.C. (2001). BACE1 is the major β-secretase for generation of Aβ peptides by neurons. *Nat. Neurosci.* 4, 233–234.
- Castaldo, P., del Giudice, E.M., Coppola, G., Pascotto, A., Annunziato, L., and Tagliatela, M. (2002). Benign familial neonatal convulsions caused by altered gating of KCNQ2/KCNQ3 potassium channels. *J. Neurosci.* 22, RC199.
- Cavaretta, J.P., Sherer, K.R., Lee, K.Y., Kim, E.H., Issema, R.S., and Chung, H.J. (2014). Polarized axonal surface expression of neuronal KCNQ potassium channels is regulated by calmodulin interaction with KCNQ2 subunit. *PLOS ONE* 9, e103655.
- Cha, A., and Bezanilla, F. (1997). Characterizing voltage-dependent conformational changes in the shakerK⁺ channel with fluorescence. *Neuron* 19, 1127–1140.
- Charlier, C., Singh, N.A., Ryan, S.G., Lewis, T.B., Reus, B.E., Leach, R.J., and Leppert, M. (1998). A pore mutation in a novel KQT-like potassium channel gene in an idiopathic epilepsy family. *Nat. Genet.* 18, 53–55.
- Choveau, F.S., Hernandez, C.C., Bierbower, S.M., and Shapiro, M.S. (2012a). Pore determinants of KCNQ3 K⁺ current expression. *Biophys. J.* 102, 2489–2498.
- Choveau, F.S., Bierbower, S.M., and Shapiro, M.S. (2012b). Pore helix-s6 interactions are critical in governing current amplitudes of KCNQ3 K⁺ channels. *Biophys. J.* 102, 2499–2509.

- Chung, H.J., Jan, Y.N., and Jan, L.Y. (2006). Polarized axonal surface expression of neuronal KCNQ channels is mediated by multiple signals in the KCNQ2 and KCNQ3 C-terminal domains. *Proc. Natl. Acad. Sci.* *103*, 8870–8875.
- Claes, L., Del-Favero, J., Ceulemans, B., Lagae, L., Van Broeckhoven, C., and De Jonghe, P. (2001). De novo mutations in the sodium-channel gene SCN1a cause severe myoclonic epilepsy of infancy. *Am. J. Hum. Genet.* *68*, 1327–1332.
- Claes, L., Ceulemans, B., Audenaert, D., Smets, K., Löfgren, A., Del-Favero, J., Ala-Mello, S., Basel-Vanagaite, L., Plecko, B., Raskin, S., et al. (2003). De novo SCN1A mutations are a major cause of severe myoclonic epilepsy of infancy. *Hum. Mutat.* *21*, 615–621.
- Cooper, E.C. (2011). Made for “anchorin”: K_v7.2/7.3 (KCNQ2/KCNQ3) channels and the modulation of neuronal excitability in vertebrate axons. *Semin. Cell Dev. Biol.* *22*, 185.
- Cooper, E.C., Aldape, K.D., Abosch, A., Barbaro, N.M., Berger, M.S., Peacock, W.S., Jan, Y.N., and Jan, L.Y. (2000). Colocalization and coassembly of two human brain M-type potassium channel subunits that are mutated in epilepsy. *Proc. Natl. Acad. Sci.* *97*, 4914–4919.
- Cooper, E.C., Harrington, E., Jan, Y.N., and Jan, L.Y. (2001). M channel KCNQ2 subunits are localized to key sites for control of neuronal network oscillations and synchronization in mouse brain. *J. Neurosci.* *21*, 9529–9540.
- Coucke, P., Van Camp, G., Djoyodiharjo, B., Smith, S.D., Frants, R.R., Padberg, G.W., Darby, J.K., Huizing, E.H., Cremers, C., Kimberling, W.J., et al. (2010). Linkage of autosomal dominant hearing loss to the short arm of chromosome 1 in two families.
- Coulter, D.A., Huguenard, J.R., and Prince, D.A. (1989). Characterization of ethosuximide reduction of low-threshold calcium current in thalamic neurons. *Ann. Neurol.* *25*, 582–593.
- Cruzblanca, H., Koh, D.-S., and Hille, B. (1998). Bradykinin inhibits M current via phospholipase C and Ca²⁺ release from IP₃-sensitive Ca²⁺ stores in rat sympathetic neurons. *Proc. Natl. Acad. Sci.* *95*, 7151–7156.
- Dedek, K., Kunath, B., Kananura, C., Reuner, U., Jentsch, T.J., and Steinlein, O.K. (2001). Myokymia and neonatal epilepsy caused by a mutation in the voltage sensor of the KCNQ2 K⁺ channel. *Proc. Natl. Acad. Sci.* *98*, 12272–12277.
- Delmas, P., and Brown, D.A. (2005). Pathways modulating neural KCNQ/M (K_v7) potassium channels. *Nat. Rev. Neurosci.* *6*, 850–862.
- Devaux, J.J., Kleopa, K.A., Cooper, E.C., and Scherer, S.S. (2004). KCNQ2 is a nodal K⁺ channel. *J. Neurosci.* *24*, 1236–1244.
- Dooley, D.J., Mieske, C.A., and Borosky, S.A. (2000). Inhibition of K⁺-evoked glutamate release from rat neocortical and hippocampal slices by gabapentin. *Neurosci. Lett.* *280*, 107–110.

- Dougherty, D.A. (1996). Cation- π interactions in chemistry and biology: a new view of benzene, phe, tyr, and trp. *Science* 271, 163–168.
- Du, X., Hao, H., Gigout, S., Huang, D., Yang, Y., Li, L., Wang, C., Sundt, D., Jaffe, D.B., Zhang, H., et al. (2014). Control of somatic membrane potential in nociceptive neurons and its implications for peripheral nociceptive transmission. *Pain* 155, 2306.
- Ettxeberria, A., Santana-Castro, I., Regalado, M.P., Aivar, P., and Villarroel, A. (2004). Three mechanisms underlie KCNQ2/3 heteromeric potassium m-channel potentiation. *J. Neurosci.* 24, 9146–9152.
- Ettxeberria, A., Aivar, P., Rodriguez-Alfaro, J.A., Alaimo, A., Villacé, P., Gómez-Posada, J.C., Areso, P., and Villarroel, A. (2008). Calmodulin regulates the trafficking of KCNQ2 potassium channels. *FASEB J.* 22, 1135–1143.
- Etzioni, A., Siloni, S., Chikvashvili, D., Strulovich, R., Sachyani, D., Regev, N., Greitzer-Antes, D., Hirsch, J.A., and Lotan, I. (2011). Regulation of neuronal M-channel gating in an isoform-specific manner: functional interplay between calmodulin and syntaxin 1a. *J. Neurosci.* 31, 14158–14171.
- Falkenburger, B.H., Jensen, J.B., and Hille, B. (2010). Kinetics of PIP2 metabolism and KCNQ2/3 channel regulation studied with a voltage-sensitive phosphatase in living cells. *J. Gen. Physiol.* 135, 99–114.
- French, J.A., Abou-Khalil, B.W., Leroy, R.F., Yacubian, E.M.T., Shin, P., Hall, S., Mansbach, H., and Nohria, V. (2011). Randomized, double-blind, placebo-controlled trial of ezogabine (retigabine) in partial epilepsy. *Neurology* 76, 1555–1563.
- Gallivan, J.P., and Dougherty, D.A. (1999). Cation- π interactions in structural biology. *Proc. Natl. Acad. Sci.* 96, 9459–9464.
- Gamper, N., and Shapiro, M.S. (2003). Calmodulin mediates Ca^{2+} -dependent modulation of M-type K^+ channels. *J. Gen. Physiol.* 122, 17–31.
- Gamper, N., Reznikov, V., Yamada, Y., Yang, J., and Shapiro, M.S. (2004). Phosphatidylinositol 4,5-bisphosphate signals underlie receptor-specific $\text{gq}/11$ -mediated modulation of n-type Ca^{2+} channels. *J. Neurosci.* 24, 10980–10992.
- Gao, Z., Zhang, T., Wu, M., Xiong, Q., Sun, H., Zhang, Y., Zu, L., Wang, W., and Li, M. (2010). Isoform-specific prolongation of K_v7 (KCNQ) potassium channel opening mediated by new molecular determinants for drug-channel interactions. *J. Biol. Chem.* 285, 28322–28332.
- Garrido, J.J., Giraud, P., Carlier, E., Fernandes, F., Moussif, A., Fache, M.-P., Debanne, D., and Dargent, B. (2003). A targeting motif involved in sodium channel clustering at the axonal initial segment. *Science* 300, 2091–2094.

- Gee, N.S., Brown, J.P., Dissanayake, V.U.K., Offord, J., Thurlow, R., and Woodruff, G.N. (1996). The novel anticonvulsant drug, gabapentin (neurontin), binds to the subunit of a calcium channel. *J. Biol. Chem.* *271*, 5768–5776.
- Gómez-Posada, J.C., Etxeberria, A., Roura-Ferrer, M., Areso, P., Masin, M., Murrell-Lagnado, R.D., and Villarroel, A. (2010). A pore residue of the KCNQ3 potassium M-channel subunit controls surface expression. *J. Neurosci.* *30*, 9316–9323.
- Gonzalez-Perez, V., Xia, X.-M., and Lingle, C.J. (2015). Two classes of regulatory subunits coassemble in the same BK channel and independently regulate gating. *Nat. Commun.* *6*, 8341.
- Gu, N., Vervaeke, K., Hu, H., and Storm, J.F. (2005). K_v7 /KCNQ/M and HCN/h, but not $KCa2$ /SK channels, contribute to the somatic medium after-hyperpolarization and excitability control in CA1 hippocampal pyramidal cells. *J. Physiol.* *566*, 689–715.
- Haitin, Y., and Attali, B. (2008). The C-terminus of K_v7 channels: a multifunctional module. *J. Physiol.* *586*, 1803–1810.
- Haley, J.E., Abogadie, F.C., Delmas, P., Dayrell, M., Vallis, Y., Milligan, G., Caulfield, M.P., Brown, D.A., and Buckley, N.J. (1998). The α subunit of Gq contributes to muscarinic inhibition of the M-type potassium current in sympathetic neurons. *J. Neurosci.* *18*, 4521–4531.
- Hansen, S.B., Tao, X., and MacKinnon, R. (2011). Structural basis of PIP2 activation of the classical inward rectifier K^+ channel Kir2.2. *Nature* *477*, 495–498.
- Hawryluk, J.M., Moreira, T.S., Takakura, A.C., Wenker, I.C., Tzingounis, A.V., and Mulkey, D.K. (2012). KCNQ channels determine serotonergic modulation of ventral surface chemoreceptors and respiratory drive. *J. Neurosci.* *32*, 16943–16952.
- Hayashi, H., Iwata, M., Tsuchimori, N., and Matsumoto, T. (2014). Activation of peripheral KCNQ channels attenuates inflammatory pain. *Mol. Pain* *10*, 15.
- Hernandez, C.C., Zaika, O., and Shapiro, M.S. (2008). A Carboxy-terminal Inter-Helix Linker As the Site of Phosphatidylinositol 4,5-Bisphosphate Action on K_v7 (M-type) K^+ Channels. *J. Gen. Physiol.* *132*, 361–381.
- Hessler, S., Zheng, F., Hartmann, S., Rittger, A., Lehnert, S., Völkel, M., Nissen, M., Edelmann, E., Saftig, P., Schwake, M., et al. (2015). B-secretase BACE1 regulates hippocampal and reconstituted M-currents in a β -subunit-like fashion. *J. Neurosci.* *35*, 3298–3311.
- Hoshi, N., Zhang, J.-S., Omaki, M., Takeuchi, T., Yokoyama, S., Wanaverbecq, N., Langeberg, L.K., Yoneda, Y., Scott, J.D., Brown, D.A., et al. (2003). AKAP150 signaling complex promotes suppression of the M-current by muscarinic agonists. *Nat. Neurosci.* *6*, 564–571.
- Howard, R.J., Clark, K.A., Holton, J.M., and Minor, D.L. (2007). Structural insight into KCNQ (K_v7) channel assembly and channelopathy. *Neuron* *53*, 663–675.

- Huang, H., and Trussell, L.O. (2011). KCNQ5 channels control resting properties and release probability of a synapse. *Nat. Neurosci.* *14*, 840–847.
- Huang, C.-L., Feng, S., and Hilgemann, D.W. (1998). Direct activation of inward rectifier potassium channels by PIP₂ and its stabilization by Gβγ. *Nature* *391*, 803–806.
- Jepps, T.A., Greenwood, I.A., Moffatt, J.D., Sanders, K.M., and Ohya, S. (2009). Molecular and functional characterization of K_v7 K⁺ channel in murine gastrointestinal smooth muscles. *Am. J. Physiol. - Gastrointest. Liver Physiol.* *297*, G107–G115.
- Kalstrup, T., and Blunck, R. (2013). Dynamics of internal pore opening in K_v channels probed by a fluorescent unnatural amino acid. *Proc. Natl. Acad. Sci.* *110*, 8272–8277.
- Kiefer, F., Arnold, K., Kunzli, M., Bordoli, L., and Schwede, T. (2009). The SWISS-MODEL Repository and associated resources. *Nucleic Acids Res.* *37*, D387–D392.
- Kim, K.S., Duignan, K.M., Hawryluk, J.M., Soh, H., and Tzingounis, A.V. (2016). The voltage activation of cortical KCNQ channels depends on global PIP₂ levels. *Biophys. J.* *110*, 1089–1098.
- Klassen, T., Davis, C., Goldman, A., Burgess, D., Chen, T., Wheeler, D., McPherson, J., Bourquin, T., Lewis, L., Villasana, D., et al. (2011). Exome sequencing of ion channel genes reveals complex profiles confounding personal risk assessment in epilepsy. *Cell* *145*, 1036–1048.
- Kobayashi, H., and Libet, B. (1968). Generation of slow postsynaptic potentials without increases in ionic conductance. *Proc. Natl. Acad. Sci. U. S. A.* *60*, 1304.
- Kosenko, A., Kang, S., Smith, I.M., Greene, D.L., Langeberg, L.K., Scott, J.D., and Hoshi, N. (2012). Coordinated signal integration at the M-type potassium channel upon muscarinic stimulation: Signal integration at the M-channel. *EMBO J.* *31*, 3147–3156.
- Kubisch, C., Schroeder, B.C., Friedrich, T., Lütjohann, B., El-Amraoui, A., Marlin, S., Petit, C., and Jentsch, T.J. (1999). KCNQ4, a novel potassium channel expressed in sensory outer hair cells, is mutated in dominant deafness. *Cell* *96*, 437–446.
- Kumar, M., Reed, N., Liu, R., Aizenman, E., Wipf, P., and Tzounopoulos, T. (2016). Synthesis and evaluation of potent KCNQ2/3-specific channel activators. *Mol. Pharmacol.* mol.115.103200.
- Kuo, C.-C. (1998). A common anticonvulsant binding site for phenytoin, carbamazepine, and lamotrigine in neuronal Na⁺ channels. *Mol. Pharmacol.* *54*, 712–721.
- Kuo, C.C., and Bean, B.P. (1994). Slow binding of phenytoin to inactivated sodium channels in rat hippocampal neurons. *Mol. Pharmacol.* *46*, 716–725.
- Kwan, P., and Brodie, M.J. (2000). Early identification of refractory epilepsy. *N. Engl. J. Med.* *342*, 314–319.

- Lacroix, J.J., Pless, S.A., Maragliano, L., Campos, F.V., Galpin, J.D., Ahern, C.A., Roux, B., and Bezanilla, F. (2012). Intermediate state trapping of a voltage sensor. *J. Gen. Physiol.* *140*, 635–652.
- Lange, W., Geißendörfer, J., Schenzer, A., Grötzinger, J., Seebohm, G., Friedrich, T., and Schwake, M. (2009). Refinement of the binding site and mode of action of the anticonvulsant retigabine on KCNQ K⁺ channels. *Mol. Pharmacol.* *75*, 272–280.
- Lerche, C., Scherer, C.R., Seebohm, G., Derst, C., Wei, A.D., Busch, A.E., and Steinmeyer, K. (2000). Molecular cloning and functional expression of KCNQ5, a potassium channel subunit that may contribute to neuronal M-current diversity. *J. Biol. Chem.* *275*, 22395–22400.
- Lerche, H., Shah, M., Beck, H., Noebels, J., Johnston, D., and Vincent, A. (2013). Ion channels in genetic and acquired forms of epilepsy: Ion channels in epilepsy. *J. Physiol.* *591*, 753–764.
- Lerman, P. (1986). Seizures induced or aggravated by anticonvulsants. *Epilepsia* *27*, 706–710.
- Li, M., Jan, Y.N., and Jan, L.Y. (1992). Specification of subunit assembly by the hydrophilic amino-terminal domain of the Shaker potassium channel. *Science* *257*, 1225–1230.
- Li, Y., Gamper, N., and Shapiro, M.S. (2004). Single-channel analysis of KCNQ K⁺ channels reveals the mechanism of augmentation by a cysteine-modifying reagent. *J. Neurosci.* *24*, 5079–5090.
- Li, Y., Gamper, N., Hilgemann, D.W., and Shapiro, M.S. (2005). Regulation of K_v7 (KCNQ) K⁺ channel open probability by phosphatidylinositol 4,5-bisphosphate. *J. Neurosci.* *25*, 9825–9835.
- Long, S.B., Tao, X., Campbell, E.B., and MacKinnon, R. (2007). Atomic structure of a voltage-dependent K⁺ channel in a lipid membrane-like environment. *Nature* *450*, 376–382.
- Loussouarn, G., Park, K.-H., Bellocq, C., Baró, I., Charpentier, F., and Escande, D. (2003). Phosphatidylinositol-4,5-bisphosphate, PIP₂, controls KCNQ1/KCNE1 voltage-gated potassium channels: a functional homology between voltage-gated and inward rectifier K⁺ channels. *EMBO J.* *22*, 5412–5421.
- Lukyanetz, E.A., Shkryl, V.M., and Kostyuk, P.G. (2002). Selective blockade of N-type calcium channels by levetiracetam. *Epilepsia* *43*, 9–18.
- Luo, Y., Bolon, B., Kahn, S., Bennett, B.D., Babu-Khan, S., Denis, P., Fan, W., Kha, H., Zhang, J., Gong, Y., et al. (2001). Mice deficient in BACE1, the Alzheimer's β-secretase, have normal phenotype and abolished β-amyloid generation. *Nat. Neurosci.* *4*, 231–232.
- Main, M.J., Cryan, J.E., Dupere, J.R.B., Cox, B., Clare, J.J., and Burbidge, S.A. (2000). Modulation of KCNQ2/3 potassium channels by the novel anticonvulsant retigabine. *Mol. Pharmacol.* *58*, 253–262.

- Malerba, A., Ciampa, C., De Fazio, S., Fattore, C., Frassine, B., La Neve, A., Pellacani, S., Specchio, L.M., Tiberti, A., Tinuper, P., et al. (2010). Patterns of prescription of antiepileptic drugs in patients with refractory epilepsy at tertiary referral centres in Italy. *Epilepsy Res.* *91*, 273–282.
- Mannuzzu, L.M., Moronne, M.M., and Isacoff, E.Y. (1996). Direct physical measure of conformational rearrangement underlying potassium channel gating. *Science* *271*, 213–216.
- Martire, M., Castaldo, P., D’Amico, M., Preziosi, P., Annunziato, L., and Tagliatela, M. (2004). M channels containing KCNQ2 subunits modulate norepinephrine, aspartate, and GABA release from hippocampal nerve terminals. *J. Neurosci.* *24*, 592–597.
- Miceli, F., Soldovieri, M., Martire, M., and Tagliatela, M. (2008). Molecular pharmacology and therapeutic potential of neuronal Kv7-modulating drugs. *Curr. Opin. Pharmacol.* *8*, 65–74.
- Mitcheson, J.S., Chen, J., Lin, M., Culberson, C., and Sanguinetti, M.C. (2000). A structural basis for drug-induced long QT syndrome. *Proc. Natl. Acad. Sci.* *97*, 12329–12333.
- Mulkey, D.K., Rosin, D.L., West, G., Takakura, A.C., Moreira, T.S., Bayliss, D.A., and Guyenet, P.G. (2007). Serotonergic neurons activate chemosensitive retrotrapezoid nucleus neurons by a pH-independent mechanism. *J. Neurosci.* *27*, 14128–14138.
- Ng, F.L., Davis, A.J., Jepps, T.A., Harhun, M.I., Yeung, S.Y., Wan, A., Reddy, M., Melville, D., Nardi, A., Khong, T.K., et al. (2011). Expression and function of the K⁺ channel KCNQ genes in human arteries. *Br. J. Pharmacol.* *162*, 42–53.
- Nguyen, H.M., Miyazaki, H., Hoshi, N., Smith, B.J., Nukina, N., Goldin, A.L., and Chandy, K.G. (2012). Modulation of voltage-gated K⁺ channels by the sodium channel β 1 subunit. *Proc. Natl. Acad. Sci.* *109*, 18577–18582.
- Osteen, J.D., Gonzalez, C., Sampson, K.J., Iyer, V., Rebolledo, S., Larsson, H.P., and Kass, R.S. (2010). KCNE1 alters the voltage sensor movements necessary to open the KCNQ1 channel gate. *Proc. Natl. Acad. Sci.* *107*, 22710–22715.
- Pan, Z., Kao, T., Horvath, Z., Lemos, J., Sul, J.-Y., Cranstoun, S.D., Bennett, V., Scherer, S.S., and Cooper, E.C. (2006). A common ankyrin-G-based mechanism retains KCNQ and Nav channels at electrically active domains of the axon. *J. Neurosci.* *26*, 2599–2613.
- Passmore, G.M., Selyanko, A.A., Mistry, M., Al-Qatari, M., Marsh, S.J., Matthews, E.A., Dickenson, A.H., Brown, T.A., Burbidge, S.A., Main, M., et al. (2003a). KCNQ/M Currents in Sensory Neurons: Significance for Pain Therapy. *J. Neurosci.* *23*, 7227–7236.
- Passmore, G.M., Selyanko, A.A., Mistry, M., Al-Qatari, M., Marsh, S.J., Matthews, E.A., Dickenson, A.H., Brown, T.A., Burbidge, S.A., Main, M., et al. (2003b). KCNA/M currents in sensory neurons: significance for pain therapy. *J. Neurosci.* *23*, 7227–7236.
- Peretz, A., Sheinin, A., Yue, C., Degani-Katzav, N., Gibor, G., Nachman, R., Gopin, A., Tam, E., Shabat, D., Yaari, Y., et al. (2007a). Pre- and postsynaptic activation of M-channels by a novel opener dampens neuronal firing and transmitter release. *J. Neurophysiol.* *97*, 283–295.

- Peretz, A., Degani-Katzav, N., Talmon, M., Danieli, E., Gopin, A., Malka, E., Nachman, R., Raz, A., Shabat, D., and Attali, B. (2007b). A tale of switched functions: from cyclooxygenase inhibition to M-channel modulation in new diphenylamine derivatives. *PLoS ONE* 2, e1332.
- Peretz, A., Pell, L., Gofman, Y., Haitin, Y., Shamgar, L., Patrich, E., Kornilov, P., Gourgy-Hacohen, O., Ben-Tal, N., and Attali, B. (2010). Targeting the voltage sensor of Kv7.2 voltage-gated K⁺ channels with a new gating-modifier. *Proc. Natl. Acad. Sci.* 107, 15637–15642.
- Perez-Reyes, E. (2003). Molecular physiology of low-voltage-activated T-type calcium channels. *Physiol. Rev.* 83, 117–161.
- Peters, H.C., Hu, H., Pongs, O., Storm, J.F., and Isbrandt, D. (2005). Conditional transgenic suppression of M channels in mouse brain reveals functions in neuronal excitability, resonance and behavior. *Nat. Neurosci.* 8, 51–60.
- Pfaffinger, P.J., Leibowitz, M.D., Subers, E.M., Nathanson, N.M., Almers, W., and Hille, B. (1988). Agonists that suppress M-current elicit phosphoinositide turnover and Ca²⁺ transients, but these events do not explain M-current suppression. *Neuron* 1, 477–484.
- Pless, S.A., Niciforovic, A.P., Galpin, J.D., Nunez, J.-J., Kurata, H.T., and Ahern, C.A. (2013a). A novel mechanism for fine-tuning open-state stability in a voltage-gated potassium channel. *Nat. Commun.* 4, 1784.
- Pless, S.A., Galpin, J.D., Niciforovic, A.P., Kurata, H.T., and Ahern, C.A. (2013b). Hydrogen bonds as molecular timers for slow inactivation in voltage-gated potassium channels. *eLife* 2, e01289.
- Porter, R.J., Partiot, A., Sachdeo, R., Nohria, V., Alves, W.M., and on behalf of the 205 Study Group (2007). Randomized, multicenter, dose-ranging trial of retigabine for partial-onset seizures. *Neurology* 68, 1197–1204.
- Qi, Y., Wang, J., Bomben, V.C., Li, D.-P., Chen, S.-R., Sun, H., Xi, Y., Reed, J.G., Cheng, J., Pan, H.-L., et al. (2014). Hyper-SUMOylation of the Kv7 Potassium Channel Diminishes the M-Current Leading to Seizures and Sudden Death. *Neuron* 83, 1159–1171.
- Ragsdale, D.S., McPhee, J.C., Scheuer, T., and Catterall, W.A. (1996). Common molecular determinants of local anesthetic, antiarrhythmic, and anticonvulsant block of voltage-gated Na⁺ channels. *Proc. Natl. Acad. Sci.* 93, 9270–9275.
- Regev, N., Degani-Katzav, N., Korngreen, A., Etzioni, A., Siloni, S., Alaimo, A., Chikvashvili, D., Villarroel, A., Attali, B., and Lotan, I. (2009). Selective interaction of syntaxin 1a with KCNQ2: possible implications for specific modulation of presynaptic activity. *PLOS ONE* 4, e6586.
- Río, E., Bevilacqua, J.A., Marsh, S.J., Halley, P., and Caulfield, M.P. (1999). Muscarinic M1 receptors activate phosphoinositide turnover and Ca²⁺ mobilisation in rat sympathetic neurones, but this signalling pathway does not mediate M-current inhibition. *J. Physiol.* 520, 101–111.

Rogawski, M.A., and Löscher, W. (2004). The neurobiology of antiepileptic drugs. *Nat. Rev. Neurosci.* 5, 553–564.

Rostock, A., Tober, C., Rundfeldt, C., Bartsch, R., Engel, J., Polymeropoulos, E.E., Kutscher, B., Löscher, W., Hönack, D., White, H.S., et al. (1996). D-23129: a new anticonvulsant with a broad spectrum activity in animal models of epileptic seizures. *Epilepsy Res.* 23, 211–223.

Rundfeldt, C. (1997). The new anticonvulsant retigabine (D-23129) acts as an opener of K⁺ channels in neuronal cells. *Eur. J. Pharmacol.* 336, 243–249.

Rundfeldt, C., and Netzer, R. (2000). The novel anticonvulsant retigabine activates M-currents in Chinese hamster ovary-cells transfected with human KCNQ2/3 subunits. *Neurosci. Lett.* 282, 73–76.

S, M., C, L., G, S., Ak, A., Ae, B., and H, L. (2003). C-terminal interaction of KCNQ2 and KCNQ3 K⁺ channels. *J. Physiol.* 548, 353–360.

Sanguinetti, M.C., Curran, M.E., Zou, A., Shen, J., Specter, P.S., Atkinson, D.L., and Keating, M.T. (1996). Coassembly of K_vLQT1 and minK (IsK) proteins to form cardiac IKS potassium channel. *Nature* 384, 80–83.

Schenzer, A., Friedrich, T., Pusch, M., Saftig, P., Jentsch, T.J., Grötzinger, J., and Schwake, M. (2005). Molecular determinants of KCNQ (K_v7) K⁺ channel sensitivity to the anticonvulsant retigabine. *J. Neurosci.* 25, 5051–5060.

Schoppa, N.E., and Sigworth, F.J. (1998). Activation of shaker potassium channels. *J. Gen. Physiol.* 111, 313–342.

Schroeder, B.C., Kubisch, C., Stein, V., and Jentsch, T.J. (1998). Moderate loss of function of cyclic-AMP-modulated KCNQ2/KCNQ3 K⁺ channels causes epilepsy. *Nature* 396, 687–690.

Schroeder, B.C., Waldegger, S., Fehr, S., Bleich, M., Warth, R., Greger, R., and Jentsch, T.J. (2000a). A constitutively open potassium channel formed by KCNQ1 and KCNE3. *Nature* 403, 196–199.

Schroeder, B.C., Hechenberger, M., Weinreich, F., Kubisch, C., and Jentsch, T.J. (2000b). KCNQ5, a novel potassium channel broadly expressed in brain, mediates M-type currents. *J. Biol. Chem.* 275, 24089–24095.

Schwake, M., Pusch, M., Kharkovets, T., and Jentsch, T.J. (2000). Surface expression and single channel properties of KCNQ2/KCNQ3, M-type K⁺ channels involved in epilepsy. *J. Biol. Chem.* 275, 13343–13348.

Schwake, M., Jentsch, T.J., and Friedrich, T. (2003). A carboxy-terminal domain determines the subunit specificity of KCNQ K⁺ channel assembly. *EMBO Rep.* 4, 76–81.

- Schwake, M., Athanasiadu, D., Beimgraben, C., Blanz, J., Beck, C., Jentsch, T.J., Saftig, P., and Friedrich, T. (2006). Structural determinants of M-type KCNQ (K_v7) channel assembly. *J. Neurosci.* *26*, 3757–3766.
- Segal, M.M., and Douglas, A.F. (1997). Late sodium channel openings underlying epileptiform activity are preferentially diminished by the anticonvulsant phenytoin. *J. Neurophysiol.* *77*, 3021–3034.
- Shah, M.M., Mistry, M., Marsh, S.J., Brown, D.A., and Delmas, P. (2002). Molecular correlates of the M-current in cultured rat hippocampal neurons. *J. Physiol.* *544*, 29–37.
- Shah, M.M., Migliore, M., Valencia, I., Cooper, E.C., and Brown, D.A. (2008). Functional significance of axonal K_v7 channels in hippocampal pyramidal neurons. *Proc. Natl. Acad. Sci.* *105*, 7869–7874.
- Shi, L., Bian, X., Qu, Z., Ma, Z., Zhou, Y., Wang, K., Jiang, H., and Xie, J. (2013). Peptide hormone ghrelin enhances neuronal excitability by inhibition of K_v7/KCNQ channels. *Nat. Commun.* *4*, 1435.
- Shyng, S.-L., and Nichols, C.G. (1998). Membrane Phospholipid Control of Nucleotide Sensitivity of KATP Channels. *Science* *282*, 1138–1141.
- Singh, N.A. (2003). KCNQ2 and KCNQ3 potassium channel genes in benign familial neonatal convulsions: expansion of the functional and mutation spectrum. *Brain* *126*, 2726–2737.
- Singh, N.A., Charlier, C., Stauffer, D., DuPont, B.R., Leach, R.J., Melis, R., Ronen, G.M., Bjerre, I., Quattlebaum, T., Murphy, J.V., et al. (1998). A novel potassium channel gene, KCNQ2, is mutated in an inherited epilepsy of newborns. *Nat. Genet.* *18*, 25–29.
- Soh, H., Pant, R., LoTurco, J.J., and Tzingounis, A.V. (2014). Conditional deletions of epilepsy-associated KCNQ2 and KCNQ3 channels from cerebral cortex cause differential effects on neuronal excitability. *J. Neurosci.* *34*, 5311–5321.
- Soldovieri, M.V., Castaldo, P., Iodice, L., Miceli, F., Barrese, V., Bellini, G., Giudice, E.M. del, Pascotto, A., Bonatti, S., Annunziato, L., et al. (2006). Decreased subunit stability as a novel mechanism for potassium current impairment by a KCNQ2 C terminus mutation causing benign familial neonatal convulsions. *J. Biol. Chem.* *281*, 418–428.
- Strulovich, R., Tobelaim, W.S., Attali, B., and Hirsch, J.A. (2016). Structural insights into the m-channel proximal c-terminus/calmodulin complex.
- Suh, B.-C., and Hille, B. (2002). Recovery from muscarinic modulation of M current channels requires phosphatidylinositol 4,5-bisphosphate synthesis. *Neuron* *35*, 507–520.
- Suh, B.-C., Inoue, T., Meyer, T., and Hille, B. (2006). Rapid chemically induced changes of ptdins(4,5)p₂ gate KCNQ ion channels. *Science* *314*, 1454–1457.

- Sutton, K.G., Martin, D.J., Pinnock, R.D., Lee, K., and Scott, R.H. (2002). Gabapentin inhibits high-threshold calcium channel currents in cultured rat dorsal root ganglion neurones. *Br. J. Pharmacol.* *135*, 257–265.
- Suzdak, P.D., and Jansen, J.A. (1995). A review of the preclinical pharmacology of tiagabine: a potent and selective anticonvulsant GABA uptake inhibitor. *Epilepsia* *36*, 612–626.
- Tatulian, L., Delmas, P., Abogadie, F.C., and Brown, D.A. (2001). Activation of expressed KCNQ potassium currents and native neuronal M-type potassium currents by the anti-convulsant drug retigabine. *J. Neurosci.* *21*, 5535–5545.
- Taverna, S., Mantegazza, M., Franceschetti, S., and Avanzini, G. (1998). Valproate selectively reduces the persistent fraction of Na⁺ current in neocortical neurons. *Epilepsy Res.* *32*, 304–308.
- Telezhkin, V., Brown, D.A., and Gibb, A.J. (2012a). Distinct subunit contributions to the activation of M-type potassium channels by PI(4,5)P₂. *J. Gen. Physiol.* *140*, 41–53.
- Telezhkin, V., Reilly, J.M., Thomas, A.M., Tinker, A., and Brown, D.A. (2012b). Structural requirements of membrane phospholipids for M-type potassium channel activation and binding. *J. Biol. Chem.* *287*, 10001–10012.
- Tinel, N., Diochot, S., Lauritzen, I., Barhanin, J., Lazdunski, M., and Borsotto, M. (2000). M-type KCNQ2-KCNQ3 potassium channels are modulated by the KCNE2 subunit. *FEBS Lett.* *480*, 137–141.
- Trott, O., and Olson, A.J. (2010). AutoDock Vina: Improving the speed and accuracy of docking with a new scoring function, efficient optimization, and multithreading. *J. Comput. Chem.* *31*, 455–461.
- Tzingounis, A.V., and Nicoll, R.A. (2008). Contribution of KCNQ2 and KCNQ3 to the medium and slow afterhyperpolarization currents. *Proc. Natl. Acad. Sci.* *105*, 19974–19979.
- Tzingounis, A.V., Heidenreich, M., Kharkovets, T., Spitzmaul, G., Jensen, H.S., Nicoll, R.A., and Jentsch, T.J. (2010). The KCNQ5 potassium channel mediates a component of the afterhyperpolarization current in mouse hippocampus. *Proc. Natl. Acad. Sci.* *107*, 10232–10237.
- Vivienne Shen, N., Chen, X., Boyer, M.M., and Pfaffinger, P.J. (1993). Deletion analysis of K⁺ channel assembly. *Neuron* *11*, 67–76.
- Wang, H.S., and McKinnon, D. (1995). Potassium currents in rat prevertebral and paravertebral sympathetic neurones: control of firing properties. *J. Physiol.* *485*, 319–335.
- Wang, A.W., Yang, R., and Kurata, H.T. (2017). Sequence determinants of subtype-specific actions of KCNQ channel openers. *J. Physiol.* *595*, 663–676.
- Wang, H.-S., Pan, Z., Shi, W., Brown, B.S., Wymore, R.S., Cohen, I.S., Dixon, J.E., and McKinnon, D. (1998). KCNQ2 and KCNQ3 potassium channel subunits: molecular correlates of the M-channel. *Science* *282*, 1890–1893.

- Wang, Q., Curran, M.E., Splawski, I., Burn, T.C., Millholland, J.M., VanRaay, T.J., Shen, J., Timothy, K.W., Vincent, G.M., de Jager, T., et al. (1996). Positional cloning of a novel potassium channel gene: K_v LQT1 mutations cause cardiac arrhythmias. *Nat. Genet.* *12*, 17–23.
- Watanabe, H., Nagata, E., Kosakai, A., Nakamura, M., Yokoyama, M., Tanaka, K., and Sasai, H. (2000). Disruption of the epilepsy KCNQ2 gene results in neural hyperexcitability. *J. Neurochem.* *75*, 28–33.
- Weight, F.F., and Votava, J. (1970). Slow synaptic excitation in sympathetic ganglion cells: evidence for synaptic inactivation of potassium conductance. *Science* *170*, 755–758.
- Wen, H., and Levitan, I.B. (2002). Calmodulin is an auxiliary subunit of KCNQ2/3 potassium channels. *J. Neurosci.* *22*, 7991–8001.
- Werry, D., Eldstrom, J., Wang, Z., and Fedida, D. (2013). Single-channel basis for the slow activation of the repolarizing cardiac potassium current, IKs. *Proc. Natl. Acad. Sci.* *110*, E996–E1005.
- Whicher, J.R., and MacKinnon, R. (2016). Structure of the voltage-gated K^+ channel Eag1 reveals an alternative voltage sensing mechanism. *Science* *353*, 664–669.
- Whorton, M.R., and MacKinnon, R. (2011). Crystal structure of the mammalian GIRK2 K^+ channel and gating regulation by G proteins, PIP2, and sodium. *Cell* *147*, 199–208.
- Wickenden, A.D., Yu, W., Zou, A., Jegla, T., and Wagoner, P.K. (2000). Retigabine, a novel anti-convulsant, enhances activation of KCNQ2/3 potassium channels. *Mol. Pharmacol.* *58*, 591–600.
- Wladyka, C.L., Feng, B., Glazebrook, P.A., Schild, J.H., and Kunze, D.L. (2008). The KCNQ/M-current modulates arterial baroreceptor function at the sensory terminal in rats. *J. Physiol.* *586*, 795–802.
- Wu, Y.-J., and Dworetzky, S. (2005). Recent developments on KCNQ potassium channel openers. *Curr. Med. Chem.* *12*, 453–460.
- Wu, Y.-J., He, H., Sun, L.-Q., L’Heureux, A., Chen, J., Dextraze, P., Starrett, J.E., Boissard, C.G., Gribkoff, V.K., Natale, J., et al. (2004). Synthesis and structure–activity relationship of acrylamides as KCNQ2 potassium channel openers. *J. Med. Chem.* *47*, 2887–2896.
- Wuttke, T.V., Seebohm, G., Bail, S., Maljevic, S., and Lerche, H. (2005). The new anticonvulsant retigabine favors voltage-dependent opening of the $K_v7.2$ (KCNQ2) channel by binding to its activation gate. *Mol. Pharmacol.* *67*, 1009–1017.
- Xiong, Q., Sun, H., and Li, M. (2007). Zinc pyrithione-mediated activation of voltage-gated KCNQ potassium channels rescues epileptogenic mutants. *Nat. Chem. Biol.* *3*, 287–296.
- Xiong, Q., Gao, Z., Wang, W., and Li, M. (2008). Activation of K_v7 (KCNQ) voltage-gated potassium channels by synthetic compounds. *Trends Pharmacol. Sci.* *29*, 99–107.

- Xu, J., Yu, W., Jan, Y.N., Jan, L.Y., and Li, M. (1995). Assembly of voltage-gated potassium channels conserved hydrophilic motifs determine subfamily-specific interactions between the α -subunits. *J. Biol. Chem.* *270*, 24761–24768.
- Yu, F.H., Mantegazza, M., Westenbroek, R.E., Robbins, C.A., Kalume, F., Burton, K.A., Spain, W.J., McKnight, G.S., Scheuer, T., and Catterall, W.A. (2006). Reduced sodium current in GABAergic interneurons in a mouse model of severe myoclonic epilepsy in infancy. *Nat. Neurosci.* *9*, 1142–1149.
- Yu, H., Wu, M., Townsend, S.D., Zou, B., Long, S., Daniels, J.S., McManus, O.B., Li, M., Lindsley, C.W., and Hopkins, C.R. (2011). Discovery, synthesis, and structure–activity relationship of a series of n-aryl-bicyclo[2.2.1]heptane-2-carboxamides: characterization of ML213 as a novel KCNQ2 and KCNQ4 potassium channel opener.
- Yue, C., and Yaari, Y. (2004). KCNQ/M channels control spike afterdepolarization and burst generation in hippocampal neurons. *J. Neurosci.* *24*, 4614–4624.
- Yus-Nájera, E., Santana-Castro, I., and Villarroel, A. (2002). The identification and characterization of a noncontinuous calmodulin-binding site in noninactivating voltage-dependent KCNQ potassium channels. *J. Biol. Chem.* *277*, 28545–28553.
- Zagotta, W.N., Hoshi, T., and Aldrich, R.W. (1994). Shaker potassium channel gating. III: Evaluation of kinetic models for activation. *J. Gen. Physiol.* *103*, 321–362.
- Zaika, O., Lara, L.S., Gamper, N., Hilgemann, D.W., Jaffe, D.B., and Shapiro, M.S. (2006). Angiotensin II regulates neuronal excitability via phosphatidylinositol 4,5-bisphosphate-dependent modulation of K_v7 (M-type) K⁺ channels: Angiotensin II regulates neuronal excitability via PIP₂ depletion. *J. Physiol.* *575*, 49–67.
- Zaydman, M.A., and Cui, J. (2014). PIP₂ regulation of KCNQ channels: biophysical and molecular mechanisms for lipid modulation of voltage-dependent gating. *Front. Physiol.* *5*.
- Zaydman, M.A., Silva, J.R., Delaloye, K., Li, Y., Liang, H., Larsson, H.P., Shi, J., and Cui, J. (2013). K_v7.1 ion channels require a lipid to couple voltage sensing to pore opening. *Proc. Natl. Acad. Sci.* *110*, 13180–13185.
- Zhang, H., Craciun, L.C., Mirshahi, T., Rohács, T., Lopes, C.M., Jin, T., and Logothetis, D.E. (2003). PIP₂ Activates KCNQ Channels, and Its Hydrolysis Underlies Receptor-Mediated Inhibition of M Currents. *Neuron* *37*, 963–975.
- Zhang, Q., Zhou, P., Chen, Z., Li, M., Jiang, H., Gao, Z., and Yang, H. (2013). Dynamic PIP₂ interactions with voltage sensor elements contribute to KCNQ2 channel gating. *Proc. Natl. Acad. Sci.* *110*, 20093–20098.
- Zhou, P., Yu, H., Gu, M., Nan, F., Gao, Z., and Li, M. (2013). Phosphatidylinositol 4,5-bisphosphate alters pharmacological selectivity for epilepsy-causing KCNQ potassium channels. *Proc. Natl. Acad. Sci.* *110*, 8726–8731.

Zhou, P., Zhang, Y., Xu, H., Chen, F., Chen, X., Li, X., Pi, X., Wang, L., Zhan, L., Nan, F., et al. (2015). P-Retigabine: An N-Propargylyed Retigabine with Improved Brain Distribution and Enhanced Antiepileptic Activity. *Mol. Pharmacol.* 87, 31–38.